*Coordination Chemistry Reviews*
Elsevier Publishing Company, Amsterdam
Printed in The Netherlands



# THE ELECTRONIC PROPERTIES AND STEREOCHEMISTRY OF MONO-NUCLEAR COMPLEXES OF THE COPPER(II) ION

B. J. HATHAWAY AND D. E. BILLING*

*The Chemistry Department, University of Essex, Wivenhoe Park, Colchester, Essex (Great Britain)*

(Received September 18th, 1969)

CONTENTS



---

* Present address. The Chemistry Department, Woolwich Polytechnic, Wellington Street, London S E. 18, Great Britain.

ABBREVIATIONS

| | | | |
|---|---|---|---|
| en | ethylenediamine | dmp | 2,2,6,6-tetramethyl-heptane-3,5-dione |
| ompa | octamethylpyrophosphoramide | | |
| hfacac | hexafluoroacetylacetone | 3-$\phi$ acac | 3-phenyl acetylacetone |
| bipy | 2,2'-bipyridyl | *N*-Me salim | *N*-methyl salicylaldimine |
| PyNO | pyridine *N*-oxide | 1,3-pn | 1,3-propylenediamine |
| acac | acetylacetone | phen | 1:10-*ortho*-phenanthroline |
| salim | salicylaldimine | dmg | dimethylglyoxime |
| t-butylsalim | *N*-t-butyl salicylaldimine | D P.P.H. | diphenylpicrylhydrazine |
| dprm | dipyrromethane | $Et_2NN'$-al | *d,l*-diethyl-*N,N'*-$\alpha$-alanine |
| $Et_4$dien | 1,1,7,7-tetraethyldiethylenetriamine | dien | diethylenetriamine |
| | | $H_2$edta | ethylene-diaminetetraacetic acid |
| dach | 1,4-diazacycloheptane | | |
| enacac$_2$ | *N,N'*-ethylenebis(acetylacetoneimine) | 3-Me acac | 3-methyl acetylacetone |

## A. INTRODUCTION

The first-row transition metals are characterised by their ability to form a wide range of coordination complexes in which the octahedral, tetrahedral and square-coplanar stereochemistries predominate[1]. The copper(II) ion is a typical transition metal ion in respect of the formation of coordination complexes[1,2], but less typical in its reluctance to take up a regular octahedral or tetrahedral stereochemistry[3,4]. The $3d^9$ outer electron configuration of the copper(II) ion lacks cubic symmetry, and hence yields distorted forms of the basic stereochemistries. The range of stereochemistries which have now been characterised[3] for the copper(II) ion are summarised in Fig. 1. The coordination numbers of four, five and six predominate, but variations of each structure occur through bond-length or bond-angle distortions. The $d^9$ configuration of the copper(II) ion is a simple

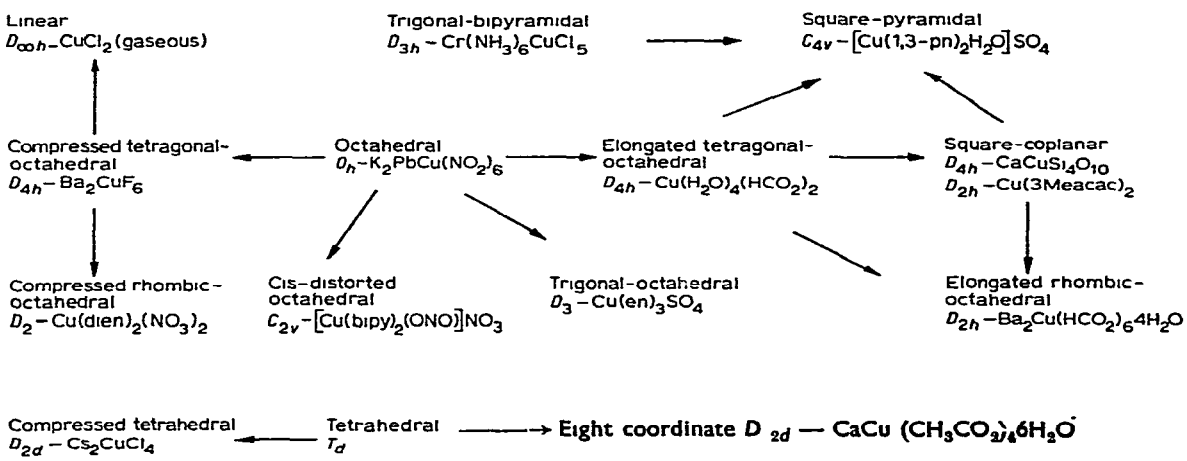


**Fig. 1. A summary of the known stereochemistries of the copper(II) ion, their idealised molecular symmetries, and the relationship between the regular and distorted geometries.**

system theoretically, as it can be considered as a single positive hole in an otherwise filled $d^{10}$ configuration. The way in which the positive hole behaves in the different stereochemistries of Fig. 1 can be understood qualitatively, using crystal-field theory[5–8] to predict the ordering of the one-electron orbital levels. The magnitudes of the splittings of the electronic energy levels in copper(II) complexes tend to be larger than for other first-row transition metals due to the large bond-length distortions present[3]. Thus, the tetragonal splittings[9] of the parent octahedral levels in $Ni(NH_3)_4(NO_2)_2$ (I)[10] are less than $2.0kK$, whereas the splitting of the $^2Eg(O_h)$ level[11] in $Cu(NH_3)_4(NO_2)_2$ (II)[12] is $13.5kK$. The electronic properties of copper(II)

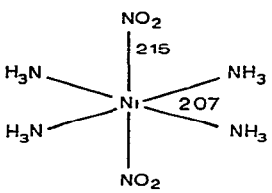


I $Ni(NH_3)_4(NO_2)_2$

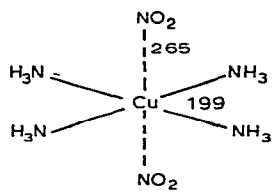


II $Cu(NH_3)_4(NO_2)_2$

complexes are thus relatively sensitive to stereochemistry, and this review examines this sensitivity for the large number of copper(II) complexes of known crystal-structure which are available[2,3]. The various stereochemistries are first summarised, and then their magnetic, ESR and electronic-spectral properties are examined, in an attempt to establish electronic criteria of their structures. Only mononuclear complexes are treated.

## B. A SURVEY OF THE STEREOCHEMISTRIES OF THE COPPER(II) ION

The range of stereochemistries available to the copper(II) ion has been summarised in Fig 1. Examples are listed in Table 1, and some typical molecular structures illustrated (II)–(XIX). This survey is not intended to be complete, but the examples given are of known crystal-structure and lend themselves to the measurement of single-crystal ESR and polarised electronic spectra.

## C. THE FACTORS WHICH INFLUENCE THE STEREOCHEMISTRY OF COPPER(II) COMPLEXES

Before discussing the electronic properties of copper(II) complexes it is worth examining some of the factors which influence the different stereochemistries.

### (i) *The Jahn–Teller theorem*

In a regular octahedral ligand-field, the $d^9$ configuration of the copper(II) ion would result in a degenerate ground state. The single unpaired electron could

TABLE 1

STEREOCHEMISTRIES ESTABLISHED FOR COPPFR(II) COMPLEXES

| *Stereochemistry* | *Examples* | *Molecular structure* | *Space group* | *Z* | *Alignment* | *Chromophore* | *Copper–ligand bond distances (Å)* | *Remarks* | *Ref* |
|---|---|---|---|---|---|---|---|---|---|
| *A Centrosymmetric complexes* | | | | | | | | | |
| Octahedral-$O_h$ | $K_2PbCu(NO_2)_6$ | III | $Fm3$ | 4 | P | $N_6$ | N-2.11 | Strictly $T_h$-dynamic Jahn–Teller | 13 |
| Elongated | $Cu(NH_3)_4(SCN)_2$ | — | $I2/m$ | 2 | P | $N_4S_2$ | N-2.08, S-3.00 | | 14 |
| tetragonal | $Cu(NH_3)_4(NO_2)_2$ | II | $C2/m$ | 2 | P | $N_4N_2'$ | N-1.99, N'-2.65 | Nitro coordination | 12 |
| octahedral | $Cu(H_2O)_4(HCO_2)_2$ | IV | $P2_1/a$ | 2 | 41° | $O_4O_2'$ | O-2.00, O'-2 36 | Formate bridging | 15 |
| | $Cu(H_2O)_{82}(UO_2)_2(AsO_4)_2$ | — | $P4_2/nmc$ | 2 | P | $O_4O_2'$ | O-2.14, O'-2.55–2.58 | Uranyl bridging | 16 |
| Square coplanar | $Cu(PyNO)_4(BF_4)_2$ | — | $P2_1/c$ | 2 | 90° | $O_4$ | O-1.91–1 93 | Nearest axial atom F-3 34 | 17 |
| $D_{4h}$ | $CaCuSi_4O_{10}$ | — | $P4/ncc$ | 4 | P | $O_4$ | O-1.91 | Nearest axial atom Cu-7.56 | 18 |
| | $Na_4Cu(NH_3)_4\{Cu(S_2O_3)_2\}_2 \cdot H_2O$ | V | $I4/m$ | 2 | P | $N_4$ | N-2.00 | Nearest axial atom O-2 88 | 19–21 |
| Elongated | $CsCuCl_3$ | — | $P6_122$ | 6 | 60° | $Cl_2Cl_2'Cl_2''$ | Cl-2 28; Cl'-2.35, Cl''-2.78 | Chloride bridging | 22 |
| rhombic | $Cu(H_2O)_6(ClO_4)_2$ | — | $P2_1/c$ | 4 | 60° | $O_2O_2'O_2''$ | O-2.09; O'-2.16, O''-2 28 | | 23 |
| octahedral | $Ba_2Cu(HCO_2)_6 \cdot 4H_2O$ | VI | $P\bar{1}$ | 1 | P | $O_2O_2'O_2''$ | O-1.97, O'-2 02, O''-2 18 | | 24 |
| | $Cu(NH_3)_2Br_2$ | — | $C2/m$ | 2 | P | $N_2Br_2Br_2'$ | N-1.93, Br-2.54; Br'-3 08 | Bromide bridging | 25 |
| $D_{4h}$ | $CuenCl_2$ | — | $P2_1$ | 2 | P | $N_2Cl_2Cl_2'$ | N-2.02–2 03, Cl-2.30; Cl'-2 91 | Chloride bridging | 26 |
| | $Cu(en)_2(BF_4)_2$ | VII | $P\bar{1}$ | 1 | P | $N_4F_2$ | N-2.02–2.03; F-2.56 | | 27, 28 |
| Square- | $Cu(3\text{-Meacac})_2$ | VIII | $P\bar{1}$ | 1 | P | $O_4$ | O-1.907 | | 29 |
| coplanar | $Cu(salim)_2$ | — | $P2_1/c$ | 2 | 10° | $O_2N_2$ | O-1.91, N-1.90 | | 30 |
| rhombic | $Cu(Et_2NN'al)_2$ | — | $P\bar{1}$ | 1 | P | $O_2N_2$ | O-1.91; N-2 03 | | 31 |
| Semi-elongated | $Cu(NH_3)_2(CH_3CO_2)_2$ | IX | $P2_1/c$ | 2 | 30° | $N_2O_2O_2'$ | N-1.97; O-2.07, O'-2.77 | O'-40° off z-axis | 32 |
| rhombic | $Cubipy(ONO)_2$ | — | $P2_1/c$ | 4 | 90° | $N_2O_2O_2'$ | N-1 98, O-1 99; O'-2.48–2 51 | O'-37° off z-axis | 33 |
| | $Cu(\phi CO_2)_2 \cdot 2H_2O$ | — | $P2_1/c$ | 2 | | $O_2O_2'O_2''$ | O-1 93; O'-1.97; O''-2.68 | O''-36° off z-axis | 34 |

*(Continued next page)*

TABLE 1 *(continued)*

| *Stereochemistry* | *Examples* | *Molecular structure* | *Space group* | *Z* | *Alignment* | *Chromophore* | *Copper ligand bond distances (Å)* | *Remarks* | *Ref.* |
|---|---|---|---|---|---|---|---|---|---|
| Compressed | $K_2CuF_4$ | — | $I4/mnm$ | 2 | — | $F_2F_4'$ | F-1.95, F′-2 08 | Fluoride bridging | 35 |
| tetragonal octahedral | $Ba_2CuF_6$ | — | $I2/m$ | 1 | P | $F_2F_4'$ | F-1.85, F′-2 08 | | 36 |
| Compressed | $Cudien_2(NO_3)_2$ | XI | $P2_12_12_1$ | 4 | 90° | $N_2N_4'$ | N-2.01, N′-2.22 | $C_2$-molecular symmetry | 37 |
| rhombic octahedral | Cu(methoxyacetate)$_2$ $2H_2O$ | — | $P2_1/n$ | 2 | 68° | $O_2O_2'O_2''$ | O-1.93, O′-2 13; O″-2.15 | | 38 |
| *B Noncentrosymmetric complexes* | | | | | | | | | |
| Compressed | $Cs_2CuCl_4$ | XIII | $Pnma$ | 4 | — | $Cl_4$ | Cl-2.22 | $D_{2d}$ symmetry | 39 |
| tetrahedral | Cu(t-butyl-salim)$_2$ | — | $P2_12_12_1$ | 4 | P | $O_2N_2$ | O-1 90, N-1.98 | | 40 |
| Trigonal | $Cu(NH_3)_2Ag(SCN)_3$ | XIV | $P\bar{6}2c$ | 2 | P | $N_2'N_3$ | N-2 00, N′-1.92 | Regular | 41 |
| bipyramidal | [Cubipy$_2$I]I | XV | $P\bar{1}$ | 2 | P | $N_4I$ | See molecular structure | Distorted | 42 |
| | $Cr(NH_3)_6CuCl_5$ | — | $Fd3c$ | 32 | — | $Cl_2Cl_3'$ | Cl-2.296, Cl′-2.391 | | 43 |
| Square-based pyramidal | $[Cu(NH_3)_4H_2O]SO_4$ | — | $Pmcn$ | 4 | 60° | $N_4OO'$ | N-2.034; O-2.34; O′-3.48 | Cu out of $N_4$ plane, $\rho = 0.19$ Å | 44, 45 |
| | [Cu(1,3-pn)$_2$H$_2$O]SO$_4$ | XVI | $Pna2_1$ | 4 | 5° | $N_4O_1$ | N-2 00; O-2.54 | Cu out of $N_4$ plane | 46 |
| $C_{2v}$ | Cu(acac)$_2$Quin | — | $P\bar{1}$ | 2 | P | $O_4N$ | O-1 95, N-2.36 | Cu out of $O_4$ plane, $\rho = 0.2$ Å | 47 |
| | $Cu(PyNO)_2(NO_3)_2$ | — | $P2_1/n$ | 4 | 40° | $O_4O'$ | O-1 96; O′-2.44 | Dimer | 48 |
| Trigonal | $Cuen_3SO_4$ | — | $P\bar{3}/c$ | 2 | P | $N_6$ | N-2.17 | Dynamic Jahn–Teller | 49 |
| octahedral | Cu(ompa)$_3$(ClO$_4$)$_3$ | — | $P\bar{3}c1$ | 2 | — | $O_6$ | O-2 065 | Dynamic Jahn–Teller | 50 |
| Cis-distorted octahedral | $[Cubipy_2(ONO)]NO_3$ | XVIII | $P2_1/n$ | 4 | P | $N_4O_2$ | See molecular structure | | 51 |
| Restricted | $Cudien_2Br_2H_2O$ | X | $P2_1/c$ | 4 | P | $N_4N_2$ | N-2.07; N-2.40 | | 52 |
| tetragonal | $CuH_2edta$ $H_2O$ | XII | $P2_1/c$ | 4 | 26° | $N_2O_4$ | see molecular structure | | 53 |
| rhombic | Cu(hfacac)$_2$bipy | XVII | $C2/c$ | 4 | — | $N_2O_2O_2'$ | N-1 976, O-1.93; O′-2.296 | $C_2$ molecular symmetry | 54 |
| Eight coordinate | $CaCu(CH_3CO_2)_4 \cdot 6H_2O$ | XIX | $I4/m$ | 4 | P | $O_4O_4'$ | O-1.97, O′-2.79 | $S_4$ molecular symmetry | 55 |

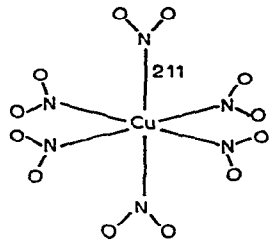


III $K_2Pb\,Cu(NO_2)_6$

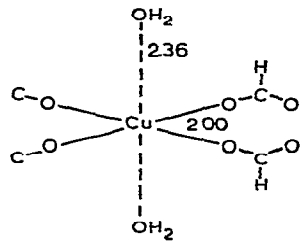


IV $Cu(H_2O)_4(HCO_2)_2$

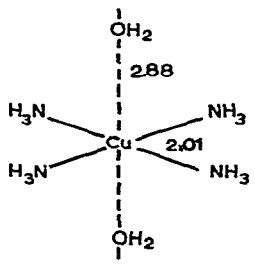


V $Na_4Cu(NH_3)_4\{Cu(S_2O_3)_2\}_2\cdot H_2O$

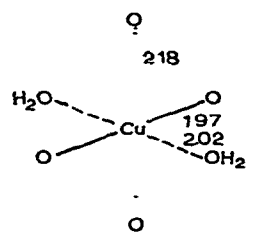


VI $Ba_2Cu(HCO_2)_6\cdot 4H_2O$

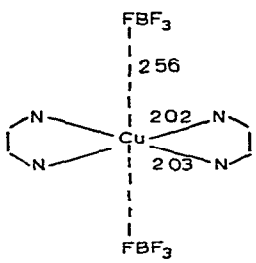


VII $Cu(en)_2(BF_4)_2$

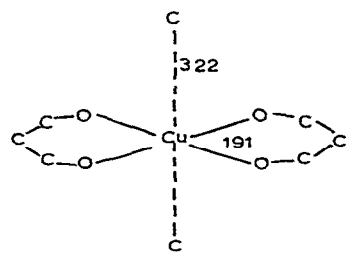


VIII $Cu(3\text{-}Me\,acac)_2$

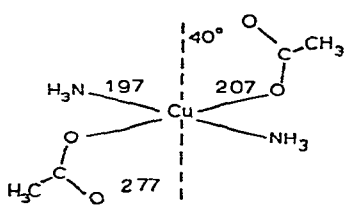


IX $Cu(CH_3CO_2)_2(NH_3)_2$

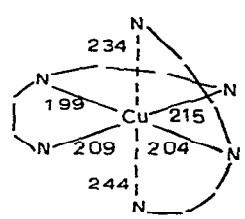


X $Cu(dien)_2Br_2\,H_2O$

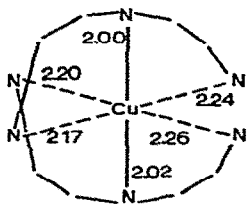


XI $Cu(dien)_2(NO_3)_2$

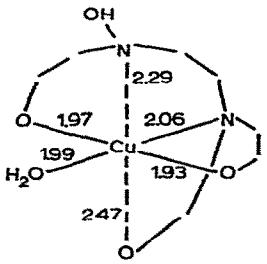


XII Cu $H_2$edta $H_2O$

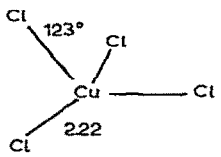


XIII $Cs_2CuCl_4$

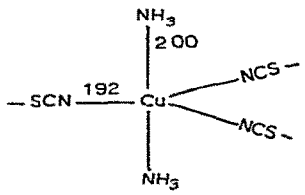


XIV $Cu(NH_3)_2Ag(SCN)_3$

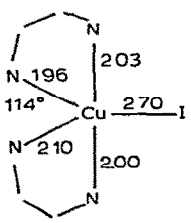


XV $[Cu(bipy)_2]I$

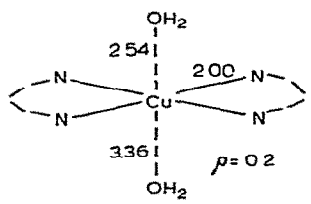


XVI $[Cu(13\text{-}pn)_2\,H_2O]SO_4$

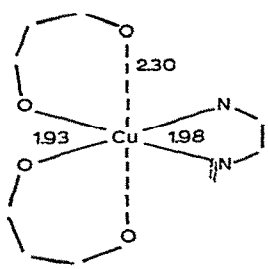


XVII $Cu(hfacac)_2(bipy)$

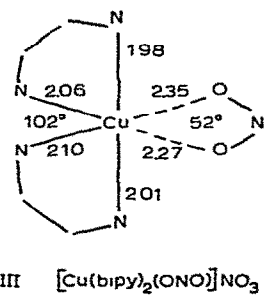


XVIII $[Cu(bipy)_2(ONO)]NO_3$

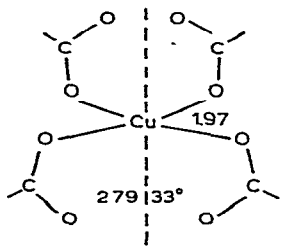


XIX Ca $Cu(CH_3CO_2)_4 \cdot 6H_2O$

be in either of the components $d_{x^2-y^2}$ or $d_{z^2}$ of the $e_g$ state. The Jahn–Teller theorem[56] requires any non-linear system with a degenerate ground state to undergo such a distortion as will remove the degeneracy. The type of distortion can be shown to be any of the non-totally symmetric normal vibrations whose representations are contained in the direct product of the ground-state representation for the appropriate point group. In this case, the representation of the ground state is $e_g$ in the $O_h$ point group. The direct product reduces to $e_g \times e_g = a_{1g}+a_{2g}+e_g$, and since $a_{1g}$ is totally symmetric and there are no $a_{2g}$ normal vibrations[57], only the components (V and VI in Fig. 2) of the $e_g$ mode can remove the degeneracy. The extrema of these vibrations are the static distortions commonly found in six-coordinate copper(II) complexes[4]. The elongated tetragonally-distorted octahedron (structure II in Fig. 2) and elongated rhombically-distorted octahedron can be thought of as resulting from having the odd electron in the $d_{x^2-y^2}$ orbital, so causing less coulombic repulsion between the copper electrons and the negatively-charged ligands in the xy-plane, than along the z-axis. The compressed structures

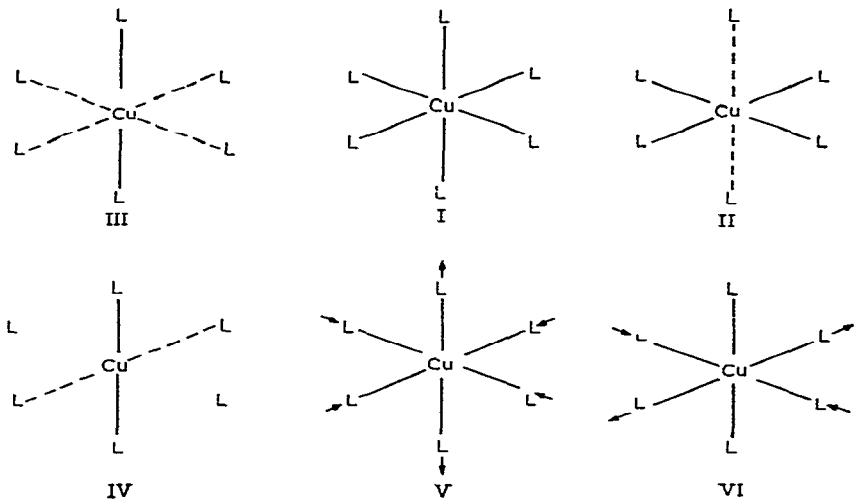


Fig 2. The forms of the tetragonal and rhombic distortions of an octahedral $CuL_6$ chromophore (II, III and IV) and the components of the $e_g$ mode of vibration (V and VI).

(III and IV) result from having the odd electron in the $d_{z^2}$ orbital. Detailed calculations[58] have shown that the elongated structures are usually more energetically favourable than the compressed structures, consistent with their more frequent occurrence[3,4]. It must be emphasized that although the Jahn–Teller theorem may in this way account for the type of distortion observed, it cannot determine the magnitude of the distortion.

This theory[56] accounts for distortion in complexes with six equivalent ligands, but at first glance does not treat the cases of inequivalent ligands, which would not give degenerate ground states. This approach to the problem of inequivalent ligands overlooks the fact that the copper(II) ion can "see" a regular octahedral field if the distances of the inequivalent ligands are so arranged that higher positions in the spectrochemical series[59] are exactly counterbalanced by longer bonds. Then, although the molecular symmetry is irregular, the "effective" electronic symmetry is regular and will require a distortion to remove the degeneracy.

The regular $CuN_6$ chromophore[13] in $K_2PbCu(NO_2)_6$ would seem to conflict with the predictions of the Jahn–Teller theorem[56], but in this complex the nuclear framework of the chromophore is believed to be undergoing a dynamic distortion[13,60–69], rather than the static distortion[4] observed in the majority of copper(II) complexes. Whether the distortion involves a true dynamic distortion or merely pseudo-rotation[70], is not certain, but the extreme distortion is probably a restricted tetragonal-octahedral stereochemistry of the form believed to exist in the complex[61,71] $K_2BaCu(NO_2)_6$. In both complexes, the restricted nature of the tetragonal distortion arises from the high symmetry of the crystals (cubic and tetragonal respectively). The regular trigonal-octahedral $CuN_6$, and $CuO_6$ chromophores present in the complexes $Cu(en)_3SO_4$ [49] and $Cu(ompa)_3(ClO_4)_2$ [50] also conflict with the predictions of the Jahn–Teller theorem[56]. In both of these complexes, the nuclear framework is also considered to undergo a dynamic Jahn–Teller distortion of the form XX now shown to exist[54] in Cu(hfacac)$_2$bipy (Table 1, XVII).

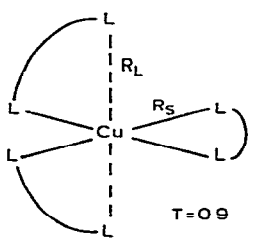


XX Cu(Chelate)$_3$X$_2$

*(ii) Pauling electroneutrality principle*

Pauling first suggested that in the formation of a dative covalent bond between a ligand and a positively-charged metal cation, the final equilibrium bond-length would be such that the charge difference between the two adjacent atoms would be no more than one electron[72]. Polarisable ligands such as halide ions would form four-coordinate species (*e.g.* $CuCl_4^{2-}$) to avoid a large negative charge-transfer to the metal by covalency, whereas less polarisable ligands, such as water, would form six-coordinate species (*e.g.* $Cu(H_2O)_6^{2+}$). In the latter, a regular octahedral stereochemistry cannot exist and the structure will distort to form a tetragonal-octahedral cation. In order to maintain the electroneutrality over the whole molecule, as the two axial bonds lengthen the equatorial bonds must shorten (see structures I and II, and the Cu–N bond-lengths in $Cu(en)_3SO_4$ [49] and $Cu(en)_2(BF_4)_2$ [28] of 2.17 and 2.025 Å, respectively). Consequently, the four equatorial ammonia ligands in $Cu(NH_3)_4(NO_2)_2$ (II) are more strongly bound than those in $Ni(NH_3)_4(NO_2)_2$ (I); this is reflected in the successive formation constants[73] of these two ions and in the Irving–Williams[74] stability series, wherein the property measured reflects the strength of the first four (equatorial) bonds.

*(iii) The concept of semi-coordination*

The arguments of the previous two sections suggest that the copper(II) ion should be dominated by a tendency to form four-coordinate square-coplanar complexes. In practice, this stereochemistry is very uncommon[3] in copper(II) complexes involving $\sigma$-bonding ligands (such as ammonia[75] or ethylenediamine[76,77]), but does occur with potentially $\pi$-bonding ligands as in $Cu(PyNO)_4(BF_4)_2$ [17] and $Cu(3\text{-Me acac})_2$ [29]. Much the preferred stereochemistry for $\sigma$-bonding ligands is a distorted tetragonal octahedron [*e.g.* $Cu(NH_3)_4(NO_2)_2$ (II) and $Cu(en)_2(BF_4)_2$ (VII)], suggesting that the bonding effects of the groups present in the axial positions cannot be ignored. The term "semi-coordination" has been introduced[27,76] to describe this situation, and the experimental justification for it has been described elsewhere[75]. This suggests that in tetragonal-octahedral copper(II) complexes involving monodentate ligands, the axial fifth and sixth ligands are weakly bonded at a definite distance (*ca.* 0.6 Å greater than the in-plane distance), and that the copper(II) ion should not be considered as spherical, but ellipsoidal (with a difference in the major and minor axes of 0.6 Å). The in-plane covalent radius of the copper(II) ion has been estimated[11] to be *ca.* 1.30 Å, and consequently its out-of-plane radius would be *ca.* 1.90 Å. This is illustrated schematically in Fig. 3. An observed bond-length would then be the sum of the covalent radii of the ligand ($r_c$) and the copper(II) ion ($r_S$ or $r_L$ as appropriate). For non-equivalent ligands, the observed bond-length will still involve the sum of the appropriate covalent radii. Using this approach, it is possible to estimate[11] the values of the

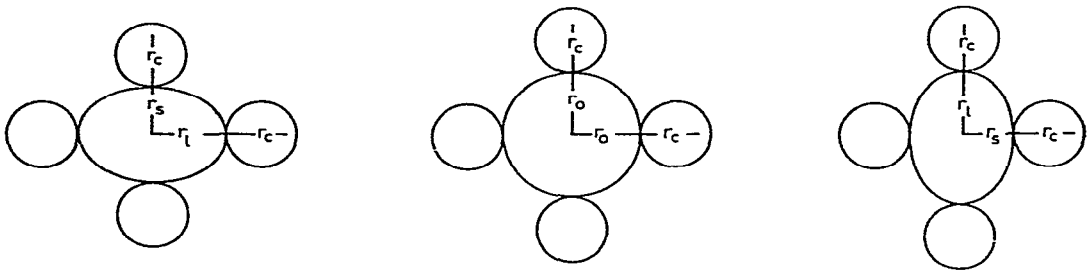


Fig 3. The copper atom and ligand atom covalent radii in octahedral and tetragonal-octahedral stereochemistries (two dimensional)

short ($R_S$) and long ($R_L$) copper–iodine bond lengths as 2 64 and 3.48 Å, respectively: these agree favourably with available observed values of 2.70 and 3.64 Å, in (Cubipy$_2$I)I (XV)[42] and Cu(imidazole)$_4$I$_2$[78], respectively. Some theoretical justification for the concept of semi-coordination has been obtained from the calculation of overlap integrals[79] for the $d_{z^2}$ and $p_z$ orbitals along the z-axes. Overlap with the $d_{z^2}$ orbital falls off to 40% of the normal equatorial value at the semi-coordinate distance. Overlap with the $p_z$ orbital actually increases up to a distance of 0.3 Å greater than the equatorial distance, and then falls off sharply.

(*iv*) *The concept of varying tetragonal distortion*

In copper(II) complexes the tetragonal distortion ($T$) may be measured by the ratio $R_S/R_L$, where $R_L$ has been corrected[11] for the presence of non-equivalent ligands The value of $T$ has been shown (Table 2) to decrease from unity for an octahedral complex, to 0.56–0.66 for a square-coplanar structure[67,80]. The range of the latter is determined by the variation of the non-bonding ligand distances of 3.0–3.5 Å in this stereochemistry[29]. Paralleling the decrease in $T$ is a decrease of the short copper–ligand distance, suggesting that the lowest values of the $R_S$ occur for a square-coplanar stereochemistry.

It might be argued that the particularly short copper–oxygen bonds[29] in these square-coplanar complexes are due to the presence of metal to ligand $\pi$-bonding, rather than to the greater tetragonal distortion. It is probable that both effects[80] are present, and the decrease of copper–oxygen bond-length, from 1.967 Å in Cu(hf acac)$_2$bipy (XVII) to 1.91 Å in Cu(3-Me acac)$_2$ (VIII), does indicate a decrease of $R_S$ with increasing tetragonal distortion, even in complexes with potentially $\pi$-bonding ligands

TABLE 2

THE VARIATION OF THE TETRAGONALITY ($T$) OF COPPER(II) COMPLEXES WITH STRUCTURE, IN-PLANE BOND LENGTH AND THE ENERGY OF THE APPROPRIATE $d$–$d$ TRANSITION

| | *Octahedral* | *Restricted tetragonal-octahedral* | *Tetragonal-octahedral* | *Square-coplanar* |
|---|---|---|---|---|
| $T$-theoretical | 1.0 | 0 9 | 0 85–0.75 | 0.66–0 56 |
| *Oxygen ligands* | | | | |
| | $Cu(ompa)_3(ClO_4)_2$ | $Cu(hfacac)_2bipy$ | $Cu(H_2O)_4(HCO_2)_2$ | $Cu(acac)_2$ 1 91 Å |
| | 2 07 Å-1 0–8 0 *kK*[a] | 1.967 Å-0.86–9 4 *kK* | 2.00 Å 0 85—9 2 *kK* | 0 6–19.2 *kK* |
| | | $Ba_2Cu(HCO_2)_64H_2O$ | | $Cu(PyNO)_4(BF_4)_2$ |
| | | 2 00 Å-0 92–8.4 *kK* | | 1 92 Å-0.575-[b] |
| *Nitrogen ligands* | | | | |
| | $K_2PbCu(NO_2)_6$ 2.11 Å | $CuH_2edtaH_2O$ 2 07 Å | | |
| | 1 0–7.02 *kK* | 0.85–8 2 *kK* | | |
| | $Cuen_3SO_4$ 2.17 Å | $Cudien_2Br_2H_2O$ 2 07 Å | $Cuen_2(BF_4)_2$ 2.03 Å | $Na_4Cu(NH_3)_4\{Cu(S_2O_3)_2\}_2 \cdot H_2O$ |
| | 1 0–8 7 *kK* | 0 86–8.8 *kK* | 0 75–18 0 *kK* | 2 00 Å-0 68–18.4 *kK* |

[a] After each complex three numbers are given, these are successively the in-plane bond length, the tetragonality $T$ and the energy of the transition from the $d_{z^2}$ to the ground stage. [b] Unknown.

*(v) The roelof π-bonding*

In all copper(II) complexes, the main contribution to bonding is of a σ-type, and with $Cu(NH_3)_4X_2$ [11] and $Cuen_2X_2$ [76,77], it is the only form of bonding in the equatorial plane. However, with these σ-bonding ligands, a strict square-coplanar stereochemistry does not occur[11,21,75], and some further capacity for bonding is required for stability. In the above complexes, this is supplied by the weak bonding of the semi-coordinating[75] anions (X), but it may also be supplied[29,30] by π-bonding, as in $Cu(3\text{-Me acac})_2$ and $Cu(salim)_2$. In these complexes, the most likely form of π-bonding is out-of-the-plane, using the copper $d_{xz}$ and $d_{yz}$ orbitals, which as they are filled, enable negative charge to be back-donated to the ligand. In this way, a square-coplanar copper(II) complex, (which has shorter in-plane copper–ligand bonds than in the tetragonal-octahedralc ase) has a mechanism for redistributing the excess negative charge, accumulated on the metal atom by the formation of four short σ-bonds, thus maintaining an internal distribution of charge consistent with Pauling's electroneutrality principle[72].

In a tetragonal-octahedral stereochemistry the redistribution required is smaller as the in-plane bonds are longer (see section C, vi), but some π-bonding could well occur via the semi-coordinated ligands and the $d_{xz}$ and $d_{yz}$ orbitals[11].

*(vi) Steric factors*

*(a) Bulk effect.*—A simple size factor may well prevent the formation of a particular stereochemistry. Thus, while the $Cuen_2X_2$ complexes involve a coplanar $CuN_4$ chromophore, the $Cubipy_2X_2$ complexes are prevented from assuming[42,51] this conformation by the steric requirements[81] of the bipyridyl 3,3'-hydrogen atoms. Consequently, the bipyridyl ligands are forced to twist out of the equatorial plane to yield a cis-conformation, as in $(Cubipy_2I)I$ (XV) and $[Cubipy_2(ONO)]NO_3$ (XVIII), or the suggested twisted conformation[82] (XXI) of $Cubipy_2(ClO_4)_2$. The latter type of twisting is also shown[39] by Cu(t-butyl salim)$_2$, ($\theta = 62°$) although[30] $Cu(salim)_2$ is strictly coplanar. The approximately tetrahedral stereochemistry[83] of $Cu(dprm)_2$ is also considered to arise from the presence of a bulky ligand which prevents a square-coplanar stereochemistry. The trigonal-bipyramidal stereochemistry[84] of $Cu(Et_4dien)BrN_3$ may result from the bulky ethyl substituents

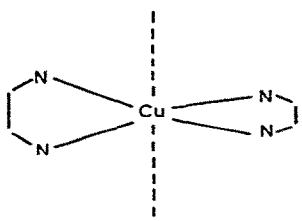


XXI $Cu(bipy)_2(ClO_4)_2$

on the diethylenetriamine ligand; the unsubstituted ligand does not give rise to this stereochemistry[85]. The trigonal-bipyramidal stereochemistry of $(Cubipy_2I)I$ may arise from the large iodide ion occupying[86] two adjacent in-plane coordinate positions of a cis-octahedral[51] stereochemistry see $[Cubipy_2(ONO)]NO_3$.

(*b*) *Blocking effect.*—The α-aminocarboxylic acids tend to form tetragonal octahedral complexes with copper(II) (*e.g.* Cu(α-alaninate)$_2 \cdot 2H_2O$)[87]. With certain substituted α-aminocarboxylates, the conformation imposed upon the ligands by coordination can result in the blocking of the axial positions, and the formation of a square-coplanar complex [*e.g.* Cu(1-aminocyclopentanecarboxylate)$_2$ [88] and Cu(*d,l*-diethyl-*N,N'*-α-alaninate)$_2$][89,31]. A similar stereochemistry has also been suggested for $Cudach_2(ClO_4)_2$ [90], in which the conformations of the methylene groups in the ligand rings effectively block the axial positions of the copper(II) ion.

(*c*) *Chelate effect.*—In axial complexes, the effect of chelation in the equatorial plane is small. Thus the in-plane bond-angle changes from 90° in $Cu(NH_3)_4X_2$ to 86° in $Cuen_2X_2$. In $Cu(dien)C_2O_4 \cdot 4H_2O$ [91], the planar tridentate diethylenetriamine ligand still involves only a total angular distortion of 25°, with the three copper–nitrogen bonds equivalent in length. The angular distortion is slightly less[52] (17°) for the in-plane dien ligand in $Cu(dien)_2Br_2 \cdot H_2O$ (X), as the terminal Cu–N bonds are slightly longer (2.10 against 2.03 Å). The out-of-plane ligand is even more distorted, due to the non-spherical symmetry of the copper(II) ion, involving a total bond-angle of 23° and a significantly longer terminal (2.40 Å), than central (2.04 Å) Cu–N bond. The difference of 0.36 Å is significantly lower than that observed in tetragonal-octahedral complexes involving monodentate ligands (*ca.* 0.6 Å), and the presence of out-of-the-plane chelation has reduced the extent of the tetragonal distortion. A similar effect has been observed in $Cu-H_2edta \cdot H_2O$ (XII)[53], $Cu(hf\ acac)_2bipy$[54], $(Cubipy_2I)I$[42] and $[Cubipy_2(ONO)]-NO_3$ [51]. In the latter complexes, the difference between the in-plane and out-of-plane Cu–N bond lengths is less than 0.15 Å. This type of restricted tetragonal distortion could occur in the trigonal complexes $Cuen_3X_2$, $Cubipy_3X_2$ and $Cuphen_3X_2$ [67].

A slightly different type of chelate effect is shown in the molecular structure[32] of $Cu(NH_3)_2(CH_3CO_2)_2$ (IX) and arises when a chelate ligand is unable to coordinate exactly along the coordinate axes. One oxygen atom of each carboxylate group coordinates in-the-plane, and the remaining oxygen occupies a position 2.77 Å from the copper(II) ion and at an angle of 40° to the z-axis. Similar stereochemistries have been observed in $Cubipy(ONO)_2$ [33] and Cu(hydrogen-*o*-phthalate)$_2 \cdot 2H_2O$ [34]. In all three molecular structures, the molecules may be described as square-coplanar, except for the presence of the offset oxygens, and the in-plane Cu–O bonds being appreciably longer than expected (see next section).

These types of chelation (out of the equatorial plane)to form a restricted

tetragonal distortion, may be considered to arise as a compromise between the desire of the copper(II) ion to distort and that of the ligand to chelate strongly. Whether or not the chelate forms a short or a long bond in the plane, depends on whether the copper(II) ion assumes the form of a prolate or oblate ellipsoid The former will result in an elongated restricted tetragonal distortion, as in $Cu(dien)_2Br_2 \cdot H_2O$ [52] and $Cu(hfacac)_2(bipy)$ [54], while the latter will result in a compressed restricted-tetragonal-distortion, as in $[Cu(bipy)_2(ONO)]NO_3$ (XVIII)[51].

*(vii) Structural factors in five-coordinate copper(II) complexes*

The discussion so far has been confined to the relationship between the idealised geometries of the tetragonal octahedron and the square-plane, both of which supplement a basic four-coordination; the former by semi-coordination, and the latter by $\pi$-bonding. This potential for further bonding above four-coordination could equally be satisfied by the formation of a five-coordinate complex. The copper(II) ion can form both trigonal-bipyramidal and square-based pyramidal complexes[26], especially the latter. The former structure frequently arises where there are particular geometric factors present. Thus, the $CuN_5$ chromophore[41] in $Cu(NH_3)_2Ag(SCN)_3$ (XIV) arises because of the trigonal packing of the $Ag(SCN)_3^{2-}$ anions. In $Cr(NH_3)_6CuCl_5$ [43], the large tri-positive cation stabilises the uncommon anion $CuCl_5^{3-}$. There are too few trigonal-bipyramidal crystal structures known to allow many generalisations, but bond-lengths are comparable to the values of $R_S$ in the tetragonal-octahedral complexes. Thus, the copper–chlorine bonds[43] in $CuCl_5^{3-}$ are in the range 2 29–2 39 Å, and compare with a mean $R_S$ value[76] of 2 31 Å in a tetragonal-octahedral complex.

Crystal-structure[2b] data for the square-based pyramidal stereochemistry is much more extensive In this, the fifth ligand is bonded at a distance of 0.2–0.6 Å greater than the in-plane ligands. In most cases, the copper(II) ion is not strictly coplanar with the equatorial ligands but is lifted *ca.* 0.2 Å towards the fifth ligand. The equatorial bonds tend to be slightly longer than those in the corresponding tetragonal-octahedral or square-coplanar complexes. In $[Cu(NH_3)_4 \cdot H_2O]SO_4$, the Cu–N bond length[45] is 2.034 Å, compared[45] with 2 005 Å in $Cu(NH_3)_4SeO_4$. The equatorial Cu–O bond-lengths in $Cu(acac)_2$ quinoline[47] are 1.95 Å, compared with 1.91 Å in $Cu(acac)_2$ [92]. In general, there is no atom within 3.0 Å in the sixth octahedral position (but see $Cu(dien)C_2O_4 \cdot 4H_2O$)[91].

Why the copper(II) ion should be so relatively stable in a square-based pyramidal stereochemistry is not clear, but the close approach of the fifth ligand must introduce considerable electrostatic asymmetry along the z-axis. This may well result in considerable asymmetry in the distribution of charge in the $d_{z^2}$ orbital, above and below the xy plane[75]. The movement of the copper(II) ion out of the plane occurs for both $\sigma$- and $\pi$-bonding equatorial ligands, but in all known crystal structures the fifth ligand has some $\pi$-bonding potential (as in water[45,46]

or quinoline[47]). The in-plane square-based pyramidal stereochemistry is believed to be present in the $Cu(NH_3)_5X_2$ complexes[93], in which the fifth ligand must be purely $\sigma$-bonded, but no crystallographic data is available.

## D. THE ELECTRONIC PROPERTIES

### (i) *The electronic properties of the complexes of the copper(II) ion*

The magnetic and ESR properties are mainly determined by the electron configuration in the ground state and only marginally by the electron configuration in the excited states The electronic spectra are primarily concerned with the energy differences between the ground state and the excited states, although a precise knowledge of the ground and excited state configurations is necessary to understand the selection rules in single-crystal polarised spectra[94]. The measurement of the ESR spectra gives the most precise information on the electronic ground state (section F); and single-crystal polarised spectra (section G) give information on the relative ordering of the excited states.

The measurement of the magnetic susceptibility of a complex can give little information, other than to indicate whether or not the copper(II) ions are magnetically dilute (section E) Before examining each of these properties in detail (sections E–G), it is worth examining, rather qualitatively, the way in which the energies of the one-electron levels are influenced by crystal-fields of various symmetries.

### (ii) *The crystal-field energy levels*

The mode of splitting of the five-fold degenerate $3d$-orbitals by crystal-fields of octahedral and tetrahedral symmetries is now well understood[5–8]. The effect of crystal-fields of even lower symmetry (as represented in the various stereochemistries of Fig. 1) is less clear[7], but the suggested orderings are shown in Figs. 4–6. Crystal-field calculations cannot give precise energies, or even detailed orderings; for example they cannot determine whether the $d_{z^2}$ orbital lies above, or below the $d_{xy}$, $d_{xz}$ and $d_{yz}$ orbitals in a square-coplanar stereochemistry. Crystal-field theory can specify which of the five $d$-orbitals has the highest energy[95] and which, therefore, will contain the odd electron (positive hole) of the $d^9$ configuration.

### (iii) *The electronic ground state in different stereochemistries*

The orbital sequences of Figs. 4–6 may be used to summarise the ground states of the various stereochemistries of Fig. 1 (Table 3). The vast majority of copper(II) complexes gives rise to orbitally non-degenerate ground states involving

a static form of distortion and a $d_{x^2-y^2}$ ground state; a substantial number of complexes have a $d_{z^2}$ ground state, and a few have a $d_{xy}$ ground state. The last group are confined to square-coplanar complexes involving chelate ligands with $\pi$-bonding potential, as in $Cu(acac)_2$ [96] and $Cu(salim)_2$ [97], and compressed tetrahedral complexes, such as Cu(t-butyl salim)$_2$ [98]. The degenerate ground-state configurations 4–6 of Table 3 are uncommon, and usually some form of dynamic Jahn–Teller[60] or pseudo-rotational[70] distortion removes the orbital degeneracy of the ground state.

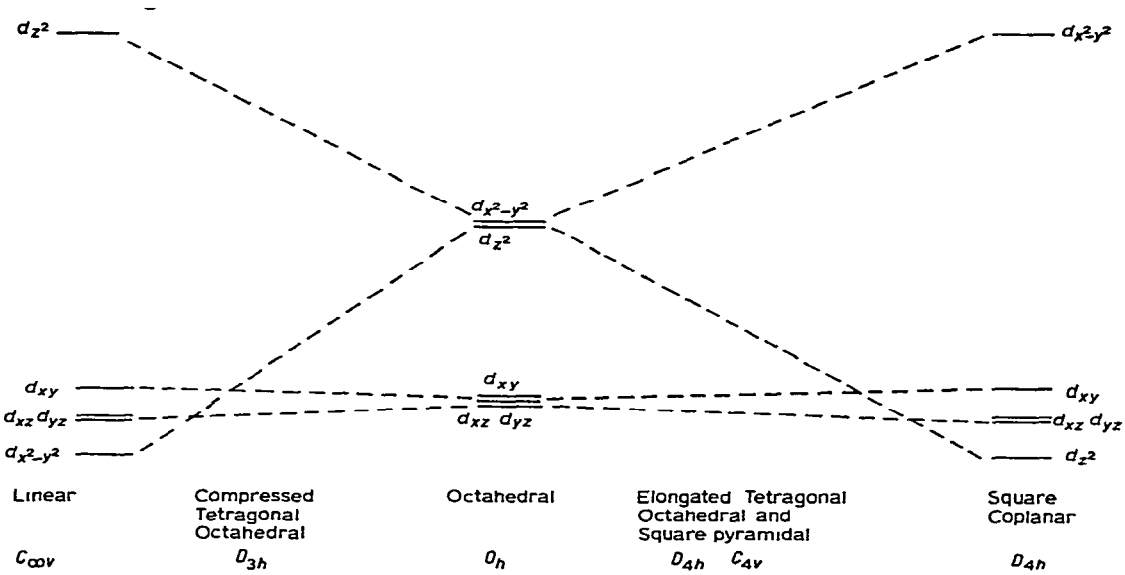


Fig 4 The splitting of the one-electron energy levels of the copper(II) ion in crystal fields of axial symmetry.

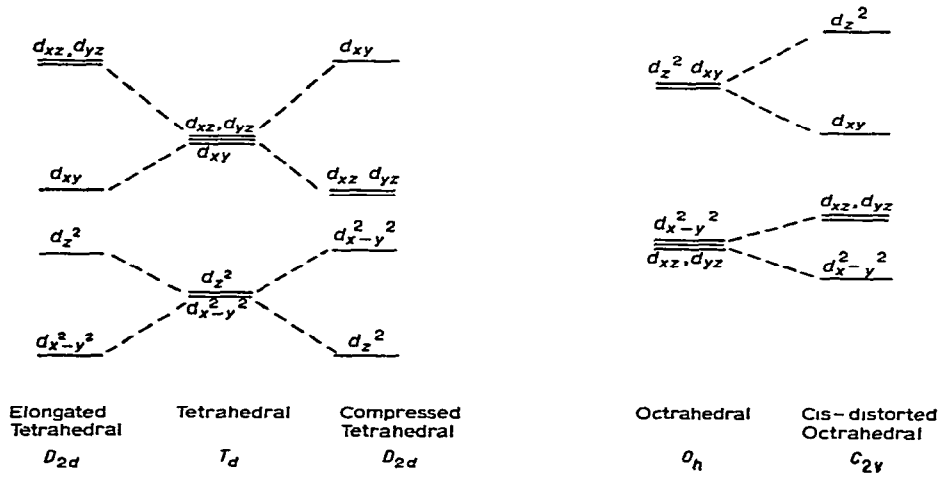


Fig. 5. The splitting of the one-electron energy levels of the copper(II) ion in crystal fields of tetrahedral and *cis*-octahedral symmetry.

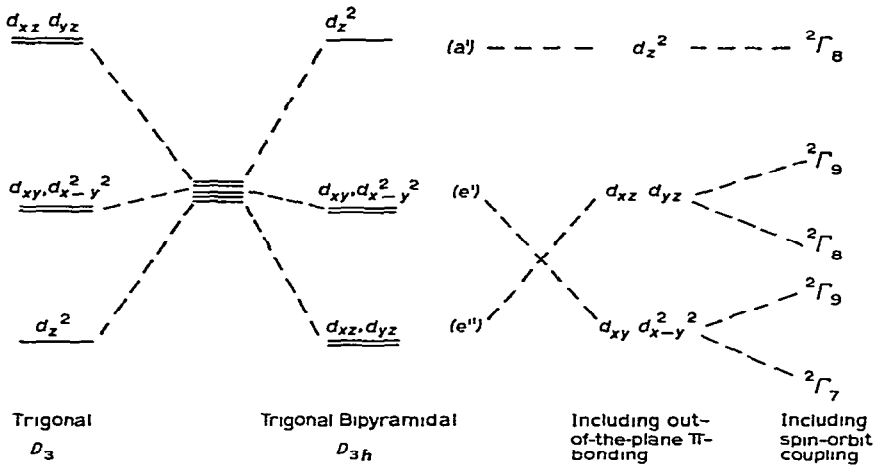


Fig. 6. The splitting of the one-electron energy levels of the copper(II) ion in crystal fields of trigonal symmetry.

TABLE 3

THE ONE-ELECTRON ORBITAL GROUND STATES FOR THE KNOWN STEREOCHEMISTRIES OF THE COPPER(II) ION, FIG 1 (for notation see section D, ii)

| | |
|---|---|
| 1 $d_{x^2-y^2}$ | Elongated tetragonal-octahedral<br>elongated rhombic-octahedral<br>square-coplanar<br>square-based pyramidal<br>(in-plane and out-of-plane) |
| 2 $d_{z^2}$ | Compressed tetragonal-octahedral<br>compressed rhombic-octahedral<br>linear<br>trigonal-bipyramidal<br>cis-distorted octahedral |
| 3 $d_{xy}$ | Compressed tetrahedral<br>square-coplanar-$Cu(acac)_2$-type |
| 4[a] $d^2_{z^2}$, $d^1_{x^2-y^2}$ or $d^1_{z^2}$, $d^2_{x^2-y^2}$ | Octahedral |
| 5[a] $d_{xz}^2$, $d_{yz}^1$ or $d_{xz}^1$, $d_{yz}^2$ | Trigonal<br>elongated tetrahedral |
| 6[a] $d_{xy}^2$, $d_{xz}^2$, $d_{yz}^1$ *etc.* | Tetrahedral |

[a] These configurations are orbitally degenerate; in 5 and 6 this orbital degeneracy is removed by spin-orbit coupling, but is not removed by this mechanism in 4 (see section C, i).

### (iv) *Electronic excited states in different stereochemistries*

The ordering of the one-electron orbital excited states, as determined by crystal-field calculations, must be considered as extremely approximate, if only because the point-charge model usually ignores the effect of $\sigma$-bonding, $\pi$-bonding,

semi-coordination and the effects of bond-angle and bond-length distortions. The only method of determining the energies of these levels with any accuracy is by using polarised single-crystal techniques, and even then the results may not be completely unambiguous (section G). An attempt to calculate[79] the energies of the one-electron orbital levels using the angular overlap model has been rather more successful, but only results in a best-fit of the single-crystal polarised spectra.

## E. MAGNETIC SUSCEPTIBILITY DATA

The magnetic properties of the copper(II) ion are primarily determined by the effective magnetic dilution in the solid state.

### (i) *Magnetically dilute complexes*

When the individual copper(II) ions in a complex are physically well separated from each other (>5 Å), then the effective magnetic moment[99] may be given by the spin-only value, ($\mu_{s\,o}$), of 1 73 B.M. In practice, the experimental values at room temperature lie in the range 1.8–2 0 B.M.; some typical values are given in Table 4. These lie appreciably above the spin-only value, due to mixing-in of

TABLE 4

SOME REPRESENTATIVE ROOM-TEMPERATURE MAGNETIC MOMENTS (B M ) FOR COPPER(II) COMPLEXES[99]

| *Compound* | $\mu_{eff}$ | *Compound* | $\mu_{eff}$ |
|---|---|---|---|
| $Na_4Cu(NH_3)_4\{Cu(S_2O_3)_2\}_2NH_3$ | 1 90 | $Cs_2CuCl_4$ | 1 92 |
| $Cu(NH_3)_4(SCN)_2$ | 1 81 | $CaCu(CH_3CO_2)_4\ 6H_2O$ | 1 94 |
| $[Cu(NH_3)_4H_2O]SO_4$ | 1.87 | Cu(t-butyl-salim)$_2$ | 1 83 |
| $Cu(NH_3)_2Ag(SCN)_3$ | 1 83 | Cu en$_2$(BF$_4$)$_2$ | 1 88 |
| Cu acac$_2$ | 1 91 | [Cu bipy$_2$(ONO)]NO$_3$ | 1 89 |
| $CuCl_2\ 2H_2O$ | 1 87 | | |

some orbital angular momentum from excited states via spin–orbit coupling The extent of mixing-in is given by the expression[99]: $\mu_{eff} = (1-4r^2\lambda/\Delta E)\mu_{s\,o}$ where $\Delta E$ is the energy separation of the ground state from the excited state being mixed in and $r$ is the combined orbital and spin–orbit reduction parameter (see section H). As in all known copper(II) complexes, the "effective" electronic ground state is orbitally non-degenerate (see D, iii), there is no inherent orbital contribution to the magnetic moment of the ground state, and hence no stereochemical information is forthcoming from this source, unlike other first-row divalent transition metal complexes[99]. Even the use of the more sophisticated technique of single-crystal magnetic anisotropy is only a little more informative[98]. In a series of complexes varying from distorted tetrahedral, [$Cs_2CuCl_4$ (XIII)], to square-coplanar [Cu(enacac)$_2$], the magnetic anisotropies were found to be only slightly sensitive

to stereochemistry, but more sensitive to the degree of covalency present (although indirectly the covalency is also a function of stereochemistry). The anisotropy in the magnetic susceptibilities is related to the anisotropy in the ESR $g$-factors by the expression $X_i = N^2 g_i^2 S(S+1)/3RT$, in which $i = x$, $y$ or $z$ directions. As the $g$-factors can generally be more readily measured than the $X_i$'s, the ESR technique is preferred (section F).

*(ii) Non-magnetically dilute complexes*

When the individual copper(II) ions in a complex are not well separated from each other, then interactions can occur. In copper(II) complexes, these are antiferromagnetic in form and result in a reduction of the observed magnetic moment below the spin-only value. Thus, the observed magnetic moment[100] of 1.4 B.M for $Cu_2(CH_3CO_2)_4 \cdot 2H_2O$ is related to the close proximity of the two copper(II) ions[101] (2.64 Å). Such interactions are typical of complexes involving bridging ligands, as found in polynuclear structures. These types of complexes involve very complicated electronic properties, which are not understood and fall outside the range of this review.

## F. ELECTRON SPIN RESONANCE SPECTRA

*(i) Theoretical principles of the E.S.R. of copper(II) complexes*[102]

In an applied magnetic field $H$, the magnetic moment $\mu_S = -2\,0023\ \beta_e S$ ($\beta_e$ = the electronic Bohr magneton), due to the electron spin angular momentum ($S$), will orient itself to lie parallel or anti-parallel to the field. The energy difference between these two states, found from the Hamiltonian $\mathcal{H} = -\mu_S H$, is $\Delta E = 2.0023\ \beta_e H_z$ for a single electron ($m_S = \pm\frac{1}{2}$). The direction of the field has been taken as the axis of quantisation (z)

For the $d^9$ configuration of copper(II), there is also an interaction between $H$ and the magnetic moment $\mu_L = -\beta_e L$ due to the orbital angular momentum ($L$) of the electrons. The total interaction, assuming Russell–Saunders coupling, is given by the Hamiltonian:

$$\mathcal{H} = -H \cdot (\mu_L + \mu_S) = \beta_e H \cdot (L + 2\,0023S)$$

The orbital degeneracy is removed by crystal-fields, but the spin-degeneracy remains even after the action of spin–orbit coupling, and is lost only in a magnetic field. The Zeeman splitting of the ground state can therefore, in principle, be observed in an electron spin resonance experiment. The orbital angular momentum is "quenched" for the ground states of most copper(II) complexes, but spin–orbit coupling mixes-in some contributions from excited states, the extent being ex-

pressed by the Landé multiplet splitting factor "$g$" in the energy equation.

$$h\nu = \Delta E = g\beta_e H \tag{1}$$

(*ii*) *The spin-Hamiltonian*

This contains those parts of the total Hamiltonian which are relevant for the purposes of ESR; *i.e.* the spin-vectors only. For copper(II) complexes, it is

$$\mathcal{H}_S = g\beta_e S \cdot H + \mathrm{A}\, S \cdot I \tag{2}$$

for crystal-fields having cubic symmetry (isotropic). The term in $g$ contains the spin–orbit ($\lambda L.S$) and electronic Zeeman interactions. The second term describes the interaction between the electron-spin and nuclear spin, which splits the ESR signal into hyperfine components. For copper(II) compounds, this structure is only resolved in dilute liquid or solid solutions[103], due to the broadness of the signals from undiluted crystals Such crystals are the subject of this review, and hyperfine structure is only important for the present purposes in that it contributes to the line-shape[104]. For crystal-fields of (z-) axial symmetry and non-axial symmetry, equation (2) becomes (respectively)

$$\mathcal{H}_S = g_{\|}\beta_e H_z S_z + g_{\perp}\beta_e (H_x S_x + H_y S_y) \tag{3}$$

and

$$\mathcal{H}_S = \beta_e (g_x H_x S_x + g_y H_y S_y + g_z H_z S_z) \tag{4}$$

Here, $g_x$, $g_y$ and $g_z$ are the principal components of the $g$ tensor along three orthogonal axes.

(*iii*) *The calculation of g-factors*

An evaluation of the effect of mixing excited states into the ground state via spin–orbit coupling, may be described by the series of matrix elements,

$$H_{L',S'} \equiv \int \psi^*_{L',S}\, \mathcal{H} \psi_{L,S}\, \mathrm{d}\tau = \langle M_{L'}, M_{S'} \mid \lambda L \cdot S \mid M_L, M_S \rangle$$

in the secular equation $| H_{L',S'} - E | = 0$. Here, $E$ is measured relative to the energy before spin–orbit coupling, $\lambda$ is the spin–orbit coupling constant, the $\psi$'s are wave functions, the $M$'s are quantum numbers for the many-electron system ($M_L$ corresponds to the component of $L$ along $z$ and $M_S$ to the component of $S$), $L$ and $S$ refer to the ground state and $L'$ and $S'$ to a series of excited states. These matrix elements are evaluated[105] using the expression

$$\begin{aligned}\langle M_{L'}, M_{S'} \mid \lambda L \cdot S \mid M_L, M_S \rangle = {} & \tfrac{1}{2}\lambda \langle M_{L'} \mid L_+ \mid M_L \rangle \langle M_{S'} \mid S_- \mid M_S \rangle \\ & + \tfrac{1}{2}\lambda \langle M_{L'} \mid L_- \mid M_L \rangle \langle M_{S'} \mid S_+ \mid M_S \rangle \\ & + \lambda \langle M_{L'} \mid L_z \mid M_L \rangle \langle M_{S'} \mid S_z \mid M_S \rangle\end{aligned}$$

and the standard[105] expressions for the non-zero elements:

$$\begin{aligned}
\langle M_{L+1} \mid L_+ \mid M_L \rangle &= [L(L+1)-M_L(M_L+1)]^{\frac{1}{2}} \\
\langle M_{L-1} \mid L_- \mid M_L \rangle &= [L(L+1)-M_L(M_L-1)]^{\frac{1}{2}} \\
\langle M_L \mid L_z \mid M_L \rangle &= M_L \\
\langle M_{S+1} \mid S_+ \mid M_S \rangle &= [S(S+1)-M_S(M_S+1)]^{\frac{1}{2}} \\
\langle M_{S-1} \mid S_- \mid M_S \rangle &= [S(S+1)-M_S(M_S-1)]^{\frac{1}{2}} \\
\langle M_S \mid S_z \mid M_S \rangle &= M_S
\end{aligned} \tag{5}$$

Here $L$ and $S$ are operators and $\lambda L \cdot S$ has been expanded

$$\lambda L \cdot S = \lambda(L_x \cdot S_x + L_y \cdot S_y + L_z \cdot S_z) = \tfrac{1}{2}\lambda(L_+ \cdot S_- + L_- \cdot S_+) + \lambda L_z \cdot S_z$$

where

$$L_\pm = L_x \pm iL_y \qquad \text{and} \qquad S_\pm = S_x \pm iS_y \tag{6}$$

For copper(II), $L = 2$ and $S = \frac{1}{2}$, giving $M_L = \pm 2, \pm 1$ or 0 and $M_S = \pm\frac{1}{2}$.

As a result of the interactions described by these matrix elements, the ground state $\mid M_L, M_S\rangle$ becomes:

$$\psi_{M_S} = \mid M_L, M_S\rangle + \sum_{M_{L'}} \sum_{M_{S'}} \frac{\mid M_{L'}, M_{S'}\rangle \langle M_{L'}, M_{S'} \mid \lambda L \cdot S \mid M_L, M_S\rangle}{-E_{L',S}}$$

There are two such states $\psi_{\frac{1}{2}}$ and $\psi_{-\frac{1}{2}}$ according as $M_S = \pm\frac{1}{2}$, and they are degenerate in the absence of a magnetic field. The application of a magnetic field is next considered along the z-, x- and y-axes, successively. The relevant Hamiltonian term corresponding to the magnetic field being along the z-axis is $\mathscr{H}_z = \beta_e H_z (L_z + 2.0023 S_z)$ and the four matrix elements $H_\pm = \langle \psi_{\pm\frac{1}{2}} \mid \mathscr{H}_z \mid \psi_{\pm\frac{1}{2}} \rangle$ can be calculated using Eqns. (5). The secular equation $\mid H_\pm - E \mid = 0$ is then solved for the energies, relative to the original energy (without the field). This gives two solutions $E_1$ and $E_2$, and hence resonance is observed at $h\nu = \Delta E = E_2 - E_1$. For $H_x$ and $H_y$, the calculation is similar, except that equations (6) must also be used.

This process has been illustrated in various references[102,105], and in all cases (except when the ground-state orbital degeneracy is removed by spin–orbit coupling rather than by low symmetry crystal-fields) the results are identical to those obtained from the equations of McGarvey[102]

$$g_j = 2.0023 + 2\lambda \sum_n \frac{\langle 0 \mid L_j \mid n\rangle \langle n \mid L_j \mid 0\rangle}{E_0 - E_n} \tag{7}$$

where $j$ is any of the $x$, $y$ or $z$ coordinates, "0" refers to the ground state and $n$ to an excited state. The matrix elements are easily evaluated using Table 5 to obtain the wavefunctions resulting[102] from the operation of $L_j$, and the knowledge that $\langle \psi_p \mid \psi_q \rangle = \delta_{pq}$. Equation (7) will now be applied to copper(II) systems of various symmetries.

Firstly, it is necessary to recognise certain similarities between the behaviour of the *d*-orbitals in different point groups. For a given ground state (D, iii), the calculation of $g$ will depend on which excited states are coupled to it through spin–orbit interactions, and therefore on any degeneracies or symmetry relationships within the excited states. An example will illustrate the importance of such relationships. Table 6 shows how the *d*-orbitals transform in the $D_{2h}$, $D_2$ and $C_{2v}$ point groups[94]. Thus, if the ground state is $d_{x^2-y^2}$ (a combination of $M_L = \pm 2$ wavefunctions) it will interact in each point group with $d_{z^2}$ ($M_L = 0$) which has the same symmetry. For all three point groups, the interaction results in a new ground state[106]

$$\psi_1 = \cos\alpha\, d_{x^2-y^2} - \sin\alpha\, d_{z^2} \tag{8}$$

while the $d_{z^2}$ excited state becomes

$$\psi_2 = \sin\alpha\, d_{x^2-y^2} - \cos\alpha\, d_{z^2} \tag{9}$$

where $\alpha$ is an angle describing the size of the non-axial component of the crystal-field, such that $\sin\alpha$ and $\cos\alpha$ are normalised mixing coefficients. In terms of orbital angular momentum, these states are rewritten

$$\psi_1 = \frac{\cos\alpha}{\sqrt{2}}(|2\rangle + |-2\rangle) + \sin\alpha\,|0\rangle$$

$$\psi_2 = \frac{\sin\alpha}{\sqrt{2}}(|2\rangle + |-2\rangle) - \cos\alpha\,|0\rangle$$

The three point groups are also similar in permitting no other mixing via symmetry. The other *d*-orbitals therefore remain expressed as

$$\psi_3 = d_{xy} = \frac{-i}{\sqrt{2}}(|2\rangle - |-2\rangle)$$

$$\psi_4 = d_{xz} = \frac{-1}{\sqrt{2}}(|1\rangle - |-1\rangle)$$

$$\psi_5 = d_{yz} = \frac{i}{\sqrt{2}}(|1\rangle + |-1\rangle)$$

The matrix elements (5) then show that, in all three point groups, $L_z$ mixes $\psi_1$ with $\psi_2$ and $\psi_3$ while $L_x$ and $L_y$ mix $\psi_1$ with $\psi_4$ and $\psi_5$, giving* from equation (7).

$$\begin{aligned} g_z &= 2 - 8\lambda\cos^2\alpha / E(\psi_3 \rightarrow \psi_1) \\ g_x &= 2 - 2\lambda(\cos\alpha + \sqrt{3}\sin\alpha)^2 / E(\psi_5 \rightarrow \psi_1) \\ g_y &= 2 - 2\lambda(\cos\alpha - \sqrt{3}\sin\alpha)^2 / E(\psi_4 \rightarrow \psi_1) \end{aligned} \tag{10}$$

where $E$ is the indicated electronic energy difference.

* In using Eqn. (7), it must be remembered that the bra $\langle M_L, M_S|$ is the complex conjugate of the ket $|M_L, M_S\rangle$ and that this affects the sign of i in the expressions for $\psi_3$ and $\psi_5$.

TABLE 5

FUNCTIONS RESULTING FROM THE OPERATION OF $\hat{L}_x$, $\hat{L}_y$ AND $\hat{L}_z$ ON THE $d$-ORBITALS[102]

| *Orbital* | $\hat{L}_x$ | $\hat{L}_y$ | $\hat{L}_z$ |
|---|---|---|---|
| $d_{z^2}$ | $-1\sqrt{3}d_{yz}$ | $i\sqrt{3}d_{xz}$ | 0 |
| $d_{x^2-y^2}$ | $-1d_{yz}$ | $-id_{xz}$ | $2id_{xy}$ |
| $d_{xy}$ | $1d_{xz}$ | $-1d_{yz}$ | $-2id_{x^2-y^2}$ |
| $d_{xz}$ | $-1d_{xy}$ | $-i\sqrt{3}d_{z^2}$ $+id_{x^2-y^2}$ | $id_{yz}$ |
| $d_{yz}$ | $id_{x^2-y^2}$ $+1\sqrt{3}d_{z^2}$ | $1d_{xy}$ | $-id_{xz}$ |

TABLE 6

REPRESENTATIONS FOR THE $d$-ORBITALS IN SEVERAL POINT-GROUPS

| *d-Orbital* | *Representation in point group* | | |
|---|---|---|---|
| | $D_{2h}$ | $D_2$ | $C_{2v}$ |
| $d_{z^2}$, $d_{x^2-y^2}$ | $A_g$ | $A$ | $A_1$ |
| $d_{xy}$ | $B_{1g}$ | $B_1$ | $A_2$ |
| $d_{xz}$ | $B_{2g}$ | $B_2$ | $B_1$ |
| $d_{yz}$ | $B_{3g}$ | $B_3$ | $B_2$ |

TABLE 7

POINT-GROUPS EQUIVALENT FOR THE MIXING OF $d$-ORBITALS

| *Key number* | *Equivalent point-groups* |
|---|---|
| 1 | $C_1$, $C_i$ |
| 2 | $C_s$, $C_2$, $C_{2h}$ |
| 3 | $D_{2h}$, $D_2$, $C_{2v}$ |
| 4 | $C_4$, $C_{4h}$, $S_4$ |
| 5 | $D_4$, $D_{4h}$, $C_{4v}$, $D_{2d}$ |
| 6 | $C_{\infty v}$, $D_{\infty h}$ |
| 7 | $C_3$, $D_3$, $C_{3v}$ |
| 8 | $O_h$, $T_d$, $O$, $T$, $T_h$ |
| 9 | $C_5$, $C_6$, $C_7$, $C_8$, $D_5$, $D_6$, $C_{5v}$ $C_{6v}$, $C_{3h}$, $C_{5h}$, $C_{6h}$, $D_{3h}$, $D_{5h}$ $D_{6h}$, $D_{3d}$, $D_{4d}$, $D_{5d}$, $D_{6d}$, $S_6$, $S_8$ |
| 10 | $I_h$, $I$ |

It has been shown here that the expressions for the $g$-values are the same for the $D_{2h}$, $D_2$ and $C_{2v}$ groups if the ground state is identical. This is a result of the way the $d$-orbitals are grouped by symmetry, and Table 7 shows the other point groups which are equivalent to this extent.

Using these similarities, and Eqns. (5) and (7), the $g$-values for most ground-states and most point-groups have been calculated for the copper(II) ion in non-degenerate ground states; the results are given in Table 8. It should be noted that in low symmetry point-groups a further mixing parameter ($\beta$) is necessary.

TABLE 8

THE EXPRESSIONS FOR THE $g$-FACTORS OF COPPER(II) IONS IN VARIOUS ENVIRONMENTS[a]

| *Ground State* | *Point Group*[b] | $-(g_z-2)$ | $-(g_x-2)$ | $-(g_y-2)$ |
|---|---|---|---|---|
| $d_{z^2}$ | 4, 5, 6 | | | |
| (a) | 7, 9 | 0 | $6\lambda/E_{a(d,e)}$ | $6\lambda/E_{a(d\,e)}$ |
| | 3 | $8\lambda \sin^2\alpha/E_{ac}$ | $2\lambda(\sin\alpha+\sqrt{3}\cos\alpha)^2/E_{ae}$ | $2\lambda(\sin\alpha-\sqrt{3}\cos\alpha)^2/E_{ad}$ |
| | 2 | $8\lambda \sin^2\alpha/E_{ac}$ | $2\lambda(\sin\alpha+\sqrt{3}\cos\alpha)^2\cos^2\beta/E_{ae}$ | $2\lambda(\sin\alpha-\sqrt{3}\cos\alpha)^2\cos^2\beta/E_{ad}$ |
| | 8 | $c$ | | |
| $d_{x^2-y^2}$ | 4, 5 | $8\lambda/E_{bc}$ | $2\lambda/E_{b(d,e)}$ | $2\lambda/E_{b(d,e)}$ |
| (b) | 3 | $8\lambda \cos^2\alpha/E_{bc}$ | $2\lambda(\cos\alpha+\sqrt{3}\sin\alpha)^2/E_{be}$ | $2\lambda(\cos\alpha-\sqrt{3}\sin\alpha)^2/E_{bd}$ |
| | 2 | $8\lambda \cos^2\alpha/E_{bc}$ | $2\lambda(\cos\alpha+\sqrt{3}\sin\alpha)^2\cos^2\beta/E_{be}$ | $2\lambda(\cos\alpha-\sqrt{3}\sin\alpha)^2\cos^2\beta/E_{bd}$ |
| | 6, 9 | $-4$ | 2 | 2 |
| | 7[c] | $-4\cos^2\alpha$ | $2\cos^2\alpha$ | $2\cos^2\alpha$ |
| | 8 | $c$ | | |
| $d_{xy}$ | 3, 5 | $8\lambda/E_{cb}$ | $2\lambda/E_{cd}$ | $2\lambda/E_{ce}$ |
| (c) | 4 | $8\lambda/E_{cb}$ | $2\lambda/E_{c(d,e)}$ | $2\lambda/E_{c(d\,e)}$ |
| | 2 | $8\lambda(\sin^2\alpha/E_{ca}+\cos^2\alpha\cos^2\beta/E_{cb})$ | $2\lambda\cos^2\beta/E_{cd}$ | $2\lambda\cos^2\beta/E_{ce}$ |
| | 6, 9 | $-4$ | 2 | 2 |
| | 7[c] | $-4\cos^2\alpha$ | $2\cos^2\alpha$ | $2\cos^2\alpha$ |
| | 8 | 0 | 0 | 0 |
| $d_{xz}$ | 3 | $2\lambda/E_{de}$ | $2\lambda/E_{ac}$ | $2\lambda(1/E_{db}+3/E_{da})$ |
| (d) | 2 | $2\lambda/E_{de}$ | $2\lambda\cos^2\alpha/E_{dc}$ | $2\lambda\cos^2\alpha(1/E_{db}+3/E_{da})$ |
| | 4, 5 | $-2$ | $2-2\lambda(1/E_{dc}-1/E_{db})$ | $2-2\lambda(1/E_{dc}-1/E_{db})$ |
| | 6, 9 | $-2$ | 2 | 2 |
| | 7[c] | $-2\cos^2\alpha$ | $2\cos^2\alpha$ | $2\cos^2\alpha$ |
| | 8 | 0 | 0 | 0 |
| $d_{yz}$ | | $d$ | | |
| (e) | | | | |

*Notes*

(a) Terms in $\lambda^2/E^2$ have been ignored, as have those in $\sin^2\beta$ (assuming that $\beta$ is small) The z-axis refers to the principal symmetry axis States $d_{z^2}$, $d_{x^2-y^2}$, $d_{xy}$, $d_{xz}$ and $d_{yz}$ are respectively referred to as *a*, *b*, *c*, *d* and *e* in the energy subscripts (In the case of mixtures of states, the reference is to the state making the greatest contribution when $\alpha$ and $\beta$ are small)

(b) Point-group 1 has been excluded due to extreme complications Point-group 10 will not occur, since a distortion is necessary to remove the degeneracy not lifted by spin–orbit coupling See Table 7 for key numbers.

(c) Ground state degeneracy is removed by distortion to satisfy the Jahn–Teller theorem, the resulting point-group is of lower symmetry

(d) Interchange x- and y-axes and treat as a $d_{xz}$ ground state

(e) See also ref. 107.

### (iv) *The practical value of the ESR spectra of copper(II) complexes*

The ESR spectra of copper(II) complexes may be measured in two ways: as polycrystalline powders, or as single crystals[102]. The former technique is the most rapid experimentally but only yields approximate[108–115] $g$-values (Appendix I), and the results may be subject to misinterpretation; the latter[116–118] not

only yields the most accurate $g$-values, but also yields their direction cosines relative to a given crystal face (Appendices II–IV). Both techniques determine the crystal $g$-values, and will only yield the local molecular $g$-values[119,120] (Appendix V) if the crystal structure is known.

The factors which determine the type of ESR spectrum observed are:

(*a*) the nature of the electronic ground state

(*b*) the symmetry of the effective ligand-field about the copper(II) ion

(*c*) the mutual orientations of the local molecular axes of the separate copper(II) chromophores in the unit cell.

Points (*a*) and (*b*) have been dealt with in section D; point (*c*) determines the amount of exchange coupling present[121], which is the major factor in reducing the amount of stereochemical information available from ESR spectra.

(*a*) *Powder ESR data.*—Fig. 7 shows some typical polycrystalline ESR spectral line-shapes, with the approximate $g$-values[109] indicated in terms of the cor-

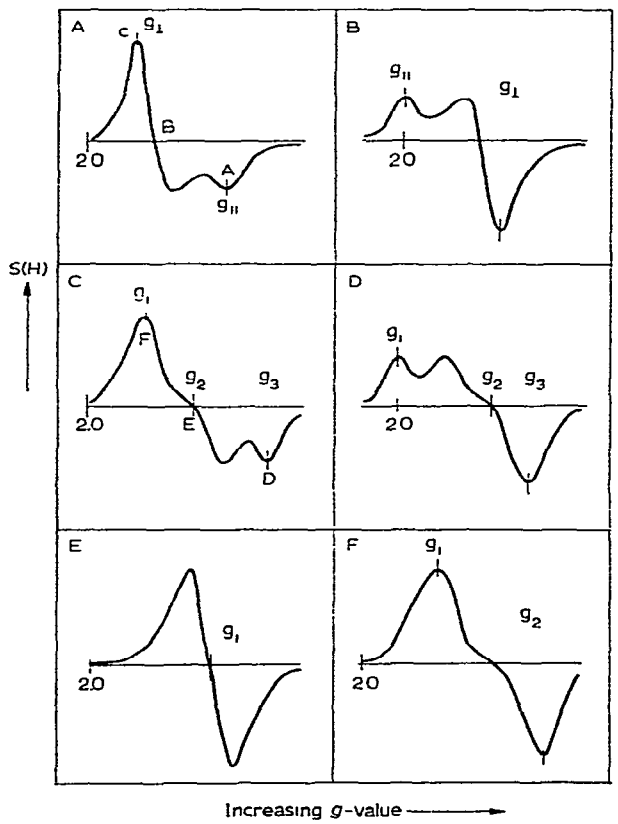


Fig. 7 The different types of ESR spectra obtained from polycrystalline samples of copper(II) complexes (1st derivative absorption curves)

responding magnetic field (see Appendix I for theory). The spectra may be considered in three general classes:

*Isotropic Spectra.* Such a spectrum (Fig. 7E) would suggest the presence of a copper(II) ion in:

1. a regular static octahedral or tetrahedral stereochemistry (neither of which occurs in practice);
2. a regular octahedral stereochemistry undergoing a dynamic[60] or pseudo-rotational[70] type of Jahn–Teller distortion. This is believed to occur in $K_2PbCu(NO_2)_6$ (III)[61,63], and in the tris-chelate complexes $Cu(en)_3SO_4$ [67] and $Cu(ompa)_3(ClO_4)_2$ [64,65];
3. a $Cu(L)_x$ chromophore of lower symmetry than octahedral, undergoing free rotation. This is believed to occur in the cubic hexaammine[62] and pentaammine[93] complexes of copper(II), in both of which the $Cu(NH_3)_5^{2+}$ cation is considered to be present;
4. a complex containing grossly misaligned "tetragonal" axes, as in $Cu\ dien_2(NO_3)_2$ (XI)[122]. This situation is probably the most common reason for the observation of an isotropic ESR spectrum.

*Axial spectra.* Two types of axial spectra are observed, depending on the value of the lowest $g$-factor (Fig 7A and B)[75]. (A) Lowest $g > 2.04$—such a spectrum can be observed for a copper(II) ion in:

1. axial symmetry with all the principal axes aligned parallel, and would be consistent with elongated tetragonal-octahedral, square-coplanar or square-based pyramidal stereochemistries, as occur in $Cu(NH_3)_4(SCN)_2$ [11], $Na_4Cu(NH_3)_4\{Cu(S_2O_3)_2\}_2\cdot H_2O$ (V)[21] and $Cu(1,3\text{-pn})_2SO_4H_2O$ (XVI)[46], respectively. In these axial spectra, the $g$-values are related by the expression[76] $G = g_{\|}-2/g_{\perp}-2 \approx 4.0$ (see section H, i, b) If $G > 4.0$, then the local tetragonal axes are aligned parallel or only slightly misaligned; if $G < 4.0$, significant exchange coupling[121] is present and the misalignment is appreciable (assuming $r_{\perp} \approx r_{\|}$ and that the energies of the electronic transitions involved are comparable),
2. rhombic symmetry with slight misalignment of the "tetragonal" axes Thus, $Cu(NH_3)_2(NO_3)_2$ [123] has a two $g$-value ESR spectrum, with $g_{\perp} = 2\,068$ and $g_{\|} = 2.231$;
3. rhombic symmetry, with the "tetragonal" axes aligned, but in which the in-plane rhombic component is small and the powder technique is insufficiently sensitive to resolve the two planar components. $Cu(NH_3)_4(CuI_2)_2$ has a two $g$-value powder ESR spectrum[11] ($g_{\perp} = 2.054$, $g_{\|} = 2\,219$ and $G = 4.21$), but gives a three $g$-value single-crystal ESR spectrum ($g_1 = 2\,054$, $g_2 = 2.058$, and $g_3 = 2\,223$);
4. compressed tetragonal or trigonal-bipyramidal molecules occupying two non-equivalent sites, with the principal axes inclined at 90°; this situation has not been observed.

(B) lowest $g < 2.03$— such spectra can be observed for a copper(II) ion in:

1. axial symmetry with all the principal axes aligned parallel, and would be consistent with compressed tetragonal-octahedral or trigonal-bipyramidal stereochemistries as in $Ba_2CuF_6$ [36] and $Cu(NH_3)_2Ag(SCN)_3$ [41] (XIV) The latter[86,124] has $g_{\|} = 2\,004$ and $g_{\perp} = 2.207$; the value of $G$ has no significance in these compressed stereochemistries;
2. compressed rhombic symmetry with slight misalignment of the "tetragonal" axes;
3. compressed rhombic symmetry with the "tetragonal" axes aligned parallel, but in which the rhombic component is so small that it is not resolved by the powder technique

*Rhombic spectra.* Two types of spectra may be observed, depending upon the value of the lowest $g$-factor. (Fig. 7, C and D.)

(C) Lowest $g > 2\,04$—such a spectrum can be observed for a copper(II) ion in:

1. elongated rhombic symmetry with all the axes aligned parallel and would be consistent with elongated rhombic-octahedral, rhombic square-coplanar or distorted square-based pyramidal stereochemistries, as in $Ba_2Cu(HCO_2)_6 \cdot 4H_2O$ (ref. 24), Cu(3-Me acac)$_2$[29] and $[Cu(1,3pn)_2 \cdot H_2O]SO_4$ [46], respectively;
2. elongated axial symmetry with slight misalignment of the principal axes. Thus, the axial environments of the $CuN_4$ chromophores in $[Cu(NH_3)_4H_2O]SO_4$ [45] are misaligned by 61° and give rise to a three $g$-value spectrum[11] ($g_1 = 2.047$; $g_2 = 2.126$ and $g_3 = 2.172$).

(D) Lowest $g < 2\,03$—such a spectrum can be observed for a copper(II) ion in:

1. compressed rhombic symmetry with all of the axes aligned parallel, and would be consistent with compressed rhombic-octahedral, cis-distorted octahedral or distorted trigonal-bipyramidal stereochemistries as in $(NH_4)_2Cu(NH_3)_2(CrO_4)_2$ [126], $[Cu(bipy)_2(ONO)]NO_3$ [51] and $[Cu(bipy)_2I]I$ [42] respectively;
2 compressed axial or rhombic symmetry with slight misalignment of the axes, as in Cu(methoxyacetate)$_2$ $2H_2O$ [38].

The spectrum of Fig. 7F is uninformative, except to indicate the presence of exchange coupling If $g_1$ lies close to 2.00 then a $d_{z^2}$ ground state is indicated

### (ii) *Single-crystal ESR data*

Not only do the single-crystal ESR spectra yield more accurate crystal $g$-values[116–118] than the powder spectra, they also yield the direction cosines of the principal axes of the $g$-tensor with respect to a given crystal face. Equally important, the directions and magnitudes of the crystal $g$-values can be used to interpret polarised single-crystal electronic spectra[75] of copper(II) complexes of known, and sometimes of unknown, crystal structure.

G. ELECTRONIC SPECTRA

The electronic absorption spectra of copper(II) complexes may be measured in solution, or in the solid state by diffuse reflectance and by single-crystal measurements[75]. All allow the measurement of the energies of the component states, although to varying accuracy. The solution spectra readily yield accurate extinction coefficients and the single-crystal spectra yield polarisation data, which under favourable circumstances allow absolute assignment of the spectral bands to the energy levels. The spectra, in favourable circumstances, may also yield data[127] on (1) spin–orbit coupling, (2) the mechanism of the excitation process, and (3), the coupling of the nuclear and electronic motions (vibronic coupling). Electronic spectra may be conveniently measured in the range 4.0–30.0 *kK* and over this range, polarised spectra may be obtained using nicol prisms, cemented by an infrared-transparent adhesive. Four types of transitions may be observed in this range[128,127]:

1. pure $d \rightarrow d$ transitions
2. charge-transfer transitions
3. internal ligand transitions
4. combination and overtone vibrations of the ligands, in the near infrared region.

In copper(II) complexes, (1) and (4) tend to occur below 20 *kK*, (2) and (3) above 20 *kK*. Spectra of type (4) tend to be sharp, relative to *d–d* spectra, and are generally easily distinguished; this may be facilitated by comparing the spectra with that of the free ligand or with that of the corresponding zinc(II) complex (which has no $d \rightarrow d$ transitions).

### (i) *Principles of* $d \rightarrow d$ *transitions*

The $d \rightarrow d$ transitions of the copper(II) ion are predominantly electric-dipolar in origin[59,95,129–132], and are controlled by two selection rules: the spin multiplicity rule which, however, is redundant in the case of copper(II), as a $d^9$ configuration only yields doublet states, and the Laporte rule.

Three mechanisms are available to account for the breakdown of the Laporte rule[129–132]:

*A.* — In non-centrosymmetric complexes (*e g.* $Cs_2CuCl_4$), *d–p* mixing may occur, and some electronic intensity may be gained from the allowed $d \rightarrow p$ transition.

*B.* — In centrosymmetric complexes (*e g.* $Cu(NH_3)_4X_2$), a vibronic mechanism is invoked, which allows an ungerade mode of vibration of the molecule to couple with the electronic excited state.

*C.* — A less common mechanism is "intensity borrowing" from a low-energy charge transfer band [*e.g.* Cu(3-$\phi$ acac)$_2$ [133] and Cu(3-Me acac)$_2$ [80]].

The importance of the first two mechanisms suggests the division of cop-

per(II) spectra into those of centrosymmetric complexes and those of non-centrosymmetric complexes. The latter should be distinguishable by a higher intensity (as seen in the reflectance spectra of Fig 8), but caution should be exercised in placing too much emphasis on differences in intensity of reflectance spectra[75].

Fig. 8 illustrates how the appearances of reflectance spectra vary with stereo-

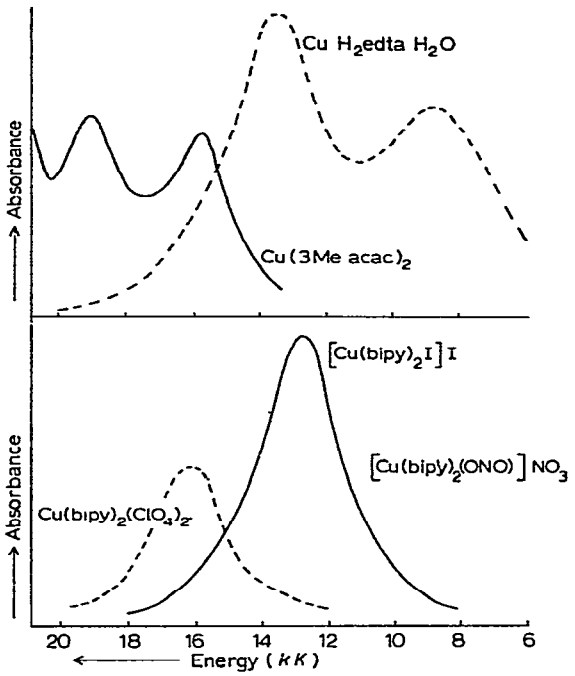


Fig 8 The electronic reflectance spectra of some copper(II) complexes

chemistry. However, not only do the spectra depend upon stereochemistry, but for a given stereochemistry, they vary with the value of 10 $Dq$[134] (see Fig. 4), and with the extent of the tetragonal distortion[67]. Consequently, although square-coplanar, tetragonal-octahedral, cis-distorted octahedral, square-based pyramidal and trigonal-bipyramidal stereochemistries, involving nitrogen ligands, may be tentatively recognised[75], less recognisable are the rhombic-octahedron, compressed tetragonal-octahedron and compressed tetrahedron. Consequently, stereochemical assignments based upon reflectance spectra should be considered as tentative.

More precise information[127] may be obtained from the measurement of polarised single-crystal spectra, but considerably more experimental work[128] is involved. A knowledge is required of:

1. the crystal structure of the complex (preferably with all molecules in the unit cell aligned), the indices of the main faces of the crystal, and the orientation of the local molecular axes to these faces;

2. the polarised single-crystal spectra, measured preferably in three mutually perpendicular directions parallel to the local molecular axes.
3. the crystal $g$-values and their direction cosines, measured with respect to a known crystal face.

Requirements 2. and 3. enable the "effective" electronic point group symmetry[67] of the crystal chromophore to be determined, and related to the crystallographic and molecular symmetry. There is little evidence, so far, to suggest that the magnetic axes do not correspond with the electronic axes (although this is not inherent), and they are assumed to do so in the present article. There is considerable evidence against the equivalence of the molecular axes and symmetries to those of the "effective" electronic axes and symmetries[67]. In practice the effective symmetry may be higher than the strict molecular symmetry, or lower than the approximate molecular symmetry. Given the "effective" point-group, the appropriate electronic selection rules[94] may be calculated, the detailed procedure being given by Cotton[94].

The single-crystal measurements give the crystal polarisations. If all the molecules in the unit cell have identical orientations, or are related by inversion in a centre of symmetry, then the measured polarisations are equivalent to the local molecular polarisations If there is more than one molecular orientation per unit cell, then the microscopic polarisations are related to the macroscopic polarisations by vector addition of $I\cos^2\theta$ (where $I$ represents a polarised molecular intensity, and $\theta$ is the angle between the direction of this polarisation and the crystal direction). Analysis of the spectra is greatly facilitated by using the single-crystal ESR direction-cosine data. A knowledge of the $g_z$ direction (for a $d_{x^2-y^2}$, $d_{xy}$ or $d_{z^2}$ ground state) permits the assignment of the z-polarised spectrum. The importance of the ESR spectra in determining the electronic ground state has been referred to earlier (section F).

Even when all of the above data is available (and it frequently is not), it may still not be possible to completely determine the one-electron orbital sequence for a copper(II) complex. This arises for a number of reasons:

1. single-crystal polarisation data alone cannot give information on the presence of a centre of symmetry; for example it cannot distinguish $D_2$ from $D_{2h}$ symmetry for a $d_{xy}$ ground state.
2 in non-centrosymmetric systems, there are only three cartesian directions, but four $d \rightarrow d$ transitions are possible. Therefore, either one band is electronically forbidden and only occurs with vibronic intensity, in the presence of three electronically allowed ones, or two transitions are electronically allowed in the same polarisation, and cannot be distinguished. In either case, it is difficult to assign all four transitions.
3. in centrosymmetric systems, the polarisation should be less marked, as a vibronic mechanism is operative, but the factors determining the most effective vibrational modes are not understood.

For the above reasons, the results summarised in the following section are

tentative and generally incomplete, but by examining the sequence of the one-electron orbitals and their energies, for a wide range of complexes of different structures, it is possible to obtain some stereochemical information.

### (*ii*) *Experimental results*

(*a*) *Octahedral.*—A single electronic transition ($t_{2g} \rightarrow e_g$; split at the most by 1.2 $kK \equiv 3\lambda/2$, due to spin–orbit coupling within the $t_{2g}$ level) and an isotropic $g$-value, would be predicted for this stereochemistry[130] (Fig. 4). $K_2PbCu(NO_2)_6$

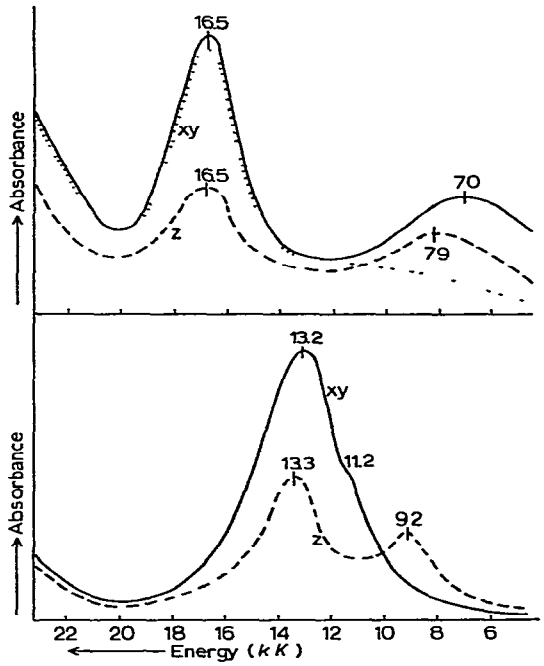


Fig. 9 The electronic reflectance spectrum of $K_2PbCu(NO_2)_6$ (———) and the polarised single-crystal electronic spectra of $K_2BaCu(NO_2)_6$ (– – – and ···· ).

Fig 10 The polarised single-crystal electronic spectra of $Cu(H_2O)_4(HCO_2)_2$

has an isotropic ESR spectrum[61] ($g = 2.10$), but the electronic reflectance spectrum (Fig. 9) involves two bands split by 9.0 $kK$. Although the crystal structure of $K_2BaCu(NO_2)_6$ is unknown, its electronic properties[61,71] are consistent with a static elongated tetragonal-octahedral stereochemistry. The polarised spectra[71] are shown in Fig. 9, and have been interpreted in approximately $D_{4h}$ symmetry, assuming a $d_{x^2-y^2}$ ground state, as suggested by the axial ESR spectrum (Table 9). The similarity of the electronic spectra suggest that $K_2PbCu(NO_2)_6$ also has an elongated tetragonal-octahedral $CuN_6$ chromophore, which, in order to be consistent with the ESR spectrum[61], must be undergoing a pseudo-rotational type of Jahn–Teller distortion[63,70].

TABLE 9

THE ASSIGNMENT OF THE ELECTRONIC ENERGY LEVELS OF COPPER(II) COMPLEXES ($kK$)(ROOM TEMPERATURE DATA); SINGLE-CRYSTAL MOLECULAR $g$-VALUES

| *Complex* | *Effective symmetry* | $d_{z^2} \rightarrow d_{x^2-y^2}$ | $d_{xy} \rightarrow d_{x^2-y^2}$ | $d_{xz} \rightarrow d_{x^2-y^2}$ | $d_{yz} \rightarrow d_{x^2-y^2}$ | $g_1$ | $g_\perp$ | $g_2$ | $g_3 = g_\parallel$ |
|---|---|---|---|---|---|---|---|---|---|
| *A $d_{x^2-y^2}$ Ground state* | | | | | | | | | |
| $K_2BaCu(NO_2)_6$ | $D_{4h}$ | 8 6 | 16 5 | 16 5 | 16 5 | 2 060 | — | 2 071 | 2 238 |
| $Cu(NH_3)_4(SCN)_2$ | $D_{4h}$ | 14 3 | 15 7 | 17 5 | 17 5 | — | 2 056 | — | 2 237 |
| $Cu(NH_3)_4(NO_2)_2$ | $D_{4h}$ | 13 4 | 16 2 | 17.1 | 17 1 | — | 2 052 | — | 2 234 |
| $Cu(H_2O)_4(UO_2)_2$ $(AsO_4)_2 \cdot 4H_2O$ | $D_{4h}$ | 13 0 | 12 0 | 15 0 | 15 0 | — | 2 0676 | — | 2 3554 |
| $Cu(H_2O)_4(HCO_2)_2$ | $D_{4h}$ | 9 2 | 11 2 | 13 2 | 13 2 | — | 2 06 | — | 2 35 |
| $Na_4Cu(NH_3)_4$ $\{Cu(S_2O_3)_2\}_2$ $H_2O$ | $D_{4h}$ | 18 4 | (19 2) | 19 2 | 19 2 | — | 2 0520 | — | 2 200 |
| $Na_4Cu(NH_3)_4$ $\{Cu(S_2O_3)_2\}_2$ $NH_3$ | $D_{4h}$ | 13 6 | (17 4) | 17 4 | 17 4 | — | 2 0567 | — | 2 227 |
| $CaCuSi_4O_{10}$ | $D_{4h}$ | 18 8 | 12 9 | 15 8 | 15 8 | — | 2 054[b] | — | 2 326[b] |
| $BaCu(HCO_4)_6 \cdot 4H_2O$ | $D_{2h}$ | 8 4 | 10 6 | 13 1 | 13 5 | 2 078 | — | 2 109 | 2 383 |
| $Cu(en)_2(BF_4)_2$ | $D_{2h}$ $D_{4h}$ | 18 0 | (18 0–19 0) | 19 0 | 19 0 | 2 0456 | — | 2 0496 | 2 1982 |
| $Cu(en)_2Cl_2$ $H_2O$ | $D_{4h}$ $D_{2h}$ | 15 0 | (15 0–18 0) | 18 1 | 18 1 | 2 0458 | — | 2 0466 | 2 2073 |
| $Cu(en)Cl_2$ | $D_2$ | 14 0 | 13 0 | *ca* 15 0 | *ca* 15 0 | 2 0523 | — | 2 0534 | 2 239 |
| $Cu(dien)_2Br_2 \cdot H_2O$ | $D_2$ | 8 8 | 9 9 | 15 4 | 15 9 | 2 0449 | — | 2 0968 | 2 2130 |
| $Cu(NH_3)_2(CH_3CO_2)_2$ | $D_{2h}$ | 17 5 | 15 0 | 17 5 | 18 0 | 2 0497 | — | 2 1100 | 2 2114 |
| $(NH_4)Cu(NH_3)_5(PF_6)_3$ | $C_{4v}$ | 11 4 | — | 15 0 | 15.0 | — | 2 0654 | — | 2 2516 |
| $[Cu(NH_3)_4H_2O]SO_4$ | $C_{4v}$ | 16 0 | — | 17 5 | 17 5 | — | — | — | — |
| $[Cu(1,3\text{-pn})_2H_2O]SO_4$ | $C_{2v}$ | 16 0 | — | 17 9 | 17 9 | 2 0503 | — | 2 0475 | 2 2073 |
| *Complex* | *Effective symmetry* | $d_{x^2-y^2} \rightarrow d_{z^2}$ | $d_{xy} \rightarrow d_{z^2}$ | $d_{xz} \rightarrow d_{z^2}$ | $d_{yz} \rightarrow d_{z^2}$ | $g_1 = g_\parallel$ | $g_2$ | $g_\perp$ | $g_3$ |
| *B. $d_{z^2}$ Ground state* | | | | | | | | | |
| $Cu(dien)_2(NO_3)_2$ | $C_2$ | 9 2 | 11 7 | 15.6 | 15 6 | 2 0518 | 2.1440 | — | 2 1589 |
| Cu(methoxyacetate)$_2$ $2H_2O$ | $D_{2h}$ | 9 8 | 16 1 | 12 3 | 12 3 | 2 0266 | 2 2241 | — | 2 3447 |
| $[Cu(bipy)_2I]I$ | $C_{2v}$ | 13.8 | 12.7 | 10 8 | (9 3) | 2.0280 | 2 1613 | — | 2.1642 |
| $[Cu(bipy)_2I]I$ | $D_2$ | (9 3) | 10 8 | 12 7 | 13 8 | — | — | — | — |
| $[Cu(bipy)_2(ONO)]NO_3$ | $C_{2v}$ | 14 6 $^2\Gamma_8 \rightarrow {}^2\Gamma_8$ | 9 5 $^2\Gamma_9 \rightarrow {}^2\Gamma_8$ | 15 0 $^2\Gamma_9 \rightarrow {}^2\Gamma_8$ | (14 6) $^2\Gamma_7 \rightarrow {}^2\Gamma_8$ | 2 029 | 2.17 | — | 2 205 |
| $CuNH_{32}AgSCN)_3$ | $D_{3h}$[a] | (11.1) | 10 5 | 13 3 | 14 6 | 2 006 | — | 2 2020 | — |

[a] Split by spin–orbit coupling [b] Powder data

(*b*) *Elongated tetragonal-octahedral*—Polarised single-crystal spectra have been observed for $Cu(NH_3)_4(SCN)_2$[11] $Cu(NH_3)_4(NO_2)_2$ (II), $Cu(UO_2)_2(AsO_4)_2$-$8H_2O$[135], and $Cu(H_2O)_4(HCO_2)_2$ (IV)[136]; those for the formate are shown in Fig. 10. The spectra of all four complexes have been vibronically assigned in $D_{4h}$ symmetry, with a $d_{x^2-y^2}$ ground state (Table 9). The most active mode of vibration in this point-group appears to be of $b_{1u}$ symmetry, and its efficiency may arise

TABLE 9 (*continued*)

| *Complex* | *Effective symmetry* | $d_{z^2} \rightarrow d_{xy}$ | $d_{x^2-y^2} \rightarrow d_{xy}$ | $d_{xz} \rightarrow d_{xy}$ | $d_{yz} \rightarrow d_{xy}$ | $g_1$ | $g_\perp$ | $g_2$ | $g_3 = g_\parallel$ |
|---|---|---|---|---|---|---|---|---|---|
| *C $d_{xy}$ Ground state* | | | | | | | | | |
| $Cu(3\text{-}Meacac)_2$ | $D_{2h}$ | 19 2 | 15 5 | 15 8 | (14 0–16 0) | 2 0569 | — | 2 0606 | 2 2550 |
| $CuH_2edtaH_2O$ | $D_2$ or $D_{2h}$ | 8 2 | 13 1 | 12 6 | 14 6 | 2 0689 | — | 2 1142 | 2 2905 |
| $Cs_2CuCl_4$ | $D_{2d}$ | 9 05 | 7 9 | 5 55[a] | 4 8[a] | 2 083 | — | 2 103 | 2 384 |
| $[Me_3(\phi CH_2)N]_2CuCl_4$ | $D_{2d}$ | 8 8 | — | 5 9 | 5 9 | — | 2.758 | — | 2.4008 |
| $Cu(hfacac)_2bipy$ | $D_2$ | 9 4 | — | 13.7 | 14 6 | 2 0722 | — | 2 0795 | 2 2919 |
| $Cu(phen)_3(ClO_4)_2$ | $D_2$ | 8 0 | — | 15 0 | 15 0 | — | — | — | — |
| $CaCu(CH_3CO_2)_4\ 6H_2O$ | $D_{2d}$ or $S_4$ | 12 7 | 15 8 | 14 4 | 14 4 | — | 2 0695 | — | 2 3602 |

from its being the only out-of-the-xy-plane vibration[136]. The tetraammines[11] and $Cu(H_2O)_4(HCO_2)_2$ [136] yield the one-electron orbital sequence

$$d_{x^2-y^2} > d_{z^2} > d_{xy} > d_{xz}, d_{yz}$$

For meta-zeunerite[135] the order of the $d_{z^2}$ and $d_{xy}$ orbitals is interchanged, probably due to the effect of $\pi$-bonding Although the crystal structure of $Na_4Cu(NH_3)_4\{Cu(S_2O_3)_2\}_2NH_3$ is not known[19,20] accurately, it is believed to be isostructural[21] with the monohydrate (V), and to involve an elongated tetragonal-octahedral stereochemistry with the fifth ammonia weakly coordinated in the axial position Its polarised spectra[11,21] are shown in Fig. 11, which is very similar to Fig. 10, but the polarisation is even more marked, the spectra have been tentatively assigned in $D_{4h}$ symmetry (Table 9).

(*c*) *Square-coplanar.*—An effectively square-coplanar stereochemistry, involving $\sigma$-bonding ligands, is believed to exist in $Na_4Cu(NH_3)_4\{Cu(S_2O_3)_2\}_2H_2O$ (V)[21] and, although the water molecules occupy positions midway between the aligned $Cu(NH_3)_4^{2+}$ cations, they are considered to be uncoordinated[21], since the distance (2.88 Å) is slightly greater than that consistent with semi-coordination[11,76] (2.55 Å). The electronic transitions (Fig. 11) occur[21] at appreciably higher energies than for the isostructural ammonia adduct[11,21], particularly the $d_{z^2} \rightarrow d_{x^2-y^2}$ transition (the spectra have been assigned in $D_{4h}$ symmetry, with a $d_{x^2-y^2}$ ground state, see Table 9). The energy of this transition has been established as a measure of the tetragonal distortion[11,135], and its high value in this complex is consistent with an effective square-coplanar stereochemistry for the monohydrate, in contrast to the elongated tetragonal-octahedron of the monoammine adduct[21].

The partial polarised spectra of Egyptian Blue[137], ($CaCuSi_4O_{10}$), which has a strictly square-coplanar stereochemistry[18] involving potentially $\pi$-bonding oxygen ligands, has been assigned[137] in $D_{4h}$ symmetry (Table 9), with the $d_{z^2} \rightarrow d_{x^2-y^2}$ transition at highest energy.

More papers have been written on the assignment of the polarised single

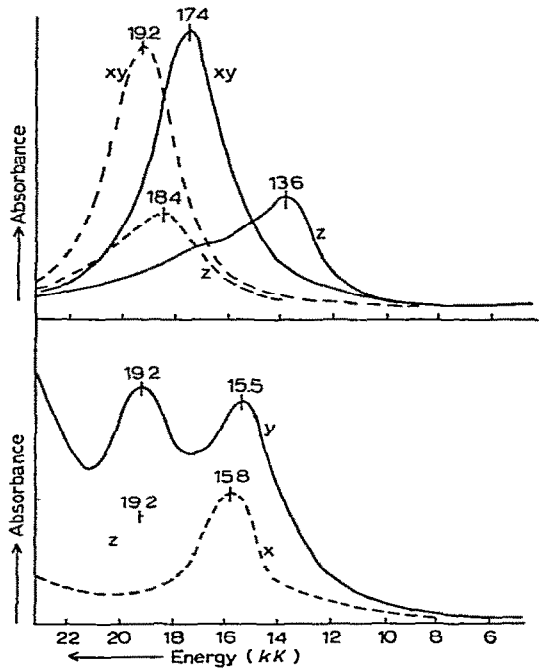


Fig 11. The polarised single-crystal electronic spectra of $Na_4Cu(NH_3)_4\{Cu(S_2O_3)_2\}_2 \cdot H_2O$ (– – –) and $Na_4Cu(NH_3)_4\{Cu(S_2O_3)_2\}_2$ $NH_3$ (———).

Fig. 12. The polarised single-crystal electronic spectra of Cu(3-Meacac)$_2$

crystal-spectra of square-coplanar bis (chelate) copper(II) complexes, involving potentially $\pi$-bonding ligands, such as acetylacetone, than on any other type of complex[127,80]. The results, for the one-electron orbital sequences of various Cu(acac)$_2$-type complexes, are listed in Table 10. The almost 90° misalignment of the two molecules in the unit cell of Cu(acac)$_2$ [92] makes the assignment uncertain[138]. The misalignment[139] in Cu(dmp)$_2$ is less (~45°), but there is some uncertainty concerning the published spectra (two of the spectra which should be the same, are not: Fig. 1, ref. 140). Cu(3-$\phi$ acac)$_2$ has two molecules, misaligned by 40°, in the unit cell[141], and the method of resolving the spectra of this complex[133] resulted in a x-polarised spectrum consisting of a continuously rising background. This is

TABLE 10

A SUMMARY OF THE ONE-ELECTRON ORBITAL ENERGIES OF THE BIS(CHELATE-OXYGEN) COPPER(II) COMPLEXES

| | *Cu(acac)$_2$* [138] | *Cu(3-$\phi$ acac)$_2$* [133] | *Cu(3-Me acac)$_2$* [80] | *Cu(dmp)$_2$* [139] |
|---|---|---|---|---|
| $d_{x^2-y^2} \rightarrow d_{xy}$ | 18 0 | 16 9 | 15 5 | 18 2 |
| $d_{xz} \rightarrow d_{xy}$ | 15 6 | 19 0 | 15 8 | 16 4 |
| $d_{y_z} \rightarrow d_{xy}$ | — | 20 6 | (14 0–16 0) | 20 0 |
| $d_{z^2} \rightarrow d_{xy}$ | 14 5 | 15 4 | 19 2 | 15.6 |

unusual, and places some doubt on the assignment, but not upon the discussion of the proposed intensity-borrowing mechanism. The crystal-structure of Cu-(3-Me acac)$_2$ involves[29] only one molecule in the unit cell, and hence avoids the complications present in the above complexes. Unfortunately, the crystals obtained are so thin that the polarised spectra[80] could only be easily obtained in one face of the crystal, and different polarisations were only obtained by tilting the crystal to the appropriate angle in the light beam. The x- and y- polarised spectra are experimentally satisfactory, but there is some doubt concerning the z-polarised spectrum. The polarised spectra[80] (Fig. 12) have been partially assigned, as in Table 9, using a vibronic mechanism in $D_{2h}$ symmetry, and an intensity borrowing mechanism[133]. The results (Table 9) are much more consistent with the previous assignments[21,137] ($Na_4Cu(NH_3)_4\{Cu(S_2O_3)_2\}_2 \cdot H_2O$ and $CaCuSi_4O_{10}$) of square-coplanar complexes, than are those of Table 10.

The polarised single-crystal spectra[97] of Cu(salim)$_2$ and Cu(*N*–Me salim)$_2$ have been reported, but in both complexes the close proximity of charge-transfer bands prevented a clear assignment.

(*d*) *Elongated rhombic octahedral*—The polarised spectra[136] of $Ba_2Cu(HCO_2)_6 \cdot 4H_2O$ (VI) are shown in Fig. 13. There is a close resemblance of the spectra to those of tetragonal-octahedral complexes[11,135], but a clear difference

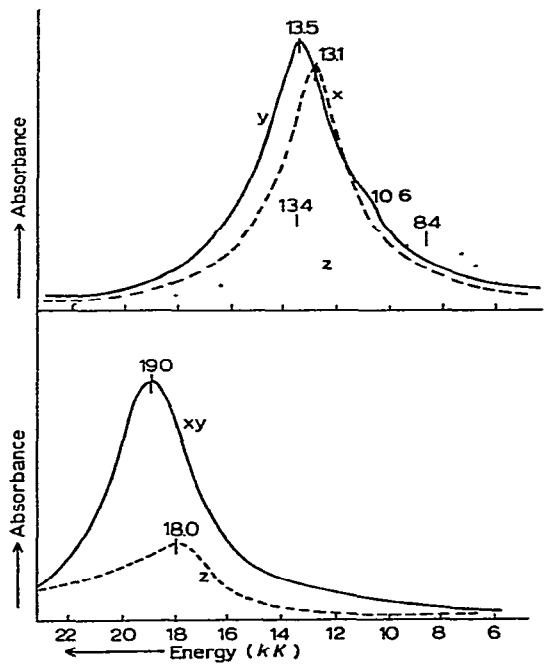


Fig. 13 The polarised single-crystal electronic spectra of $Ba_2Cu(HCO_2)_6 \cdot 4H_2O$.

Fig 14. The polarised single-crystal electronic spectra of $Cu(en)_2(BF_4)_2$.

is seen between the x- and y-polarisations. The spectra have been assigned in $D_{2h}$ symmetry (Table 9), and yield a one-electron orbital sequence comparable[136] to that in $Cu(H_2O)_4(HCO_2)_2$, except for the splitting of the $d_{xz}$ and $d_{yz}$ orbitals. The strict molecular symmetry[27,28] of $Cu\,en_2(BF_4)_2$ (VII) is $C_i$, and three $g$-values are observed (Table 9), but the difference between $g_x$ and $g_y$ is very small[77]. The polarised spectra[77] (Fig. 14) do not distinguish the x- and y-polarisations and have been partially assigned in the effective symmetry of $D_{4h}$ with a $d_{x^2-y^2}$ ground state (Table 9). This suggests that the methylene groups of the ethylenediamine ligands do not seriously influence the electronic properties[77]. The polarised single-crystal spectra of $Cu(en)Cl_2$ [134] (Fig. 15) have been interpreted in the non-centrosymmetric point-group $D_2$, with a $d_{x^2-y^2}$ ground state (Table 9). The electronic properties clearly correspond with a principal axis perpendicular to the chelate plane, rather than with the principal axis of the approximate $C_2$ molecular symmetry, and this again suggests that the methylene links in the ethylenediamine ligands are not electronically important.

The polarised single-crystal spectra[67] of $Cu(dien)_2Br_2 \cdot H_2O$ are shown in Fig 16. Although there are four molecules in the unit cell of this complex, the local molecular axes are aligned, if the x- and y-axes lie along the equatorial Cu–N bonds This has been established through a correlation of the single-crystal electronic and ESR spectra[67] with the crystallographic data[52]. The spectra have been

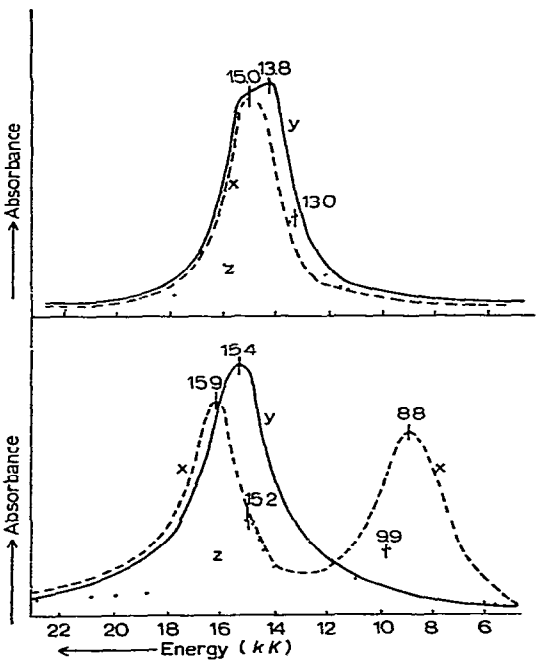


Fig 15. The polarised single-crystal electronic spectra of $Cu(en)Cl_2$.

Fig. 16 The polarised single-crystal electronic spectra of $Cu(dien)_2Br_2 \cdot H_2O$.

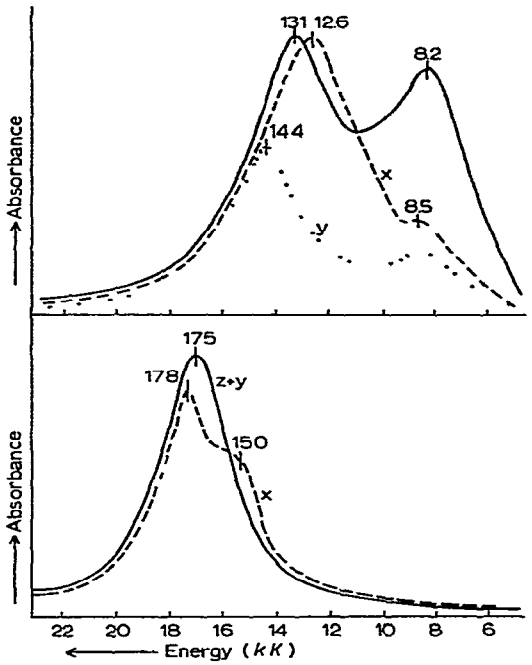


Fig. 17. The polarised single-crystal electronic spectra of $CuH_2edta \cdot H_2O$.
Fig. 18. The polarised single-crystal electronic spectra of $Cu(NH_3)_2(CH_3CO_2)_2$.

assigned in $D_2$ symmetry (Table 9), and much less satisfactorily in $C_{2v}$ symmetry, suggesting that, in this case, the methylene groups are important in removing the center of symmetry. However, this could also be removed by the accumulative bond-angle distortion (12°) imposed by the diethylenetriamine ligands.

The polarised single-crystal spectra[67] of $CuH_2edtaH_2O$ are shown in Fig. 17. A correlation between the polarisation directions, the crystal $g$-values and the crystal structure[53] requires that the x- and y-axes lie between the equatorial bonds, rather than along them. The spectra can then be assigned, with a $d_{xy}$ ground state, in the non-centrosymmetric point-group, $D_2$, and equivalently, in the centrosymmetric point-group $D_{2h}$, notwithstanding the clear lack of a centre of inversion in the molecular structure (XII).

The low energies of the first transitions[67], in $Cu(dien)_2Br_2 \cdot H_2O$ and $CuH_2edta \cdot H_2O$, reflect the restricted-tetragonal distortion imposed by the out-of-the-xy-plane chelation of these polydentate ligands (X) and (XII).

(*e*) *Semi-elongated rhombic-octahedral.*—The polarised single-crystal spectra[75] of $Cu(NH_3)_2(CH_3CO_2)_2$ are shown in Fig. 18. The polarisation is not very marked, due to misalignment[32] of the "tetragonal" axes by 60°, but the spectra have been tentatively assigned in $D_{2h}$ symmetry (Table 9). The $d_{z^2} \rightarrow d_{x^2-y^2}$ transition (17.5 $kK$) is intermediate in energy between that (18.4 $kK$) of the effectively

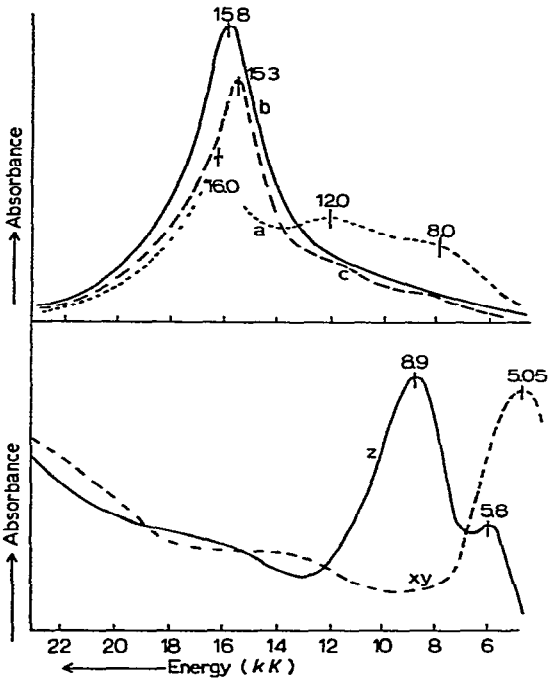


Fig 19. The polarised single-crystal electronic spectra of $Cu(dien)_2(NO_3)_2$.
Fig. 20. The polarised single-crystal electronic spectra of $Cs_2CuCl_4$.

square-coplanar $Na_4Cu(NH_3)_4\{Cu(S_2O_3)_2\}_2 \cdot H_2O$ [21] complex, and that (13.6 *kK*) of the tetragonal-octahedral ammonia analogue[11]. This is consistent with its stereochemistry being intermediate between a square-plane and a tetragonal-octahedron, due to the inability of the terminal acetate oxygen atoms to coordinate effectively along the z-axis (IX).

(*f*) *Compressed tetragonal octahedral.*—No polarised single-crystal spectra of copper(II) complexes having exactly this stereochemistry are known (see ref. 143). $Cu(dien)_2(NO_3)_2$ has almost this structure (XI)[37] and its spectra[125] are shown in Fig. 19. The alignment of the four molecules in the unit cell[37] is not ideal, but allows a reasonable spectral assignment in $C_2$ symmetry, using the $d_{z^2}$ ground state established by the single-crystal ESR data (Table 9). This yields the one-electron orbital sequence $d_{z^2} > d_{x^2-y^2} > d_{xy} > d_{xz}, d_{yz}$, the order of the last three orbitals conflicting with the prediction of crystal field calculations[144]. The low energy of the $d_{x^2-y^2} \rightarrow d_{z^2}$ transition, in this complex, is consistent with the restricted tetragonal distortion due to chelation from the short-bonded axial positions to the long-bonded equatorial positions[67].

(*g*) *Compressed rhombic-octahedral.*—The polarised single-crystal spectra[125] of $Cu(methoxyacetate)_2 \cdot 2H_2O$ [38] have been assigned in the effective electronic

symmetry $D_{2h}$ (Table 9). The ESR data indicate a predominantly $d_{z^2}$ ground state, with the z-axis along the short Cu–O, bonds and the x- and y-axes close to the other bonds.

(*h*) *Compressed tetrahedral.*—The polarised single-crystal spectra[145,149] of $Cs_2CuCl_4$ are shown in Fig. 20. Partial data[146] have been obtained for $[(CH_3)_3N(C_6H_5CH_2)]_2CuCl_4$, using a crystal-tilting technique. The spectra of both complexes have been assigned in the $D_{2d}$ point-group, with a $d_{xy}$ ground state (Table 9).

(*i*) *Trigonal-bipyramidal.*—The polarised single-crystal spectra[147] of $Cu(NH_3)_2Ag(SCN)_3$ are shown in Fig. 21, and the ESR spectrum[124] clearly establishes a $d_{z^2}$ ground state. The observation of three clear bands rules out the assignment of this spectra in the simple $D_{3h}$ point-group, as only two transitions are predicted (Fig. 6). The spectra have been assigned[147] (Table 9) in the $D'_{3h}$ double group (including spin–orbit coupling[148]), with the interesting result that the parent $d_{xy}$, $d_{x^2-y^2}$ level is lower in energy than $d_{xz}$, $d_{yz}$ (Fig. 6). This reversal has been accounted for by out-of-the-plane $\pi$-bonding of the thiocyanate ligands with the $d_{xz}$ and $d_{yz}$ copper orbitals[147]. The polarised single-crystal spectra (Fig. 22)[147] of the distorted trigonal-bipyramidal complex $[Cu(bipy)_2I]I$ (XV) may be assigned (Table 9) in $C_{2v}$ or $D_2$ symmetry, with a $d_{z^2}$ ground state. The former point-group is preferred, and yields the inverted sequence of one-electron orbitals, as above.

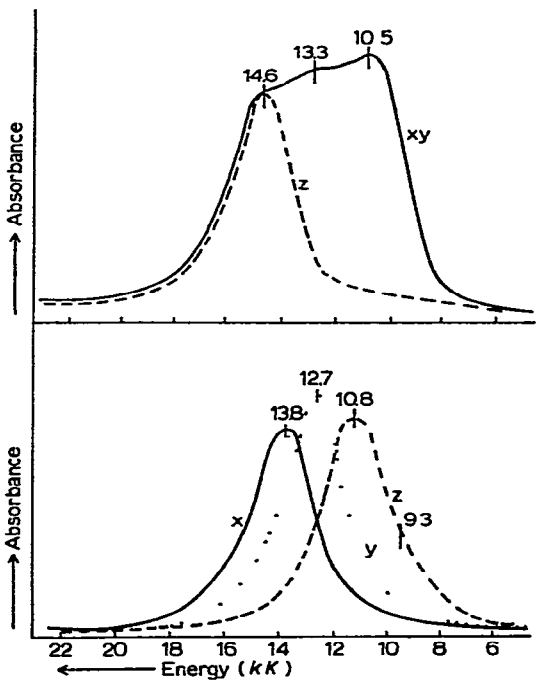


Fig. 21. The polarised single-crystal electronic spectra of $Cu(NH_3)_2Ag(SCN)_3$.
Fig. 22. The polarised single-crystal electronic spectra of $[Cu(bipy)_2I]I$.

(*j*) *Square-based pyramidal.*—The polarised single-crystal spectra[149] of $[Cu(1,3\text{-pn})_2 \cdot H_2O]SO_4$, are shown in Fig. 23, and merely show a change of intensity between the two polarisations. The spectra may be assigned in $C_{4v}$ symmetry, with a $d_{x^2-y^2}$ ground state (Table 9). Comparable results have been obtained[75] for $[Cu(NH_3)_4 \cdot H_2O]SO_4$. Although[93] $NH_4[Cu(NH_3)_5](PF_6)_3$ is of unknown crystal structure, it is believed to contain a square-based pyramidal $CuN_5$ chromophore, and the polarised single-crystal spectra[75] have been assigned in

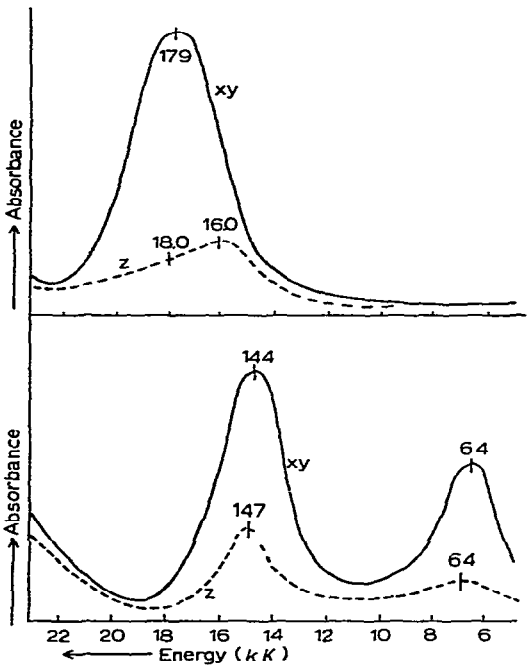


Fig 23 The polarised single-crystal electronic spectra of $[Cu(1,3\text{-pn})_2H_2O]SO_4$.

Fig 24 The polarised single-crystal electronic spectra of $Cu/Zn(bipy)_3Br_2 \cdot 6H_2O$.

$C_{4v}$ symmetry, using the single-crystal ESR data. The polarised single-crystal spectra[150] of $Cu[S_2CN(C_2H_5)_2]_2$ (which has a dimeric square-based pyramidal structure[151]) have been partially assigned in $C_{4v}$ symmetry and a single broad band at 22.0 *kK* attributed to the $d_{xz}, d_{yz} \rightarrow d_{x^2-y^2}$ transition.

(*k*) *Trigonal-octahedral* ($D_3$).—The polarised single-crystal[66,149] spectra of copper(II) doped into $Zn(bipy)_3Br_2 \cdot 6H_2O$ and $Zn(bipy)_3SO_4 \cdot 7H_2O$, are the same (Fig. 24) and comparable to those of the undiluted complex $Cu(bipy)_3Br_2 \cdot 6H_2O$ (ref. 149). A slightly different type of spectrum has been observed for Cu $(phen)_3(ClO_4)_2$, which is closely comparable to that of $Cu(hfacac)_2bipy$ (Fig. 25)[149]. The spectra of the latter have been tentatively assigned in $D_2$ symmetry, with a $d_{xy}$

ground state (Table 9), and a comparable assignment[149] has been suggested for $Cu(phen)_3(ClO_4)_2$, and less certainly for $Cu(bipy)_3Br_2 \cdot 6H_2O$.

(*l*) *Cis-distorted octahedral.*—The polarised single-crystal spectra[152] of $[Cu(bipy)_2(ONO)]NO_3$ are shown in Fig. 26. The ESR spectrum[152] establishes a $d_{z^2}$ ground state, (all four molecules in the unit cell[51] have their molecular axes aligned) and the spectra are assigned in $C_{2v}$ symmetry, with a principal x-axis.

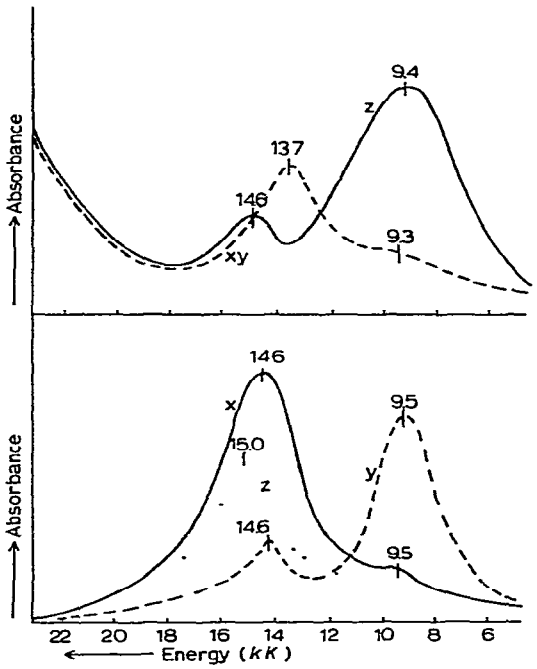


Fig 25 The polarised single-crystal electronic spectra of $Cu(hfacac)_2bipy$.

Fig 26. The polarised single-crystal electronic spectra of $[Cu(bipy)_2(ONO)]NO_3$

(*m*) *Coordination numbers greater than six.*—The polarised single-crystal spectra[125] of $CaCu(CH_3CO_2)_4 \cdot 6H_2O$ (XIX)[55] are shown in Fig. 27. These are assigned in $S_4$ and $D_{2d}$ symmetry, using a $d_{xy}$ ground state.

(*iii*) *Conclusions from the electronic spectra*

A number of generalisations may be drawn from the data on the electronic energy levels of copper(II) complexes presented in this section.

(*a*) *Orbital sequence.*—For a given stereochemistry the sequence of one-electron orbitals is essentially constant; *e.g.* for a tetragonal octahedron[11,77,135]:

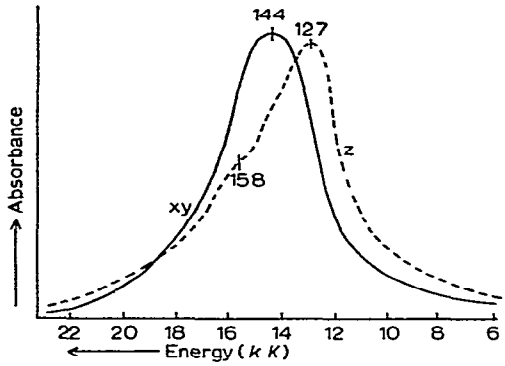


Fig. 27. The polarised single-crystal electronic spectra of $CaCu(CH_3CO_2)_4 \cdot 6H_2O$

$d_{x^2-y^2} > d_{z^2} > d_{xy} > d_{xz}, d_{yz}$. The effect of different ligands is reflected in their contribution to the value of $10Dq$. Thus, in $Cu(en)_2(BF_4)_2$ the above order applies, but in $Cu(en)Cl_2$ [134] the order of the $d_{z^2}$ and $d_{xy}$ levels is reversed, as the chloride ion lies much lower in the spectrochemical series[59] than does ethylenediamine. In a square-coplanar stereochemistry, the $d_{z^2}$ level lies below $d_{xz}$, $d_{yz}$ in $CaCuSi_4O_{10}$ [137] but above it in $Na_4Cu(NH_3)_4\{Cu(S_2O_3)_2\}_2H_2O$ [21], for a comparable reason. The effect of $\pi$-bonding on the sequence varies; in $Cu(H_2O)_4(HCO_2)_2$ [136] it is negligible, in meta-zeunerite[135] it interchanges the relative positions of the $d_{z^2}$ and $d_{xy}$ levels, and in $Cu(NH_3)_2Ag(SCN)_3$ [147] and $[Cu(bipy)_2I]I$ it completely changes the point-charge sequence.

(*b*) *Correlation diagram*.—The results substantiate a correlation diagram which relates the energy levels of a restricted-tetragonal-octahedron, through those of a tetragonal-octahedron to those of a square-plane, for $CuO_x$ and $CuN_x$ chromophores (Fig 4). In general, the spectra are much more sensitive to differences in bond-length[135] (as above), than to differences in bond-angle (*e.g.* $Cu(NH_3)_4X_2$ [11] and $Cu(en)_2X_2$ [77]). The evidence for correlation diagrams relating the square-plane and square-based pyramid (see section G, iii, c), and relating the cis-octahedron and trigonal-bipyramid, is less clearly established[147,152].

(*c*) *The concept of varying tetragonal distortion*.—This concept, established[11] on the basis of crystallographic bond-length data, finds substantial support from the correlation[135] between the tetragonality ($T$) and the energy of the $d_{z^2} \rightarrow d_{x^2-y^2}$ transition (Table 2). There is no such clear relationship between the energy of the $d_{z^2} \rightarrow d_{x^2-y^2}$ transition and the bond-length of the fifth ligand in square-based pyramidal complexes. The energy of this transition is reduced from its value in the parent square-coplanar chromophore (compare 18.4 $kK$ in $Na_4Cu(NH_3)_4\{Cu(S_2O_3)_2\}_2H_2O$ [21] with 16.0 $kK$ in $[Cu(NH_3)_4H_2O]SO_4$ [11]) but not to the value ($\sim$14.0 $kK$) observed in tetragonal-octahedral complexes (*i.e.* $Cu(NH_3)_4(SCN)_2$ [11])

notwithstanding the closer approach of the single fifth ligand {2.34 Å in $[Cu(NH_3)_4H_2O]SO_4$[45]}. This insensitivity of the energy of the $d_{z^2} \rightarrow d_{x^2-y^2}$ transition to the effect of a fifth ligand may be enhanced by the ability of the copper(II) ion to move out of the plane of the equatorial ligands, towards the fifth ligand {(XVI), $\rho = 0.19$ Å in $[Cu(NH_3)_4OH_2]SO_4$[45]}. This crystallographic effect, which may be associated with the $\pi$-bonding potential of the fifth ligand, could possibly "cushion" the effect of the fifth ligand on the energy of the $d_{z^2} \rightarrow d_{x^2-y^2}$ transition. In contrast, a fifth ligand without any $\pi$-bonding potential, such as ammonia in $(NH_4)Cu(NH_3)_5(PF_6)_3$[93] has much more effect on the energy of the $d_{z^2} \rightarrow d_{x^2-y^2}$ transition, (it is reduced to 11.4 *kK* in this complex); this suggests that the fifth ammonia group will bond at a shorter distance than 2 3 Å, in order to satisfy the additional bonding potential of the $Cu(NH_3)_4^{2+}$ cation (section C, iii).

(*d*) *Chelate effect.*—The consequence of a change, from a monodentate ligand to a chelate ligand, is minimal, as long as there is no change in the bond-lengths or bond-angles (*e.g.* $Cu(NH_3)_4X_2$[11] and $Cu(en)_2X_2$[77]). If the chelation occurs in a way that restricts the extent of elongation or compression ($Cu\ dien_2Br_2 \cdot H_2O$[52] and $Cu\ dien_2(NO_3)_2$[37]), then it has a major electronic effect (Table 2), significantly lowering the energy of the $d_{z^2} \rightarrow d_{x^2-y^2}$ or $d_{xy}$ transitions[67,125].

(*e*) *Electronic ground state.*—There is no electronic spectral evidence that the ground state of the copper(II) ion in its complexes is ever orbitally degenerate. The $d_{x^2-y^2}$ orbital is the most common ground state, the $d_{z^2}$ is quite common, and the $d_{xy}$ occurs occasionally. The difference between a $d_{x^2-y^2}$ and a $d_{z^2}$ ground state, for the same symmetry, is not observable in the electronic spectra, but can be readily distinguished by the ESR data (*e.g.* $Cu(dien)_2Br_2 \cdot H_2O$[67] and $Cu(dien)_2(NO_3)_2$[125]). A $d_{xy}$ ground state, in the $Cu(acac)_2$-type complexes[138], is associated with enhanced intensity in y-polarisation, due to intensity-borrowing[133] from a low-energy charge-transfer band. It is not possible to say whether this mechanism is primarily a consequence of the ground state configuration, or of the particular ligand involved.

(*f*) *The active mode of vibration in a vibronic mechanism.*—In practice, the vibronic mechanism has been restricted to $D_{4h}$ and $D_{2h}$ symmetries. In both, independent of the ligand atom or whether it is involved as a chelate, the most active normal vibrations are the out-of-plane bending modes[11,77,136] ($a_{2u}$ and $b_{2u}$ in $D_{4h}$, and $b_{1u}$ in $D_{2h}$ symmetry).

(*g*) *The electronic consequence of a centre of inversion.*—The polarised spectra, described in this section, cover a wide range of stereochemistries, some centrosymmetric and some non-centrosymmetric. The former spectra have been assigned using vibronic selection rules, the latter using an electronic mechanism, and the

sensitivity of the electronic spectra to the presence or absence of a centre of inversion is of interest. The spectral intensities of $Cu(NH_3)_4X_2$, $[Cu(NH_3)_4OH_2]SO_4$[11], $NH_4[Cu(NH_3)_5](PF_6)_3$ [93], $Ba_2Cu(HCO_2)_6 \cdot 4H_2O$ [136], $Cu(acac)_2$ [138] and $CuH_2edta \cdot H_2O$ [67] are quite similar. The intensity appears to be a function of the ligand atom, nitrogen atoms producing more intensely coloured complexes than oxygen ligands. This could result from lower energy charge-transfer bands in the latter. The extents of polarisations observed for centrosymmetric complexes are only slightly less than those observed for non-centrosymmetric structures: compare $Na_4Cu(NH_3)_4\{Cu(S_2O_3)_2\}_2 \cdot NH_3$ [21] with $Cu(dien)_2Br_2 \cdot H_2O$ [67]; or $Ba_2Cu(HCO_2)_6 \cdot 4H_2O$ [136] with $CuH_2edta \cdot H_2O$ [67]. There is no experimental test for the presence of a centre of inversion (see the assignment of $CuH_2edta \ H_2O$ in both $D_2$ and $D_{2h}$ symmetries[67]). Probably, the presence of a chelate ligand is not sufficient an electronic effect to remove a centre of inversion, but a gross bond-angle distortion is important. Thus, the distorted tetrahedron ($D_{2d}$), trigonal-bipyramid ($D_{3h}$) and square-based pyramid ($C_{4v}$) clearly lack a centre of inversion, while $CuH_2edta \cdot H_2O$ does not, since it is basically a tetragonal octahedron[53]. In $Cu(dien)_2Br_2 \cdot H_2O$ [52] and $Cu(dien)_2(NO_3)_2$ [37], it is probably not the presence of methylene links themselves, but their accumulative distortion of the Cu–N bond-angles, which removes the centre of symmetry

(*h*) *The electronic consequences of π-bonding.*—The effect of π-bonding on the electronic energy levels of a copper(II) ion is relatively small, compared with the effect of σ-bonding, and consequently the former effect is difficult to establish. It is believed to be responsible for (*a*) the reversal of the order of the $d_{xy}$, $d_{x^2-y^2}$ and $d_{xz}$, $d_{yz}$ levels in $Cu(NH_3)_2Ag(SCN)_3$ [147] (and less certainly[147] in $[Cubipy_2I]I$), (*b*) the existence of strictly square-coplanar $Cu(acac)_2$-type complexes[80], their relatively short copper-oxygen bonds and hence the high energies of their $d_{z^2} \rightarrow d_{xy}$ transitions, and (*c*) the relatively low values of the combined orbital and spin-orbit reduction factors in complexes, particularly with oxygen ligands[135]. It may also be present in complexes involving semi-coordinated ligands[11], such as, the nitro groups in $Cu(NH_3)_4(NO_2)_2$, and the thiocyanate groups in $Cu(NH_3)_4(SCN)_2$ and $Cu(en)_2(NCS)_2$ [77]. π-bonding may also play a significant part in satisfying the additional bonding capacity of a four-coordinate chromophore in forming a square-based pyramidal structure, as in $[Cu(NH_3)_4H_2O]SO_4$. The π-bonding of the fifth water ligand may partially account for the energy of the $d_{z^2} \rightarrow d_{x^2-y^2}$ transition in this complex.

## H. ORBITAL REDUCTION FACTORS AND THEIR SIGNIFICANCE

Under favourable circumstances, it is possible to combine the ESR spectra of copper(II) complexes with their electronic energy-levels, and from the expres-

sions of Table 8, to obtain values for the combined orbital and spin-orbit reduction parameters. Before examining the results, it is worth considering the origin of these reductions.

(*i*) *Spin-orbit reduction*

Two mechanisms have been suggested[59,153] to account for the apparent numerical reduction of the spin-orbit coupling constant from its free-ion value[99] (−0 829 *kK*). It appears that both factors are important[154], but their relative influences have not yet been established.

(*a*) *Central-field-covalency.*—This causes a real reduction of $L$ and of $\lambda L$, and depends on the variation of the effective charge in the partly filled shell, due to transfer of electrons from the ligands into metal orbitals. Hence $L$ and $\lambda L$ become $kL$ and $R\lambda L$, where the coefficients $k$ and $R$ describe[154] "orbital reduction" and "spin-orbit reduction".

The introduction of these parameters modifies the expressions of Table 8, to the extent that $\lambda$ must be replaced by $kR\lambda$. (It has been assumed that the reduction factors associated with the matrix elements between two $t_{2g}$ orbitals are the same as those associated with the matrix elements between a $t_{2g}$ and an $e_g$ orbital.) Now if the crystal-field is not cubic, then $k$ and $R$ will display the same anisotropy as does $g$. Thus, in Table 8, $\lambda$ must be replaced by $k_iR_i\lambda$ in the $g_i$ ($i = x, y, z$) expressions.

In the axial case, $k_{\|}R_{\|}$ and $k_{\perp}R_{\perp}$ may be determined from $g_{\|}$, $g_{\perp}$ and the electronic energies. The individual $k$ and $R$ values cannot therefore, be measured, but only parameters $r_{\|} = \sqrt{k_{\|}} \cdot R_{\|}$ and $r_{\perp} = \sqrt{k_{\perp}} \cdot R_{\perp}$. These have previously[77,136,152] been referred to as "combined orbital reduction-factors", or simply as "orbital reduction-factors".

In the non-axial cases, the three measured $g$-values, and the electronic energies must be used to determine one ($\alpha$) or two ($\alpha$, $\beta$) angles which describe the crystal-field, and also the three parameters $r_x$, $r_y$ and $r_z$. Solutions are only possible if some approximations are made. Generally $\beta$ will be assumed to be zero, and $r_x \approx r_y$. This allows $\alpha$, $r_{\perp}$ and $r_{\|}$ to be calculated.

(*b*) *Symmetry-restricted-covalency*—This causes an apparent reduction of $\lambda$ through delocalisation of the metal electrons, and has been treated by means of molecular-orbital theory[96,102,156,157]. The case of tetragonal[96,157] symmetry ($D_{4h}$) will be illustrated, since the derived expressions are often assumed[96,157–162] to be relevant in other point-groups ($D_{2h}$ expressions have also been given[163,164]). For a $d_{x^2-y^2}$ ground state, the d-orbitals contribute to the following antibonding molecular orbitals, which are based on the metal atom and the coordinating atoms of four ligands (denoted by superscripts 1, 2, 3, 4) arranged in a plane.

$$\phi_1 = a(d_{x^2-y^2}) - a'[-\sigma_x^{(1)} + \sigma_y^{(2)} + \sigma_x^{(3)} - \sigma_y^{(4)}]/2$$
$$\phi_2 = a_1(d_{z^2}) - a_1'[\sigma_x^{(1)} + \sigma_y^{(2)} - \sigma_x^{(3)} - \sigma_y^{(4)}]/2$$
$$\phi_3 = b_1(d_{xy}) - b_1'[p_y^{(1)} + p_x^{(2)} - p_y^{(3)} - p_x^{(4)}]/2$$
$$\phi_4 = b(d_{xz}) - b'[p_z^{(1)} - p_z^{(3)}]/\sqrt{2}$$
$$\phi_5 = b(d_{yz}) - b'[p_z^{(2)} - p_z^{(4)}]/\sqrt{2}$$

(The $\sigma$-orbitals are hybrids of the ligand s and p orbitals). The $g$-values derived by operating on these wavefunctions with the axial Hamiltonian (3) are

$$\left.\begin{aligned} g_{\parallel} - 2 &= -8\rho[ab_1 - a'b_1 S - a'(1-b_1^2)^{\frac{1}{2}}T(n)/2] \\ g_{\perp} - 2 &= -2\mu[ab - a'bS - a'(1-b^2)^{\frac{1}{2}}T(n)/\sqrt{2}] \end{aligned}\right\} \quad (11)$$

where $S$ is the overlap integral involving $d_{x^2-y^2}$ (the small overlaps for $d_{xy}$, $d_{xz}$ and $d_{yz}$ are ignored); $T(n)$ is a function of the metal-ligand distance, the effective nuclear charge and the extent of $s$–$p$ hybridisation of the ligand orbitals; $\rho = \lambda ab_1/E(\phi_1 - \phi_3)$, $\mu = \lambda ab/E(\phi_1 - \phi_{4,5})$ and $E$ is the energy of the indicating transition. An interesting case arises if there is no metal-ligand $\pi$-bonding (hence $b_1 = b = 1$ and $b_1' = b' = 0$), then (using $a^2 + (a')^2 - 2aa'S = 1$, for the normalisation of $\phi_1$)

$$g_{\parallel} - 2 = -8\lambda\left[\frac{a^2}{2} - \frac{(a')^2}{2} + \tfrac{1}{2}\right]/E(\phi_1 - \phi_3)$$
$$g_{\perp} - 2 = -2\lambda\left[\frac{a^2}{2} - \frac{(a')^2}{2} + \tfrac{1}{2}\right]/E(\phi_1 - \phi_{4,5})$$

and

$$G = \frac{g_{\parallel} - 2}{g_{\perp} - 2} = \frac{4 \cdot E(\phi_1 - \phi_{4,5})}{E(\phi_1 - \phi_3)} \quad (12)$$

The best test of this relationship involves the complexes[21] $Na_4Cu(NH_3)_4[Cu(S_2O_3)_2]_2L$, where L = $NH_3$ or $H_2O$. In both cases, no equatorial $\pi$-bonding is possible with the $NH_3$ ligands, and $E(\phi_1 - \phi_{4,5}) \approx E(\phi_1 - \phi_3)$. No axial $\pi$-bonding is possible for the monoammine adduct, resulting in a $G$-value (4.01) very close to 4.00. The slightly lower value (3.85) for the monoaquo adduct could be due to (*a*) slight axial $\pi$-bonding, although any electronic effect of the $H_2O$ molecules has been ruled-out[21], (*b*) the effect of central-field covalency, or (*c*) inaccuracies in measuring the broad $g_{\parallel}$ resonance, or locating the $d_{xy} \rightarrow d_{x^2-y^2}$ transition.

When $\pi$-bonding is present it is necessary to simplify equations (11) (unless nuclear and ligand hyperfine structure provide extra data) by ignoring overlap and the small terms in $T(n)$. This leads to expressions previously derived by Stevens[156]:

$$\left.\begin{aligned} g_{\parallel} &= 2 - 8\lambda a^2 b_1^2/E(\phi_1 - \phi_3) \\ g_{\perp} &= 2 - 2\lambda a^2 b^2/E(\phi_1 - \phi_{4,5}) \end{aligned}\right\} \quad (13)$$

These expressions are those of Table 8, modified by replacing $\lambda$ with $a^2b^2{}_1\lambda$ or

$a^2b^2\lambda$. Thus, the parameters $ab_1$ and $ab$ in the symmetry-restricted description have the same function as $r_\parallel$ and $r_\perp$ in the central-field description. When both mechanisms are important, $\lambda$ must be replaced in Table 8 by $r_\parallel ab_1\lambda$ or $r_\perp ab\lambda$.

For $D_{2h}$ symmetry, the orbitals $\phi_4$ and $\phi_5$ are no longer degenerate (because $d_{xy}$ and $d_{yz}$ lose their degeneracy), and the following expressions are used[164,165]:

$$\left.\begin{aligned} g_z &= 2-8\lambda a^2 b_1{}^2/E(\phi_1-\phi_3) \\ g_x &= 2-2\lambda a^2 c^2/E(\phi_1-\phi_5) \\ g_y &= 2-2\lambda a^2 b^2/E(\phi_1-\phi_4) \end{aligned}\right\} \qquad (14)$$

where the parameter $b$ in the degenerate $\phi_{4,5}$ orbitals has been replaced by $b$ and $c$ for $\phi_4$ and $\phi_5$, respectively. These expressions should be modified due to the mixing of $\phi_1$ and $\phi_2$ via symmetry.

If terms in $a_1$ and $a_1'$ (introduced through spin-orbit coupling between $\phi_1$ and $\phi_2$, in their symmetry-mixed forms) can be ignored, then instead of Eqns. (14), the expressions of Table 8 may be used, with $\lambda$ replaced by $a^2b_1{}^2\lambda$, $a^2b^2\lambda$ or $a^2c^2\lambda$. As with the central-field mechanism, it is necessary to assume that $b \approx c$ if any solutions are to be obtained.

Since $a$, $b_1$, $b$ and $c$ are molecular-orbital coefficients, their values must be less than or equal to unity. Further, unless most of the $d$-electron density is in the ligand orbitals, the coefficients must be greater than 0.5.

The extent of the departure of these coefficients from unity measures the extent of delocalisation of the metal electrons due to metal–ligand bonding. Thus, "$a$" measures[96] $\sigma$-bonding "$b$" measures out-of-(xy)plane $\pi$-bonding, and $b_1$ measures in-(xy)plane $\pi$-bonding. It is often assumed[157,159,160,164] that there is no out-of-plane $\pi$-bonding ($b = 1$), when the MO description is used, but the examples discussed below will illustrate that such a generalisation is invalid.

### (*ii*) *Measured reduction factors*

The most accurate data are obtainable only when ESR and polarised electronic spectra are recorded on single-crystals of known structure. Table 11 lists all such available data on the anisotropy of $\lambda'/\lambda$ ($\lambda'$ is the effective value of the spin-orbit coupling constant, $\lambda$ its free-ion value).

It is impossible to determine all of the parameters $r_\parallel$, $r_\perp$, $a$, $b_1$ and $b$ from this data, but consider first the possibility that the dominant factor is symmetry-restricted covalency. Then in the absence of in-plane $\pi$-bonding ($b_1 = 1$) $a$ and $b$ may be determined. The bis-ethylenediamine complexes[77] involve this situation ($b_1 = 1$), since ethylenediamine is incapable of $\pi$-bonding and the "semi-ordinated" axial ligands can only $\pi$-bond with the $d_{xz}$ and $d_{yz}$ orbitals. Table 12 lists the values obtained for "$a$" and "$b$". Only ranges can be given, since $E(\phi_1-\phi_3)$ is only known within limits. The values of $b$ are all close to unity, as expected for little out-of-plane $\pi$-bonding (with axial ligands), but not equal to unity. $Cu(en)_2$-

TABLE 11

ANISOTROPY IN THE REDUCTION OF THE SPIN-ORBIT COUPLING CONSTANT, CALCULATED FROM CRYSTAL DATA†

| *Compound* | $(\lambda'_{\parallel}/\lambda)^{\pm}$ | $(\lambda'_{\perp}/\lambda)^{\pm}$ | *Ref.* |
|---|---|---|---|
| $Cu(en)_2(BF_4)_2$ | .73–.75 | .74 | 77 |
| $Cu(en)_2(ClO_4)_2$ | .76–.77 | .74 | 77 |
| $Cu(en)_2(SCN)_2$ | .71–.75 | .71 | 77 |
| $Cu(en)_2(NO_3)_2$ | .70–.76 | .78 | 77 |
| $Cu(en)_2Cl_2$ $H_2O$ | .68–.75 | .71 | 77 |
| $Cu(en)_2Br_2$ $H_2O$ | .69–.76 | .72 | 77 |
| $Cu(en)Cl_2$ | .68 | .67 | 134 |
| $Na_4Cu(NH_3)_4\{Cu(S_2O_3)_2\}_2 \cdot NH_3$ | .77 | .78 | 21 |
| $Na_4Cu(NH_3)_4\{Cu(S_2O_3)_2\}_2 \cdot H_2O$ | .76 | .78 | 21 |
| $Cu(NH_3)_4(CuBr_2)_2$ | .65–.75 | .72 | 11 |
| $Cu(NH_3)_4(NO_2)_2$ | .74 | .73 | 11 |
| $Cu(NH_3)_4SO_4$ $H_2O$ | — | .75 | 11 |
| $Cu(NH_3)_4(SCN)_2$ | .74 | .76 | 11 |
| $Cu(NH_3)_4(CuI_2)_2$ | .78–.72 | .71–.78 | 11 |
| $Cu(UO_2)_2(AsO_4)_2 \cdot 8H_2O$ | .80 | .78 | 135 |
| $Ba_2Cu(HCO_2)_6$ $4H_2O$ | .78 | .86 | 136 |
| $Cu(HCO_2)_2 \cdot 4H_2O$ | .77 | .69 | 136 |
| $(MeNH_3)_2CuCl_4$ | .71 | .66 | 166 |
| $CuH_2edta$ $H_2O$ | .82 | .72 | 67 |
| $CaCu(CH_3CO_2)_4$ $6H_2O$ | .926 | .78 | 125 |
| $(Me_3\phi CH_2N)_2CuCl_4$ | — | .52 | 146, 25 |
| $Cs_2CuCl_4$ | .69 | .51 | 167 |
| $Cu(dmg)_2$ | — | .60 | 168, 169 |
| $(NH_4)Cu(NH_3)_5(PF_6)_3$ | — | .77 | 93, 75 |
| $K_2BaCu(NO_2)_6$ | .81 | .77 | 71 |
| $Cu(N\text{-Mesalim})_2$ | .75 | .77 | 170 |
| $Cu(3\text{-Meacac})_2$* | .77 | .74 | 80 |
| $Cu(NH_3)_2Ag(SCN)_3$ | — | .68 | 147 |

* Other acetylacetone systems are omitted, since no agreement has been reached on the electronic assignment (section G, II, c)

† No corrections are applied to the electronic energies in respect of vibrational quanta, nor is the relativistic correction to the free-electron's $g$-value included

$(ClO_4)_2$ has the highest value of "$a$", and this is consistent with its having[171] the longest Cu–N bonds (2.04 Å), and hence the least covalency. The ranges of the other "$a$" values overlap, but that of the chloride extends to the lowest value. The chloride would be expected to have the greatest covalency, since it has [172] the shortest Cu–N bonds (1.985 Å). Previous data on the bis-ethylenediamine complexes have not been considered, since the frozen solution results[160] were based upon incorrect guesses for the electronic energies, and the crystal data[119,173] were interpreted on the incorrect basis of pure axial symmetry. There is now no reason to make an axial assumption, since expressions have been developed (see Appendix V) for calculating non-axial $g$-values for crystals containing two inequivalent molecular orientations. $Cu(dmg)_2$ has a lower value of $\lambda'$, in agreement with the probability of considerable out-of-plane $\pi$-bonding.

TABLE 12

MOLECULAR ORBITAL COEFFICIENTS FOR COPPER(II) BIS-ETHYLENEDIAMINE AND TETRAAMMINE COMPLEXES, CALCULATED FROM CRYSTAL DATA

| *Compound* | *a* | *b* |
|---|---|---|
| $Cu(en)_2(BF_4)_2$ | .73–.75 | 98–1 00[a] |
| $Cu(en)_2(ClO_4)_2$ | 76–77 | 96–98 |
| $Cu(en)_2(SCN)_2$ | .71–75 | 94–1 00 |
| $Cu(en)_2(NO_3)_2$ | .70–.76 | [b] |
| $Cu(en)_2Cl_2 \cdot H_2O$ | .68–75 | 94–1 00 |
| $Cu(en)_2Br_2 \ H_2O$ | .69–76 | .95–1 00 |
| $Na_4Cu(NH_3)_4\{Cu(S_2O_3)_2\}_2 \ H_2O$ | .76 | 1 00 |
| $Na_4Cu(NH_3)_4\{Cu(S_2O_3)_2\}_2 \ NH_3$ | 77 | 1 00 |
| $Cu(NH_3)_4(CuBr_2)_2$ | 65–75 | 96–1 00 |
| $Cu(NH_3)_4(NO_2)_2$ | 74 | .99 |
| $Cu(NH_3)_4(SCN)_2$ | 74 | [b] |
| $Cu(NH_3)_4(CuI_2)_2$ | .78–.72 | 91–1 00 |

[a] The values of "b" have been curtailed at 1 00, since b cannot have a value greater than unity
[b] All calculated values of "b" are greater than unity This has been explained[77] for $Cu(en)_2(NO_3)_2$ in terms of an ambiguity in $g_1$ and $g_2$ values affecting only this complex For $Cu(NH_3)_4(SCN)_2$, there may be a slight error in $g_\perp$ due to large angles of misalignment resulting from awkwardly shaped crystals

The values of $\lambda'_{\|}$ and $\lambda'_{\perp}$ for the mono-chelate $Cu(en)Cl_2$ are both less than the respective values in the bis-species. This is expected, since the structure[26] of Cu en $Cl_2$ involves chlorine atoms in the equatorial plane and these may contribute both to in-plane and to out-of-plane $\pi$-bonding. The involvement of considerable metal–ligand $\pi$-bonding with the chlorine atom is also suggested by the low values[66] of $\lambda'_{\|}$ and $\lambda'_{\perp}$ for the tetragonal-octahedral complex $(MeNH_3)_2CuCl_4$, and the flattened tetrahedral complexes[167] $Cs_2CuCl_4$ and $[Me_3\phi CH_2N]_2CuCl_4$.

The assumption of no in-plane $\pi$-bonding, should also be valid for the tetraammines[11], and Table 12 gives the MO coefficients then obtained. Again the values of "*b*" are close to unity, and the iodide may have the lowest b-value, consistent with its having[11] the smallest tetragonal distortion. Further the range of *a*-values extends highest in the iodide, and lowest in the bromide. If the actual values behave in the same way, covalency is greatest in the bromide, and least in the iodide. This agrees with the Cu–N bonds in the iodide[174] (2.14 Å mean), being the longest of all the tetraammines and almost the shortest in the bromide[174] (1.996 Å).

No simplification can be made for the other complexes listed in Table 11, since in-plane $\pi$-bonding cannot be discounted for chlorine or oxygen atoms. No M.O. coefficients can therefore be calculated. However, certain trends can be seen. In most cases $\lambda'_{\|} > \lambda'_{\perp}$, suggesting the presence of more out-of-plane $\pi$-bonding than inplane $\pi$-bonding Only for $Ba_2Cu(HCO_2)_6 \cdot 4H_2O$ and Cu(*N*-Mesalim)$_2$ is this not true.

The layer structure[15] of $Cu(HCO_2)_2 \cdot 4H_2O$ requires that the oxygen (for-

mate) $p$-orbital, unused in $sp^2$ $\sigma$-bonding (to copper and carbon, leaving a lone pair), is perpendicular to the plane of the $CuO_4$ (formate) unit, and can therefore form $\pi$-MO's with the $d_{xz}$ and $d_{yz}$ (and carbon) orbitals The lone pair is directed parallel to one lobe of the $d_{xy}$ orbital, and can give little overlap. The crystal structure therefore agrees with the anisotropy in $\pi$-bonding which is suggested by the $\lambda'$ values.

The situation in the structure[24] of $Ba_2Cu(HCO_2)_6 \cdot 4H_2O$ is complicated by the presence of Ba–O(formate) bonds. These require the formate groups of the (water)O–Cu–O(formate) plane to be orientated so that the oxygen $p$-orbitals are directed towards the $d_{xy}$ orbital. This leads, as observed, to $\pi$-bonding anisotropy of the opposite type to that of $Cu(HCO_2)_2 \cdot 4H_2O$. In $Cu(UO_2)_2(AsO_4)_2 \cdot 8H_2O$[16], the $\pi$-orbitals of the uranyl ion can bond with the copper $d_{xz}$ and $d_{yz}$ orbitals, to produce the observed anisotropy. Acetate groups perform the same function in $CaCu(CH_3CO_2)_4$ $6H_2O$ [55], the anisotropy of $CuH_2edta \cdot H_2O$ is not understood[67]. Cu(*N*-Mesalim)$_2$[170] appears to have more in-plane $\pi$-bonding, than out-of-plane $\pi$-bonding, and is also not understood.

The five-coordinate complexes $Cu(NH_3)_2Ag(SCN)_3$ [147] and $(NH_4)Cu(NH_3)_5(PF_6)_3$ [75] are interesting, in that the $\lambda'_\perp$ values indicate more out-of-plane bonding in the former. This is expected, due to the presence of thiocyanate ligands[147]. If a square-based pyramidal stereochemistry is appropriate for the latter, then no $\pi$-bonding can be present and $(\lambda'_\parallel/\lambda)^{\frac{1}{2}} \approx (\lambda'_\perp/\lambda)^{\frac{1}{2}}$, as in $NaCu(NH_3)_4\{Cu(S_2O_3)_2\}_2NH_3$ [21] (Table 11). Using an estimated value of $(\lambda'_\parallel/\lambda)^{\frac{1}{2}} = 0.77$, and $g_\parallel = 2.2516$ a value of the energy of the $d_{xy} \rightarrow d_{x^2-y^2}$ transition of 15.7 $kK$ is obtained, in reasonable agreement with a value of 15.0 $kK$ for the energy of the $d_{xz}$, $d_{yz} \rightarrow d_{x^2-y^2}$ transition. This suggests that, in axial copper(II) complexes involving $\sigma$-bonding ligands, the values of $(\lambda'_\parallel/\lambda)^{\frac{1}{2}}$ and $(\lambda'_\perp/\lambda)^{\frac{1}{2}}$ may be reasonably equated, and used to evaluate the energy of the $d_{xy} \rightarrow d_{x^2-y^2}$ transition The recent attempt[175] to calculate the effect of covalency on the second moments of the ESR spectrum of $Na_4Cu(NH_3)_4\{Cu(S_2O_3)_2\}_2$ (assuming that the ammonia adduct was used[21]) must be incorrect, as the energy of the $d_{xz}$, $d_{yz} \rightarrow d_{x^2-y^2}$ transition was "estimated" to be at 25 0 $kK$.

In spite of the partial success of this treatment, it has ignored central-field covalency and although, on this basis, the data can be understood in terms of varying metal–ligand $\pi$-bonding, the presence of metal–ligand $\pi$-bonding is not established.

Hitchman[176] has considered the interpretation of rhombic $g$-tensors and has obtained the probability distribution of the unpaired electron along the x-, y- and z-axes. In the case of two complexes. $Cu(MeOAc)_2 \cdot 2H_2O$ and $[Cu(bipy)_2ONO]NO_3$, Hitchman's treatment differs from ours[152] in the definition of molecular axes. The dominant perturbation in the stereochemistry of these complexes appears to be an axial compression. We, therefore, take this to be the z-axis, while Hitchman defines it as the x-axis. This labelling will not effect the physical proper-

ties, however, it probably invalidates Hitchman's approximation that $r_x = r_y$ for these complexes. Plots of $r_y$ and $r_z$, for varying $r_x$, indicate relatively small changes, but are more valuable in showing that the wavefunction coefficients are relatively constant.

## APPENDIX

### 1 LINE SHAPES FOR NON-DILUTE POWDERED SAMPLES[104]

In a polycrystalline sample, all possible orientations of the molecules are presented to the magnetic field, and therefore a spread of the signal is observed, this being the envelope for all $g$-values between the principal values[104] Each $g$-value contributes to the line-shape according to its statistical weight. Several analyses of the line-shape have been used[104 108–115], varying in sophistication, according to whether the $g$-value, hyperfine and line-width tensors are considered to be isotropic, axial or completely anisotropic This allows computer simulation of the line-shape for a given set of parameters

For each hyperfine component (nuclear quantum number $I$), the absorption intensity at field $H$ is

$$S(H) = \frac{1}{(2I+1)} f(\theta) \cdot \frac{dH}{dN} \tag{27}$$

where for the axial case, $f(\theta) = g_\perp^2[(g_\parallel/g)^2+1]/8$ (and $g^2 = g_\parallel^2 \cos^2\theta + g_\perp^2 \sin^2\theta$, when the field is at angle $\theta$ to the $g_\parallel$ vector) and takes into account the variation of transition moment

TABLE 13

A COMPARISON OF SOME CRYSTAL AND (UNCORRECTED) POWDER ESR DATA

| *Complex* | *Crystal g-values* | | | | *Powder g-values* | | | |
|---|---|---|---|---|---|---|---|---|
| | $g_1$ | $g_2$ | $g_3$ | *Ref.* | $g_1$ | $g_2$ | $g_3$ | *Ref* |
| $CuF_2$ 5HF $5H_2O$ | | 2 090 | 2 410 | 103 | | 2 084 | 2 383 | 103 |
| $CuCl_2$ $2H_2O$ | 2 037 | 2.187 | 2 252 | 103 | 2 050 | 2 195 | 2 250 | 125 |
| $CuSO_4 \cdot 5H_2O$ | | 2 07 | 2 28 | 109 | | 2 07 | 2 28 | 125 |
| $(NH_4)_2Cu(SO_4)_2 \cdot 6H_2O$ | 2 09 | 2 25 | 2 32 | 103 | 2.07 | 2 21 | 2 35 | 125 |
| $(NH_4)_2Zn(SO_4)_2$ $6H_2O$ | 2 04 | 2 26 | 2.26 | 103 | 2 06 | 2 28 | 2 28 | 125 |
| $K_2CuCl_4$ $2H_2O$ | 2 06 | 2.22 | 2 22 | 103 | 2 07 | 2 24 | 2 24 | 125 |
| $(NH_4)_2CuCl_4 \cdot 2H_2O$ | 2 07 | 2 24 | 2 24 | 103 | 2 07 | 2 26 | 2 26 | 125 |
| $Cu(salim)_2$ | 2.040 | 2 050 | 2 200 | 103 | | 2 055 | 2 180 | 125 |
| Cu$\alpha, \beta, \gamma, \delta, \phi_4$ porphyrin* | | 2 05 | 2 17 | 103 | | 2 07 | 2 19 | 103 |
| $Cu(NH_3)_4SO_4 \cdot H_2O$ | 2 054 | 2 104 | 2 181 | 103 | 2 050 | 2 100 | 2 183 | 125 |
| $Cu(en)_3SO_4$ | | 2.110 | 2 126 | 177 | | 2.130 | 2 130 | 125 |
| $Cu(en)_2(NO_3)_2$ | 2 059 | 2 059 | 2 189 | 103 | | 2 050 | 2 180 | 125 |
| $Cu(en)Cl_2$ | | 2 049 | 2.239 | 103 | | 2 045 | 2 240 | 125 |
| $Cu(NH_3)_5(NH_4)(PF_6)_3$ | 2 0643 | 2 0666 | 2 2516 | 125 | | 2 053 | 2 240 | 93 |
| $CuCl_2(py)_2$ | 2.0611 | 2 0854 | 2 2198 | 125 | 2 065 | 2 09 | 2 22 | 125 |
| $Cu(NCS)_2(py)_2$ | 2 0573 | 2 0599 | 2.2790 | 125 | | 2 055 | 2 27 | 125 |
| $Cu(NH_3)_2(CH_3CO_2)_2$ | 2 0497 | 2.1100 | 2 2114 | 125 | 2 049 | 2.113 | 2 214 | 123 |
| $Cutren(NCS)_2$ | 2 0835 | 2 1321 | 2 1572 | 125 | 2 060 | 2.178 | 2 178 | 124 |
| $(NH_4)_2CuCl_4$ | 2.0652 | 2 1714 | 2.1734 | 125 | 2 152 | 2 152 | 2 152 | 125 |
| $K_3Cu(NO_2)_5$ | 2.1016 | 2 1214 | 2 1794 | 125 | 2.10 | 2 10 | 2 174 | 125 |
| $Cu(dmp)Cl_2H_2O$ | 2 0299 | 2 1325 | 2 2752 | 125 | 2 033 | 2.171 | 2 234 | 125 |

* Measurements at liquid nitrogen temperatures

with angle. $dN$ is the number of spins (from the total of $N_0$) with their principal axes inclined between angles $\theta$ and $(\theta+d\theta)$ to the field, and is given by $dN = (N_0/2) \sin\theta\, d\theta$. Eqn. (27) must be integrated over all $\theta$, and the results summed for all hyperfine components Typical results (as derivative curves) are given in Fig 7.

When these curves are compared with the parameters used for plotting them, it is found that the fields at points A, C, D, E and F correspond[109] quite closely to the values of $g_{\parallel}$ and $g_{\perp}$ (axial case), $g_3$, $g_2$ and $g_1$ (non axial case with $g_3 > g_2 > g_1$) For $g_{\perp}$, the agreement is even better[115] with the field at a point dividing BC in the ratio of $(\Delta H/P - K\Delta H)\cdot K\Delta H$ The difference between the fields at B and C is $\Delta H/P$, and can be used to estimate the crystal line-width (assumed isotropic) The values[115] of the coefficients $P$ and $K$ depend on whether the line-shape is gaussian.

$$S(H) = S(H_0) \exp\left[-4 \ln 2 \frac{(H-H_0)^2}{\Delta H}\right]$$

or lorentzian,

$$S(H) = S(H_0)/\left[1+4\frac{(H-H_0)^2}{\Delta H}\right].$$

(where $H_0$ is the field at the centre of the signal). In the gaussian case $P = 1.8$ and $K = 0\,2$, while for a lorentzian curve $P = 2\,28$ and $K = 0\,15$

Table 13 shows a comparison between some powder ($g_{\perp}$ uncorrected), and crystal, $g$-values. Table 14 gives a further comparison[125], for the tetraammines and bis(ethylenediamine) complexes, which shows the advantage of the above correction procedure for $g_{\perp}$. For better results from powder data, it is necessary to use computer simulation techniques[111-114].

By whatever method the powder $g$-values are measured they can only yield the crystal $g$-values, rather than the molecular $g$-values

## II. ANGULAR VARIATION OF $g$-VALUES

It has been shown[102] that the solution of the wave equation, using the axial Hamiltonian (3), gives $\Delta E = g\beta H$ with $g^2 = g_{\parallel}^2 \cos^2\theta + g_{\perp}^2 \sin^2\theta$, where $\theta$ is the angle between the applied field and the principal axis For the non-axial case, the solution is similar and

$$g^2 = g_x^2 l^2 + g_y^2 m^2 + g_z^2 n^2 \qquad (15)$$

TABLE 14

A COMPARISON OF SOME CRYSTAL AND POWDER ESR DATA SHOWING THE EFFECTIVENESS OF THE CORRECTION OF $g_{\perp}$ FOR LINE-SHAPE DEPENDENCE[125,76]

| *Complex* | *Crystal g-values* | | *Powder g-values** | | | |
|---|---|---|---|---|---|---|
| | $g_{\parallel}$ | $g_{\perp}$ | $g_{\parallel}$ | $g_{\perp}(u)$ | $g_{\perp}(G)$ | $g_{\perp}(L)$ |
| $Cu(NH_3)_4(CuBr_2)_2$ | 2 214 | 2 047 | 2 206 | 2 041 | 2 044 | 2 044 |
| $Cu(NH_3)_4(CuI_2)_2$ | 2 223 | 2 056 | 2 219 | 2 051 | 2 055 | 2 055 |
| $Cu(NH_3)_4(NO_2)_2$ | 2 234 | 2 052 | 2 239 | 2 048 | 2 050 | 2 050 |
| $Cu(NH_3)_4Ag(SCN)_3$ | 2 232 | 2 052 | 2 228 | 2 046 | 2 050 | 2 050 |
| $Cu(NH_3)_4(SCN)_2$ | 2 237 | 2 056 | 2 233 | 2 047 | 2 052 | 2.051 |
| $Cu(en)_2(ClO_4)_2$ | 2 209 | 2 048 | 2 200 | 2 045 | 2 048 | 2 048 |
| $Cu(en)_2(NCS)_2$ | 2 199 | 2 044 | 2 195 | 2 043 | 2 044 | 2 044 |
| $Cu(en)_2(BF_4)_2$ | 2 198 | 2.048 | 2 192 | 2 043 | 2 048 | 2 048 |
| $Cu(en)_2Cl_2 \cdot H_2O$ | 2 205 | 2 047 | 2 205 | 2 043 | 2 045 | 2 045 |
| $Cu(en)_2Br_2 \cdot H_2O$ | 2 208 | 2 049 | 2 205 | 2 042 | 2 045 | 2 045 |
| $Cu(en)_2(NO_3)_2$ | 2 184 | 2 066 | 2 180 | 2 050 | 2 057 | 2 057 |
| $Cu(en)_2Ni(CN)_4$ | 2 213 | 2 050 | 2 206 | 2 047 | 2 049 | 2 049 |

* $g_{\perp}(u)$ is the uncorrected value, while $g_{\perp}(G)$ and $g_{\perp}(L)$ are corrected respectively for gaussian and lorentzian line-shapes

where $l$, $m$ and $n$ are direction cosines of $H$, with respect to the magnetic x-, y- and z-axes This relationship may be used to derive[116] others, which express the $g$-value relative to an arbitrary, orthogonal, set of axes X, Y and Z

$$\begin{aligned} g_X^2 &= g_{yy}^2 \cos^2 \phi_x + g_{zz}^2 \sin^2 \phi_x + 2g_{yz}^2 \cos \phi_x \sin \phi_x \\ g_Y^2 &= g_{zz}^2 \cos^2 \phi_y + g_{xx}^2 \sin^2 \phi_y + 2g_{zx}^2 \cos \phi_y \sin \phi_y \\ g_Z^2 &= g_{xx}^2 \cos^2 \phi_z + g_{yy}^2 \sin^2 \phi_z + 2g_{xy}^2 \cos \phi_z \sin \phi_z \end{aligned} \quad (16)$$

Here, $g_X$, $g_Y$ and $g_Z$ are the $g$-values at angles $\phi_x$, $\phi_y$ and $\phi_z$, during rotations of the magnetic field about the X-, Y- and Z-axes, respectively The $g_{ij}^2$ coefficients are the elements of the $3 \times 3$ matrix $[g_{ij}^2]$ Measurements of the $g$-values at several angles, during the three rotations about X, Y and Z, allow these coefficients to be evaluated by means of a Fourier, or a least-squares, analysis (see section C) If the $[g_{ij}^2]$ matrix is transformed by rotating from the (X, Y, Z) reference system to the (x, y, z) frame, the diagonal matrix

$$\begin{bmatrix} g_x^2 & 0 & 0 \\ 0 & g_y^2 & 0 \\ 0 & 0 & g_z^2 \end{bmatrix}$$

results. This gives the desired principal $g$-values if a matrix can be found which does diagonalise $[g_{ij}^2]$ This problem is the standard eigenvalue problem, and can be solved by a computer to give eigenvalues $g_x^2$, $g_y^2$ and $g_z^2$, and also the transformation matrix of eigenvectors.

$$\begin{bmatrix} l_x & l_y & l_z \\ m_x & m_y & m_z \\ n_x & n_y & n_z \end{bmatrix} \quad (17)$$

where $l_i$, $m_i$ and $n_i$ are the direction cosines of the $g_i$-axis ($i = x$, $y$ or $z$), with respect to the X-, Y- and Z-axes Thus, the angles between the principal $g$-axes and the experimental X-, Y- and Z-axes, can be evaluated (from matrix 17). The latter axes will be defined relative to the $a$, $b$ and $c$ crystallographic axes The method, given above, is of general application and must be employed for triclinic crystals A simpler method, given by Schonland[117], is available for monoclinic crystals. Once the triclinic computer programme has been written, it is convenient to use it for monoclinic, trigonal, hexagonal and orthorhombic crystals also (without modification). Further, corrections for misalignments (see section III) are easily included in the same programme For tetragonal crystals, it is often possible to obtain the principal $g$-values by making two measurements on the appropriately orientated crystal For cubic crystals, there is no anisotropy to measure

Data on the orientation of the principal $g$-axes have been little used until now, more emphasis being put on the actual values of the $g$-factors However, it is possible to use angular data to establish the electronic ground state, when other data are ambiguous Thus the ground state in the bis-ethylenediamine complexes[77] is $d_{x^2-y^2}$ rather than $d_{xy}$ (in the "hole" formalism), because the axes of $g_x$ and $g_y$ point almost along the Cu–N bonds, rather than between them Further, in cases where the effective crystal-field symmetry does not correspond to the crystallographic molecular symmetry, the former can be determined by locating the principal magnetic axis Thus, $Cu(en)Cl_2$ behaves electronically[134] as if it had $D_2$ symmetry, with the z axis perpendicular to the chelate plane, rather than the crystallographic $C_2$ symmetry.

### III MEASUREMENT OF THE PRINCIPAL $g$-VALUES OF SINGLE-CRYSTALS

As discussed above, the method depends on rotating the crystal about three orthogonal axes, measuring the $g$-value dependence on angle in each case. Eqns (16) are then solved It has been found convenient to mount, using grease, the same face of the crystal ($\sim 2$ mm $\times$ 1 mm $\times$ 0 5 mm) on to mutually perpendicular faces, A and B, of the perspex rod illustrated in Fig. 28 This rod can then be mounted vertically in the cavity of the ESR spectrometer, and rotated in the horizontal magnetic field (or the field rotated about the cavity), a scale of angle being attached to the rod (or to the magnet) The rod is placed in the Varian variable-temperature quartz dewar insert, where it is centralised by ring D and cone C. The $g$-value is measured by recording the first derivative signal, as the field is scanned. Calibration is achieved using a speck of DPPH

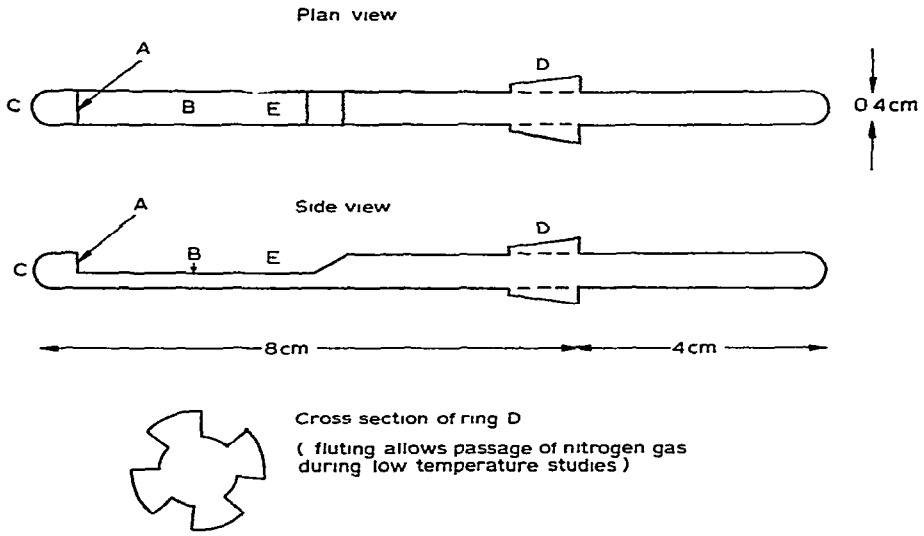


Fig 28 The perspex rod used for single-crystal ESR measurements

($g = 2\ 0036$) on the rod (E), and by measuring the hyperfine splitting of a sample of MgO powder (containing $Mn^{2+}$ impurity), at the same chart speed Using the central 86 7-gauss interval in the $Mn^{2+}$ spectrum, the scale on the chart can be calibrated in gauss/cm, while the DPPH signal fixes the field at one point on the chart (if the klystron frequency is measured, since $h\nu_0 = 2\ 0036\ \beta H_0$) Hence the field at which the sample resonance occurs can be calculated from the distance on the chart between it, and the sharp DPPH signal

A prominent face of the crystal is first mounted on to rod-face A, with the edge of the crystal face lying along the intersection of faces A and B Then the rotation about the rod-axis, may be defined as the X-rotation, if the perpendicular to the crystal face is defined as X The crystal is then slid around on to face B of the rod, and under a microscope, the edge (which may be defined as the Z-axis) of the crystal face is aligned perpendicularly to the rod-axis (using the microscope cross-wires) Rotation about the rod-axis gives the Y-rotation Finally, using the microscope, the crystal is reorientated on rod-face B, so that the Z-axis lies along the rod-axis (rotation about which gives the Z-rotation).

The Geusic–Brown Eqns.[116] (16) have, implicit within them, angular origins, such that

$$\left.\begin{array}{l}\phi_x = 0° \text{ when } H \text{ is parallel to Y}\\ \phi_x = 90° \text{ when } H \text{ is parallel to Z}\\ \phi_y = 0° \text{ when } H \text{ is parallel to Z}\\ \phi_y = 90° \text{ when } H \text{ is parallel to X}\\ \phi_z = 0° \text{ when } H \text{ is parallel to X}\\ \phi_z = 90° \text{ when } H \text{ is parallel to Y}\end{array}\right\} \quad (18)$$

If these origins are not located exactly, then angular errors $\varepsilon_x$, $\varepsilon_y$ and $\varepsilon_z$ will occur in the measurements Fortunately, it is possible to correct for these misalignments (and all errors, since these may be represented as contributions to $\varepsilon$, for example, in the Y-rotation, if the edge of the crystal is not accurately aligned perpendicularly to the rod-axis, there is a contribution to $\varepsilon_x$), using three matrix elements, which would otherwise be redundant. Reference 118 shows how this is done, and also gives equations for the least-squares analysis

The angles $\varepsilon$ are given by

$$2\varepsilon_x = \pm[\cos^{-1} | (a_z - a_y)/2(b_x^2 + c_x^2)^{\frac{1}{2}} | - \tan^{-1} | c_x/b_x |]$$
$$2\varepsilon_y = \pm[\cos^{-1} | (a_x - a_z)/2(b_y^2 + c_y^2)^{\frac{1}{2}} | - \tan^{-1} | c_y/b_y |]$$
$$2\varepsilon_z = \pm[\cos^{-1} | (a_y - a_x)/2(b_z^2 + c_z^2)^{\frac{1}{2}} | - \tan^{-1} | c_z/b_z |]$$

The angles on the right-hand-side of these equations may be taken in the first quadrant, if the sign ($\pm$) is that of $c/b$. Here, $a = g_{ii}^2+g_{jj}^2$, $b = \frac{1}{2}(g_{ii}^2-g_{jj}^2)\cos 2\varepsilon+g_{ij}^2 \sin 2\varepsilon$, and $c = g_{ij}^2 \cos 2\varepsilon-\frac{1}{2}(g_{ii}^2-g_{jj}^2)\sin 2\varepsilon$.

Ayscough[178] suggests that the maximum and minimum $g$-values in each rotation may be used to calculate the off-diagonal elements of the $[g_{ij}^2]$ matrix:

$$g_{ij}^2 = \tfrac{1}{2}[(\Delta X)^2-(g_{ii}^2-g_{jj}^2)^2]^{\frac{1}{2}} \tag{21}$$

(Ayscough's equation 5.18 is incorrect[147]) where $\Delta X$ is the difference between the maximum and minimum values of $g^2 = X$. It is also possible to obtain the diagonal elements, in the same way[147], in terms of the $X' = X_{max} + X_{min}$:

$$\left.\begin{aligned} g_{xx}^2 &= \tfrac{1}{2}(X'_{xy}+X'_{xz}-X'_{yz}) \\ g_{yy}^2 &= \tfrac{1}{2}(X'_{yz}+X'_{xy}-X'_{xz}) \\ g_{zz}^2 &= \tfrac{1}{2}(X'_{yz}+X'_{xz}-X'_{xy}) \end{aligned}\right\} \tag{22}$$

where the subscripts $xy$, $xz$ and $yz$ refer to the planes perpendicular to the rotation axes. $g_{ij}^2$ is taken to be positive if $g^2$ reaches a maximum in the quadrant between the positive i- and j-axes, and negative if $g^2$ reaches a minimum in this quadrant.

Thus, all the diagonal and off-diagonal elements of $[g_{ij}^2]$ may be evaluated, using eqns (21) and (22), from only six measurements—the maximum and the minimum value of $g^2$ in each of three rotations. These measurements can easily be made with an instrument such as the JEOL JES-3BS-X ESR spectrometer, where the oscilloscope display is sufficiently sensitive to the variation of $g$-value, so that the positions of the extrema may be located visually. A further advantage of this simple method is that angular misalignments are taken into account automatically.

## IV ESR LINE WIDTHS FOR SINGLE CRYSTALS[102,103 179 180]

Electron spin resonance consists not only in an absorption of energy to give an excited state, but also the decay ("relaxation") of this excited state. If the relaxation is fast, the excited state lifetime is short, and hence the energy uncertainty is large (via the Heisenberg principle), resulting in a broad spectral absorption line. The line-width (expressed as a magnetic field) is

$$\Delta H \sim 1/(2\pi T_1)$$

where $T_1$ is the relaxation time. The relaxation mechanism is, therefore, important, and can be of two forms—spin-lattice relaxation, or spin-spin relaxation. Uusually, the energy is transferred from the electron spin-system to the lattice vibrations. The spin–lattice coupling (characterised by $T_1$) is provided by the spin–orbit interaction.

$T_1$ decreases ($\Delta H$ increases) as the temperature increases, because the lattice vibrations increase in amplitude. $T_1$ also depends on $g$, and hence on the sensitivity of $g$ to stereochemistry. This sensitivity depends on the presence of low-lying excited states which are spin–orbit coupled to the ground-state. For tetrahedral copper(II) compounds[167] (*e g* $CuCl_4^{2-}$), there often is such a low-lying state (due to the splitting of the $^2T_{2g}$ state), hence $T_1$ is short and $\Delta H$ large.

There may be an interaction between two or more spin-systems (*i e* metal ions) and this is characterised by the spin–spin relaxation time ($T_2$). There are two mechanisms for this process —a dipole/dipole interaction between ions regarded as fixed magnets, and an exchange interaction, through the correlation of electron spins via orbital overlap. Neither of these effects is temperature dependent, but both are proportional to the inverse-cube of the inter-spin distance. Thus, dilution reduces the spin–spin contributions to $\Delta H$.

Spin–spin interactions may broaden the resonance line, because the electron spin produces a magnetic field of $\sim 600G$ at a typical distance of 4 Å. This adds or subtracts from the applied field, thus spreading it. However, electron delocalisation results in line-narrowing because the electron "sees" the average of all the local variations in magnetic field. The combined effects of the dipolar and exchange contributions are given by[181]

$$\Delta H = 20H_P^2/3H_e$$

where the dipolar component $H_P$ is $1.849\ 10^4\ g/a_0^3$ ($a_0$ = unit-cell length in Å) for a cubic lattice, and the exchange component $H_e$ is $2[2\ 83S(S+1)]^{\frac{1}{2}}Jhc/g\beta$ ($J$ = exchange energy in $cm^{-1}$).

The results of these two factors can be described by distinguishing four cases:

(*i*) Identical ($S = \frac{1}{2}$) spin-sites give rise to line-narrowing through contributions to the fourth moment of the line $[\int (H-H_0)^4 I(H)\,dH$, where $H_0$ is the resonance value of the field, and $I(H)$ gives the shape of the absorption curve, as a function of $H$]

(*ii*) Non-identical spin-sites give rise, in addition, to a broadening, through contributions to the second moment of the line $[\int (H-H_0)^2 I(H)\,dH]$. However, lines due to each of the non-equivalent sites will be observed.

(*iii*) Relatively strong exchange between non-equivalent ions causes the narrowing effect to become dominant Further, the several lines draw together as the exchange interaction increases, and finally coalesce [when $J > (g-g')\beta H$, where $g$ and $g'$ refer to different sites] at the root-mean-square $g$-value This effect is shown[182] at 9000 Mc/s (X-band) by $CuSO_4 \cdot 5H_2O$, but at higher frequencies the two separate lines are observed

(*iv*) Strong exchange results when identical ions are grouped in isolated pairs The effect, then, is of a single spin-system with $S = 1$ or 0 This situation is present[183] in $[Cu(CH_3CO_2)_2 \cdot H_2O]_2$ The triplet state gives a zero-field splitting and hence absorptions at two values of the magnetic field. It is not the purpose of this review to discuss these binuclear complexes

Now, if the unit cell of the copper(II) complex contains molecules in only one orientation, spin–spin interactions will affect the line-width, but not the $g$-values, until the strong exchange of case (iv) is reached However, if the unit cell contains two or more sets of crystallographically non-equivalent ions, the spin–spin interaction will not only affect the line-width, but may cause the individual signals to draw together[182] or coalesce before the exchange interaction becomes strong ($J \sim 0.03$ cm$^{-1}$ compared with $J \sim 300$ cm$^{-1}$ for $[Cu(CH_3CO_2)_2\ H_2O]_2$). In fact, virtually all non-dilute mononuclear copper(II) complexes, with non-equivalent ions exhibit only the single coalesced signal at X-band frequencies[103]. This is probably due to the dependence of $J$ on $\lambda^2$, which is relatively large for copper(II)

Other contributions to the crystal line-width come from unresolved hyperfine structure[104], and from the avoidable instrumental effects of saturation broadening (too much power) or modulation broadening (too large a sweep field)

## V THE CALCULATION OF MOLECULAR $g$-VALUES FROM CRYSTAL $g$-VALUES

Consider the case of a unit cell containing only two sets of crystallographically non-equivalent (but chemically equivalent) axial molecules Let the two principal axes of the molecules (along the directions-of $g'_{\parallel}$ and $g''_{\parallel}$ for the two sets of molecules) be inclined at angle $2\gamma$, and let the y and z axes bisect this angle, while the x axis is perpendicular to the plane containing

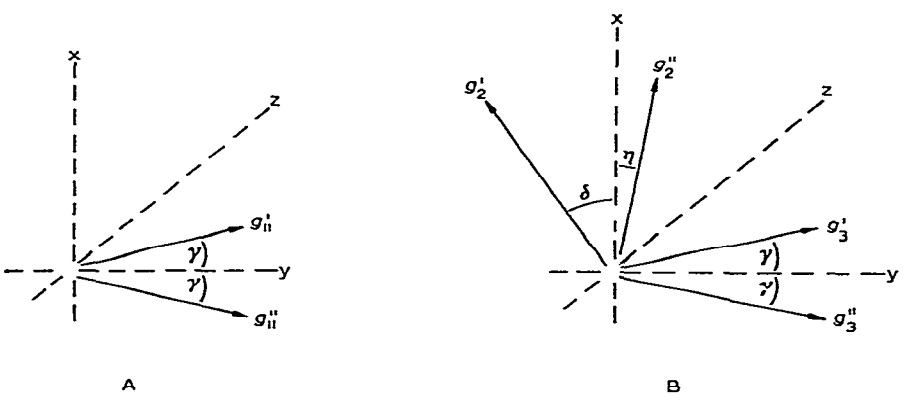


Fig. 29. A, the relationship between two axial molecules and B, the relationship between two non-axial molecules

the $g'_{\parallel}$ and $g''_{\parallel}$ vectors (Fig 29A) Then it has been shown[119] that the crystal has principal $g$-values which are along the x-, y- and z-axes, and given by:

$$\left.\begin{aligned} g_x &= g_\perp \\ g_y &= [g_\parallel^2 \cos^2\gamma + g_\perp^2 \sin^2\gamma]^{\frac{1}{2}} \\ g_z &= [g_\parallel^2 \sin^2\gamma + g_\perp^2 \cos^2\gamma]^{\frac{1}{2}} \end{aligned}\right\} \quad (23)$$

Thus, if $\gamma = 45°$, $g_y = g_z$ and the crystal could be mistaken for one with effective $g$-values of "$g_\parallel$" $= g_\perp$ and "$g_\perp$" $= [(g_\parallel^2 + g_\perp^2)/2]^{\frac{1}{2}}$.

Until recently[120], equations were not available for the non-axial case. This requires two further angles ($\delta$ and $\eta$) to specify the inclination of the two sets of $g_z$ axes to the x-axis The x-axis is defined as perpendicular to the plane containing the two $g_3$ axes, these being inclined at an angle $2\gamma$ to each other, and the y- and z-axes bisect the angle $2\gamma$ internally and externally (Fig. 29b). Hypothetical rotations of the magnetic field are performed, about the x-, y- and z-axes to give a matrix $[(g_{ij}^*)^2]$, in the same way that $[g_{ij}^2]$ is obtained experimentally The elements of this matrix are[120].

$$\left.\begin{aligned} (g_{xx}^*)^2 &= g_1^2 + \tfrac{1}{2}(g_2^2 - g_1^2)(\cos^2\delta + \cos^2\eta) \\ (g_{yy}^*)^2 &= g_3^2\cos^2\gamma + g_2^2\sin^2\gamma - \tfrac{1}{2}(g_2^2 - g_1^2)\sin^2\gamma(\cos^2\delta + \cos^2\eta) \\ (g_{zz}^*)^2 &= g_3^2\sin^2\gamma + g_2^2\cos^2\gamma - \tfrac{1}{2}(g_2^2 - g_1^2)\cos^2\gamma(\cos^2\delta + \cos^2\eta) \\ (g_{yz}^*)^2 &= \tfrac{1}{8}(g_2^2 - g_1^2)\sin 2\gamma(\cos 2\delta - \cos 2\eta) \\ (g_{xz}^*)^2 &= \tfrac{1}{4}(g_2^2 - g_1^2)\cos\gamma(\sin 2\delta + \sin 2\eta) \\ (g_{xy}^*)^2 &= -\tfrac{1}{4}(g_2^2 - g_1^2)\sin\gamma(\sin 2\delta - \sin 2\eta) \end{aligned}\right\} \quad (24)$$

If this matrix is diagonalised, the principal $g$-values are obtained Conversely, from the measured principal crystal $g$-values ($g_a$, $g_b$ and $g_c$), the molecular $g$-values $g_1$, $g_2$ and $g_3$ may be calculated The problem is complicated, unless (as usual, since molecules are often related by screw diad axes) $\delta = \eta$ when $g_{yz}^* = g_{xy}^* = 0$ In this case, $g_1$, $g_2$ and $g_3$ may be obtained from the measured values and the crystallographic angles $\gamma$ and $\delta$ using the simultaneous equations

$$\left.\begin{aligned} g_b^2 &= (g_{yy}^*)^2 \\ g_a^2 + g_c^2 &= (g_{xx}^*)^2 + (g_{zz}^*)^2 \\ g_a^2 \cdot g_c^2 &= (g_{xx}^*)^2 \cdot (g_{zz}^*)^2 - (g_{xz}^*)^4 \end{aligned}\right\} \quad (25)$$

The problem is generally more complicated for more than two non-equivalent sets of molecules, but may be simplified if the sets are related by symmetry elements Thus, if there are four sets of axial molecules in an orthorhombic unit cell, all making the same angle $\rho$ between their z-axes and the crystallographic c-axis they may often divide into two pairs Within each pair, the z-axes are inclined at angle $2\rho$, and the planes containing the z-axes of each pair are inclined at the same angle ($\omega$) to the a-axis, and at angle $2\omega$ to each other Due to exchange narrowing, each pair forms a system with principal $g$-values given by equations (23) (with $\gamma = \rho$). The pairs interact through exchange narrowing, according to equation (24) (where $\gamma = \omega$ and $\delta = \eta = 0$), giving the following principal $g$-values[125]

$$\left.\begin{aligned} g_p &= [g_\perp^2 + (g_\parallel^2 - g_\perp^2)\sin^2\rho\sin^2\omega]^{\frac{1}{2}} \\ g_q &= [g_\perp^2 + (g_\parallel^2 - g_\perp^2)\cos^2\rho]^{\frac{1}{2}} \\ g_r &= [g_\perp^2 + (g_\parallel^2 - g_\perp^2)\sin^2\rho\cos^2\omega]^{\frac{1}{2}} \end{aligned}\right\} \quad (26)$$

In particular, if the four axial molecules are arranged with their z-axes pointing towards the corners of a tetrahedron, $\rho = 54°44'$, and $\omega = 45°$, giving $g_p = g_q = g_r = [(2g_\perp^2 + g_\parallel^2)/3]^{\frac{1}{2}}$, and only one $g$-value is observed at all orientations A similar, apparently isotropic, signal is produced from three mutually perpendicular molecules. Other combinations may give principal $g$-values which are so close that they cannot be resolved The case of four non-axial molecules in an orthorhombic unit cell has also been considered[125] However, exchange is not the only mechanism which can produce isotropic signals, alternative explanations involve the presence of free-rotation, or of pseudo-rotation of the dynamic Jahn–Teller type[70]

VI. THE ELECTRONIC SELECTION RULES FOR THE COPPER(II) ION IN VARIOUS SYMMETRIES AND GROUND STATES: VIBRATIONS ALLOWING THE TRANSITIONS

| Point group | a[a] b c d e | a-Ground state | | | | b-Ground state | | | | c-Ground state | | | |
|---|---|---|---|---|---|---|---|---|---|---|---|---|---|
| | | b→a | c→a | d→a | e→a | a→b | c→b | d→b | e→b | a→c | b→c | d→c | e→c |
| *A. Centrosymmetric* | | | | | | | | | | | | | |
| $C_{2h}$ | $A_g\ A_g\ A_g\ B_g\ B_g$ z($A_u$) | $a_u$ | $a_u$ | $b_u$ | $b_u$ | $a_u$ | $a_u$ | $b_u$ | $b_u$ | $a_u$ | $a_u$ | $b_u$ | $b_u$ |
| | x,y($B_u$) | $b_u$ | $b_u$ | $a_u$ | $a_u$ | $b_u$ | $b_u$ | $a_u$ | $a_u$ | $b_u$ | $b_u$ | $a_u$ | $a_u$ |
| $C_{4h}$ | $A_g\ B_g\ B_g\ E_g\ E_g$ z($A_u$) | $b_u$ | $b_u$ | $e_u$ | $e_u$ | $b_u$ | $a_u$ | $e_u$ | $e_u$ | $b_u$ | $a_u$ | $e_u$ | $e_u$ |
| | xy($E_u$) | $e_u$ | $e_u$ | $2a_u+2b_u$ | $2a_u+2b_u$ | $e_u$ | $e_u$ | $2a_u+2b_u$ | $2a_u+2b_u$ | $e_u$ | $e_u$ | $2a_u+2b_u$ | $2a_u+2b_u$ |
| $D_{2h}$ | $A_g\ A_g\ B_{1g}B_{2g}B_{3g}$z($B_{1u}$) | $b_{1u}$ | $a_u$ | $b_{3u}$ | $b_{2u}$ | $b_{1u}$ | $a_u$ | $b_{3u}$ | $b_{2u}$ | $a_u$ | $a_u$ | $b_{2u}$ | $b_{3u}$ |
| | y($B_{2u}$) | $b_{2u}$ | $b_{3u}$ | $a_u$ | $b_{1u}$ | $b_{2u}$ | $b_{3u}$ | $a_u$ | $b_{1u}$ | $b_{3u}$ | $b_{3u}$ | $b_{1u}$ | $a_u$ |
| | x($B_{3u}$) | $b_{3u}$ | $b_{2u}$ | $b_{1u}$ | $a_u$ | $b_{3u}$ | $b_{2u}$ | $b_{1u}$ | $a_u$ | $b_{2u}$ | $b_{2u}$ | $a_u$ | $b_{1u}$ |
| $D_{4h}$ | $A_{1g}B_{1g}B_{2g}E_g\ E_g$ z($A_{2u}$) | $b_{2u}$ | $b_{1u}$ | $e_u$ | $e_u$ | $b_{2u}$ | $a_{1u}$ | $e_u$ | $e_u$ | $b_{1u}$ | $a_{1u}$ | $e_u$ | $e_u$ |
| | xy($E_u$) | $e_u$ | $e_u$ | $a_{1u}+a_{2u}+b_{1u}+b_{2u}$ | $a_{1u}+a_{2u}+b_{1u}+b_{2u}$ | $e_u$ | $e_u$ | $a_{1u}+a_{2u}+b_{1u}+b_{2u}$ | $a_{1u}+a_{2u}+b_{1u}+b_{2u}$ | $e_u$ | $e_u$ | $a_{1u}+a_{2u}+b_{1u}+b_{2u}$ | $a_{1u}+a_{2u}+b_{1u}+b_{2u}$ |
| *B. Non centrosymmetric* | | | | | | | | | | | | | |
| $C_s$ | $A'\ A'\ A'\ A''\ A''$ z($A''$) | $a''$ | $a''$ | $a'$ | $a'$ | $a''$ | $a''$ | $a'$ | $a'$ | $a''$ | $a''$ | $a'$ | $a'$ |
| | x,y($A'$) | $a'$ | $a'$ | $a''$ | $a''$ | $a'$ | $a'$ | $a''$ | $a''$ | $a'$ | $a'$ | $a''$ | $a''$ |
| $C_2$ | $A\ A\ A\ B\ B$ z($A$) | $a$ | $a$ | $b$ | $b$ | $a$ | $a$ | $b$ | $b$ | $a$ | $a$ | $b$ | $b$ |
| | x,y($B$) | $b$ | $b$ | $a$ | $a$ | $b$ | $b$ | $a$ | $a$ | $b$ | $b$ | $a$ | $a$ |
| $C_3$ | $A\ E\ E\ E\ E$ z($A$) | $e$ | $e$ | $e$ | $e$ | $b$ | $b$ | $b$ | $b$ | $b$ | $b$ | $b$ | $b$ |
| | xy($E$) | $2a+e$ | $2a+e$ | $2a+e$ | $2a+e$ | $b$ | $b$ | $b$ | $b$ | $b$ | $b$ | $b$ | $b$ |
| $C_4$ | $A\ B\ B\ E\ E$ z($A$) | $b$ | $b$ | $e$ | $e$ | $b$ | $a$ | $e$ | $e$ | $b$ | $a$ | $e$ | $e$ |
| | xy($E$) | $e$ | $e$ | $2a+2b$ | $2a+2b$ | $e$ | $e$ | $2a+2b$ | $2a+2b$ | $e$ | $e$ | $2a+2b$ | $2a+2b$ |
| $D_2$ | $A\ A\ B_1\ B_2\ B_3$ z($B_1$) | $b_1$ | $a$ | $b_3$ | $b_2$ | $b_1$ | $a$ | $b_3$ | $b_2$ | $a$ | $a$ | $b_2$ | $b_3$ |
| | y($B_2$) | $b_2$ | $b_3$ | $a$ | $b_1$ | $b_2$ | $b_3$ | $a$ | $b_1$ | $b_3$ | $b_3$ | $b_1$ | $a$ |
| | x($B_3$) | $b_3$ | $b_2$ | $b_1$ | $a$ | $b_3$ | $b_2$ | $b_1$ | $a$ | $b_2$ | $b_2$ | $a$ | $b_1$ |

| | | | | | | | | | | | | | | | | | | | |
|---|---|---|---|---|---|---|---|---|---|---|---|---|---|---|---|---|---|---|---|
| $D_3$ | $A_1$ | $E$ | $E$ | $E$ | $E$ | z($A_2$) | $e$ | | $e$ | | $e$ | | $e$ | | [b] | [b] | [b] | [b] | [b] | [b] | [b] | [b] |
| | | | | | | xy($E$) | $a_1+a_2+e$ | | $a_1+a_2+e$ | | $a_1+a_2+e$ | | $a_1+a_2+e$ | | [b] | [b] | [b] | [b] | [b] | [b] | [b] | [b] |
| $D_4$ | $A_1$ | $B_1$ | $B_2$ | $E$ | $E$ | z($A_2$) | $b_2$ | | $b_1$ | | $e$ | | $e$ | | $b_2$ | $a_1$ | $e$ | | $e$ | | $b_1$ | $a_1$ | $e$ | | $e$ | |
| | | | | | | xy($E$) | $e$ | | $e$ | | $a_1+a_2+b_1+b_2$ | | $a_1+a_2+b_1+b_2$ | | $e$ | $e$ | $a_1+a_2+b_1+b_2$ | | $a_1+a_2+b_1+b_2$ | | $a_1+a_2+b_1+b_2$ | $a_1+a_2+b_1+b_2$ | | | | |
| $C_{2v}$ | $A_1$ | $A_1$ | $A_2$ | $B_1$ | $B_2$ | z($A_1$) | $a_1$ | | $a_2$ | | $b_1$ | | $b_2$ | | $a_1$ | $a_2$ | $b_1$ | | $b_2$ | | $a_2$ | $a_2$ | $b_2$ | | $b_1$ | |
| | | | | | | x($B_1$) | $b_1$ | | $b_2$ | | $a_1$ | | $a_2$ | | $b_1$ | $b_2$ | $a_1$ | | $a_2$ | | $b_2$ | $b_2$ | $a_2$ | | $a_1$ | |
| | | | | | | y($B_2$) | $b_2$ | | $b_1$ | | $a_2$ | | $a_1$ | | $b_2$ | $b_1$ | $a_2$ | | $a_1$ | | $b_1$ | $b_1$ | $a_1$ | | $a_2$ | |
| $C_{3v}$ | $A_1$ | $E$ | $E$ | $E$ | $E$ | z($A_1$) | $e$ | | $e$ | | $e$ | | $e$ | | [b] | [b] | [b] | [b] | [b] | [b] | [b] | [b] | [b] | [b] | [b] | [b] |
| | | | | | | xy($E$) | $a_1+a_2+e$ | | $a_1+a_2+e$ | | $a_1+a_2+e$ | | $a_1+a_2+e$ | | [b] | [b] | [b] | [b] | [b] | [b] | [b] | [b] | [b] | [b] | [b] | [b] |
| $C_{4v}$ | $A_1$ | $B_1$ | $B_2$ | $E$ | $E$ | z($A_1$) | $b_1$ | | $b_2$ | | $e$ | | $e$ | | $b_1$ | $a_2$ | $e$ | | $e$ | | $b_2$ | $a_2$ | $e$ | | $e$ | |
| | | | | | | xy($E$) | $e$ | | $e$ | | $a_1+a_2+b_1+b_2$ | | $a_1+a_2+b_1+b_2$ | | $e$ | $e$ | $a_1+a_2+b_1+b_2$ | | $a_1+a_2+b_1+b_2$ | | $a_1+a_2+b_1+b_2$ | $a_1+a_2+b_1+b_2$ | | | | |
| $D_{2d}$ | $A_1$ | $B_1$ | $B_2$ | $E$ | $E$ | z($B_2$) | $a_2$ | | $a_1$ | | $e$ | | $e$ | | $a_2$ | $b_1$ | $e$ | | $e$ | | $a_1$ | $b_1$ | $e$ | | $e$ | |
| | | | | | | xy($E$) | $e$ | | $e$ | | $a_1+a_2+b_1+b_2$ | | $a_1+a_2+b_1+b_2$ | | $e$ | $e$ | $a_1+a_2+b_1+b_2$ | | $a_1+a_2+b_1+b_2$ | | $a_1+a_2+b_1+b_2$ | $a_1+a_2+b_1+b_2$ | | | | |
| $D_{4d}$ | $A_1$ | $E_2$ | $E_2$ | $E_3$ | $E_3$ | z($B_2$) | $e_2$ | | $e_2$ | | $e_1$ | | $e_1$ | | [b] | [b] | [b] | [b] | [b] | [b] | [b] | [b] | [b] | [b] | [b] | [b] |
| | | | | | | xy($E_1$) | $e_1+e_3$ | | $e_1+e_3$ | | $b_1+b_2+e_2$ | | $b_1+b_2+e_2$ | | [b] | [b] | [b] | [b] | [b] | [b] | [b] | [b] | [b] | [b] | [b] | [b] |
| $C_{3h}$ | $A'$ | $E'$ | $E'$ | $E''$ | $E''$ | z($A''$) | $e''$ | | $e''$ | | $e'$ | | $e'$ | | [b] | [b] | [b] | [b] | [b] | [b] | [b] | [b] | [b] | [b] | [b] | [b] |
| | | | | | | xy($E'$) | $2a'+e'$ | | $2a'+e'$ | | $2a''+e''$ | | $2a''+e''$ | | [b] | [b] | [b] | [b] | [b] | [b] | [b] | [b] | [b] | [b] | [b] | [b] |
| $D_{3h}$ | $A_1'$ | $E'$ | $E'$ | $E''$ | $E''$ | z($A_2''$) | $e''$ | | $e''$ | | $e'$ | | $e'$ | | [b] | [b] | [b] | [b] | [b] | [b] | [b] | [b] | [b] | [b] | [b] | [b] |
| | | | | | | xy($E'$) | $a_1'+a_2'+e'$ | | $a_1'+a_2'+e'$ | | $a_1''+a_2''+e''$ | | $a_1''+a_2''+e''$ | | [b] | [b] | [b] | [b] | [b] | [b] | [b] | [b] | [b] | [b] | [b] | [b] |
| $S_4$ | $A$ | $B$ | $B$ | $E$ | $E$ | z($B$) | $a$ | | $a$ | | $e$ | | $e$ | | $a$ | $b$ | $e$ | | $e$ | | $a$ | $b$ | $e$ | | $e$ | |
| | | | | | | xy($E$) | $e$ | | $e$ | | $2a+2b$ | | $2a+2b$ | | $e$ | $e$ | $2a+2b$ | | $2a+2b$ | | $e$ | $e$ | $2a+2b$ | | $2a+2b$ | |

[a] The letters $a$, $b$, $c$, $d$ and $e$ represent the $d_{z^2}$, $d_{x^2-y^2}$, $d_{xy}$, $d_{xz}$ and $d_{yz}$ orbitals, respectively [b] These ground states are not appropriate as they would be doubly degenerate and subject to a Jahn–Teller distortion to a lower symmetry, or the degeneracy is lifted by spin–orbit coupling, in which case the double group must be considered

REFERENCES


1 F A COTTON AND G. WILKINSON, *Advanced Inorganic Chemistry*, Interscience, London, 2nd ed , 1966
2 (*a*) N V SIDGWICK, *The Eleme ts and Their Compounds*, Vol I, Oxford University Press, Oxford, 1950; (*b*) E L MUETTERTIES and R A SCHUNN, *Quart Rev* , 20 (1966) 245; (*c*) W. E. HATFIELD AND R WHYMAN, *Trans Metal Chem* , 5 (1969) 47; (*d*) C FURLANI, *Coordin Chem. Rev* , 3 (1968) 141
3 A F. WELLS, *Structural Inorganic Chemistry*, University Press, Oxford, 3rd ed , 1962
4 J D. DUNITZ AND L. E. ORGEL, *Nature*, 179 (1957) 462
5 C. J BALLHAUSEN, *Dan Mat Fys Medd* , 29 (1954) No 4
6 C. J. BALLHAUSEN AND C. K JØRGENSON, *Dan Mat Fys Medd* , 29 (1955) No 14
7 A. L. COMPANION AND M. A KOMARYNSKI, *J Chem Educ* , 41 (1964) 257
8 P. DAY, *Proc Chem Soc* , (1964) 84, W. E HATFIELD AND T S PIPER, *Inorg Chem* , 3 (1964) 841; G. C. ALLEN AND N S. HUSH, *Inorg Chem* , 6 (1967) 4
9 C. R HARE AND C J. BALLHAUSEN, *J Chem Phys* , 40 (1964) 792
10 M. A. PORAI-KOSHITZ AND L M DIKAREVA, *Kristallografiya*, 4 (1959) 650
11 A A G. TOMLINSON, B J HATHAWAY, D E BILLING AND P. NICHOLLS, *J Chem Soc. (A)*, (1969) 65
12 M BUKOVSKA AND M A PORAI-KOSHITZ, *Zhur strukt Khim* , 7 (1961) 712
13 N W. ISAACS, C H L KENNARD AND D A WHEELER, *Chem Commun* , (1967) 587; N W. ISAACS AND C H. L. KENNARD, *J. Chem. Soc (A)*, (1969) 386
14 M A PORAI-KOSHITZ, *Zhur strukt Khim* , 4 (1963) 584
15 R. KIRIYAMA, H IBAMOTO AND K MATSUO, *Acta Cryst* , 11 (1954) 482
16 F. HANIC, *Czech J. Phys* , B10 (1960) 169
17 D. S. BROWN, J D LEE AND B G A MELSON, *Chem Commun* , (1968) 852, *Acta Cryst* , *B25 (1969) 1378*
18 A PABST, *Acta Cryst* , 12 (1959) 733
19 A. FERRARI, A. BRAIBANTI AND A. TIREPICCHIO, *Acta Cryst* , 21 (1966) 605
20 B MOROSIN AND A C LARSON, *Acta Cryst* , B25 (1969) 1417.
21 B. J HATHAWAY AND F. S STEPHENS, *J. Chem. Soc (A)*, (1970) 884
22 A. W SCHLUCTER, R A. JACOBSON AND R E. RUNDLE, *Inorg Chem* , 5 (1966) 277
23 N V. MANI AND S RASASERSHAN, *Z Krist* , 115 (1961) 97
24 R V G SUNDARA RAO, K SUNDARAMMA AND G SWASANKARA RAO, *Z. Krist* , 110 (1958) 231.
25 F. HANIC, *Acta Cryst* , 12 (1959) 739
26 G GIUSEPPETTI AND F. MAZZI, *Rend Soc mineral ital* , 11 (1955) 202
27 D S BROWN, J D LEE, B G A MELSON, B J HATHAWAY, I. M PROCTER AND A A G TOMLINSON, *Chem Commun* , (1967) 369
28 D S BROWN, J. D LEE AND B G. A MELSON, *Acta Cryst* , B24 (1968) 730
29 I. ROBERTSON AND M. R TRUTER, *J Chem Soc (A)*, (1967) 309
30 E. N. BAKER, I. HALL AND N. WATERS, *J. Chem Soc (A)*, (1966) 680
31 C P. NASH AND W. P SCHAEFER, *J Amer. Chem Soc* , 91 (1969) 1319
32 Y. A. SIMONOV, A. V ABLOV AND T. I MALINOVSKI, *Kristallografiya*, 8 (1963) 205.
33 F. S. STEPHENS, *J. Chem. Soc. (A)*, (1969) 2081
34 M B CINGI, C GUASTINI, A. MUSATTI AND M. NARDELLI, *Acta Cryst* , B25 (1969) 1833.
35 K. KNOX, *J Chem Phys.*, 30 (1959) 991.
36 H G VON SCHNERING, *Z. Anorg Allgem Chem* , 353 (1967) 13
37 F S STEPHENS, *J Chem Soc. (A)*, (1969) 883
38 C. K PROUT, R A ARMSTRONG, J R CARRUTHERS, J. G FORREST, P MURRAY-RUST AND F J. C. ROSSOTTI, *J Chem. Soc. (A)*, (1968) 2791.
39 B MOROSIN AND E. C LINGAFELTER, *J Phys. Chem* , 65 (1961) 50.
40 T. P. CHEESEMAN, D. HALL AND T. N WATERS, *J Chem. Soc.*, (1966) 685.
41 HUANG JIN-LING, LI JIEN MING AND LI JIA-XI, *Acta Chim. Sinica*, 32 (1966) 162.
42 G. A. BARCLAY, B. F. HOSKINS AND C. H. L KENNARD, *J. Chem Soc* , (1963) 5691
43 K. N. RAYMOND, D. W. MEEK AND J. A IBERS, *Inorg. Chem* , 7 (1968) 1111

44 F MAZZI, *Acta Cryst*, 8 (1955) 137.
45 B. MOROSIN, *Acta Cryst*, B24 (1969) 19.
46 J HOWATSON AND B MOROSIN, private communication
47 P JOSE, S. OOI, Q FERNANDO, *J Inorg Nucl Chem*, 31 (1969) 1971
48 S SCAVNICAR AND B MATKOVIC, *Chem Commun*, (1967) 297
49 M COLA, G GUISEPPETTI AND F. MAZZI, *Atti Accad Sci Torino*, 96 (1962) 381
50 M D. JOESTEN, M SAKHAWAT HUSSAIN, P G. LENHERT AND J H VENABLES, *J Amer. Chem. Soc*, 90 (1968) 5623
51 I M. PROCTER AND F S STEPHENS, *J. Chem Soc (A)*, (1969) 1248
52 F. S STEPHENS, *J. Chem Soc (A)*, (1969) 2233
53 F. S STEPHENS, *J Chem Soc (A)*, (1969) 1723
54 M V VEIDIS, G H SCHREIBER, T E GRUGH AND G T PALENIK, *J Amer Chem Soc*, 91 (1969) 1859
55 D A LANGS AND C R HARE, *Chem Commun*, (1970) 890
56 H A JAHN AND E TELLER, *Proc Roy Soc*, A161 (1937) 220
57 K. NAKAMOTO, *Infrared Spectra of Inorganic and Coordination Compounds*, Wiley, New York, 1963.
58 M H L. PRYCE, K P SINHA AND Y. TANABE, *Mol Phys*, 9 (1965) 33, A ABRAGAM AND M. H. L PRYCE, *Proc Roy Soc*, A206 (1951) 164
59 C K JØRGENSON, *Absorption Spectra and Chemical Bonding in Complexes*, Pergamon Press Ltd, Oxford, 1962.
60 H C LONGUET-HIGGINS, *Adv Spectros*, 2 (1961) 429, M C M O'BRIAN, *Proc. Roy Soc*, A281 (1964) 323.
61 H ELLIOTT, B J HATHAWAY AND R C SLADE, *Inorg Chem*, 5 (1966) 669
62 H ELLIOTT AND B J HATHAWAY, *Inorg Chem*, 5 (1966) 885
63 B J. HATHAWAY AND R C SLADE, *J Chem Soc (A)*, (1968) 85.
64 M D JOESTEN AND J F FORBES, *J Amer Chem Soc*, 88 (1966) 5465
65 K P LANNERT AND M D JOESTEN, *Inorg Chem*, 7 (1968) 2048
66 R A PALMER AND T. S PIPER, *Inorg Chem*, 5 (1966) 864
67 B J. HATHAWAY, M J. BEW, D E BILLING, R J DUDLEY AND P. NICHOLLS, *J Chem Soc (A)*, (1969) 2312.
68 H C ALLEN, G F KOKOSZKA AND R G. INSKEEP, *J Amer Chem Soc*, 86 (1964) 1023
69 G. F. KOKOSZKA, C. W. REIMANN, H C. ALLEN AND G GORDON, *Inorg Chem.*, 6 (1967) 1657.
70 A D LIEHR AND C J. BALLHAUSEN, *Ann. Phys (N Y)*, 3 (1958) 304
71 B J. HATHAWAY, R DUDLEY AND P. NICHOLLS, *J Chem Soc (A)*, 1969, 1845
72 L PAULING, *The Nature of the Chemical Bond*, University Press, Oxford, 2nd ed, 1940
73 *Stability Constants of Metal Ion Complexes, Chem Soc. Special Publ* No 17 (1964)
74 H IRVING AND R J P. WILLIAMS, *J Chem Soc*, (1953) 3192
75 B J. HATHAWAY AND A A. G TOMLINSON, *Coordin. Chem Rev*, 5 (1970) 1.
76 I. M PROCTER, B J HATHAWAY AND P NICHOLLS, *J. Chem. Soc (A)*, (1968) 1678
77 B J. HATHAWAY, D E. BILLING, P NICHOLLS AND I M PROCTER, *J. Chem Soc. (A)*, (1969) 319
78 F AKHTAR, D M L. GOODGAME, M. GOODGAME, G W RAYNER-CANHAM AND A C. SKAPSKI, *Chem Commun*, (1968) 1389
79 D. SMITH, private communication
80 B J HATHAWAY, D E BILLING AND R J. DUDLEY, *J. Chem Soc (A)*, (1970) 1420.
81 F. P. DWYER, H. A. GOODWIN AND E C GYARFAS, *Aust. J Chem*, 16 (1963) 544, E. D MACKENZIE, Ph D Thesis, University of New South Wales, 1962.
82 B. J HATHAWAY, I M. PROCTER, R C SLADE AND A A. G TOMLINSON, *J. Chem Soc (A)*, (1969) 2219
83 M. ELDER AND B. R. PENFOLD, private communication.
84 Z. DORI, *Chem Commun*, (1968) 714
85 M. J. BEW AND B J. HATHAWAY, unpublished results.
86 H. ELLIOTT, B J. HATHAWAY AND R C SLADE, *J. Chem Soc (A)*, (1966) 1443
87 A DYKSTRA, *Acta Cryst*, 20 (1966) 588

88 G. A BARCLAY AND F. S STEPHENS, *J. Chem Soc*, (1963) 2027.
89 D. P. GRADDON AND L. MUNDAY, *J. Inorg. Nucl Chem*, 25 (1963) 215
90 W. K. MUSKER AND M. S HUSSAIN, *Inorg Chem*, 8 (1969) 528
91 F. S STEPHENS, *J. Chem. Soc (A)*, (1969) 2493.
92 H. KOYAMA, Y. SAITO AND H KUROYA, *J Inst Polytech Osaka City Univ*, C4 (1953) 43; L F DAHL, 1961 private communication referred to in T. S PIPER AND R. L BELFORD, *Mol Phys*, 5 (1962) 169
93 A. A G TOMLINSON AND B J HATHAWAY, *J Chem Soc (A)*, (1968) 1905.
94 F A COTTON, *Chemical Applications of Group Theory*, Interscience, Wiley, New York, 1963.
95 T M. DUNN, in J LEWIS AND R G. WILKINS (Eds), *Modern Coordination Chemistry*, Interscience, New York, 1960, p 229
96 A. H MAKI AND B. R. MCGARVEY, *J. Chem Phys*, 29 (1958) 31.
97 J FERGUSON, *J. Chem. Phys.*, 35 (1961) 1612.
98 B N FIGGIS, M GERLOCH, J. LEWIS AND R. C SLADE, *J. Chem Soc (A)*, (1968) 2028.
99 B. N. FIGGIS AND J. LEWIS, *Progr Inorg Chem*, 6 (1964) 37
100 B. N FIGGIS AND R. S NYHOLM, *J Chem Soc.*, (1954) 12.
101 J. A VAN NIERKERK AND F. R. L SCHOENING, *Acta Cryst*, 6 (1953) 227.
102 B. R. MCGARVEY, *Transition Metal Chemistry*, 3 (1966) 89.
103 E. KONIG, *Landolt-Bornstein*, New Series, Group II, Vol. 2, Springer, Berlin, 1966.
104 C. P. POOLE, JR, *Electron Spin Resonance*, Interscience, New York, 1967, Ch 20.
105 A CARRINGTON AND H. C. LONGUET-HIGGINS, *Quart Rev*, 14 (1960) 427.
106 A. ABRAGAM AND M H L PRYCE, *Proc Roy Soc*, 206A (1951) 164
107 R E. DIETZ, H. KAMIMURA, M D STURGE AND A. YARIV, *Phys Rev.*, 132 (1963) 1559.
108 R H SANDS, *Phys Rev.*, 99 (1955) 1222
109 F. K. KNEUBUHL, *J. Chem Phys*, 33 (1960) 1074.
110 R. NEIMAN AND D. KIVELSON, *J. Chem. Phys*, 35 (1961) 156.
111 T. VANNGÅRD AND R. AASA, in W. LOW (Ed), *Paramagnetic Resonance*, Vol 2, Academic Press, 1963, p. 509.
112 F K. KNEUBUHL AND B. NATTERER, *Helv Phys Acta*, 34 (1961) 710
113 V. S. KOROLKOV AND A. K. POTAPOVICH, *Optics and Spectroscopy*, 16 (1964) 251
114 T. S JOHNSTON AND H. G HECHT, *J Mol. Spec*, 17 (1965) 98
115 J. W. SEARL, R. C SMITH AND S J WYARD, *Proc Phys Soc*, 78 (1961) 1174.
116 J. E GEUSIC AND L. CARLTON-BROWN, *Phys. Rev*, 112 (1958) 64
117 D. S SCHONLAND, *Proc Phys. Soc*, 73 (1959) 788.
118 D. E BILLING AND B J. HATHAWAY, *J Chem Phys*, 50 (1969) 2258.
119 H ABE AND K. ONO, *J. Phys Soc. Japan*, 11 (1956) 947.
120 D. E. BILLING AND B. J. HATHAWAY, *J Chem. Phys*, 50 (1969) 1476.
121 J. C. EISENSTEIN, *J. Chem. Phys*, 28 (1958) 323.
122 B J. HATHAWAY, M. J. BEW AND D. E BILLING, *J. Chem. Soc. (A)*, (1969) 1090.
123 A. A. G TOMLINSON AND B. J. HATHAWAY, *J Chem Soc. (A)*, (1968) 2578
124 R. C SLADE, A A G TOMLINSON, B J HATHAWAY AND D E. BILLING, *J Chem Soc (A)*, (1968) 61
125 M J. BEW, D E. BILLING AND B J. HATHAWAY, unpublished results.
126 M. HAREL, C. KNOBLER AND J D. MCCULLOUGH, *Inorg. Chem.*, 8 (1969) 11.
127 N S. HUSH AND R J. M. HOBBS, *Progr Inorg. Chem*, 10 (1968) 259.
128 B J. HATHAWAY, P. NICHOLLS AND D. BARNARD, *Spectrovision*, 22 (1969) 4.
129 J. S GRIFFITH, *Theory of Transition Metal Ions*, Cambridge University Press, Cambridge, 1961.
130 C J. BALLHAUSEN, *Introduction to Ligand Field Theory*, McGraw-Hill, New York, 1962
131 D. S MCCLURE, *Solid State Physics*, 9 (1959)
132 J. FERGUSON *Rev. Pure Appl. Chem*, 14 (1964) 1.
133 R L BELFORD AND J W. CARMICHAEL, JR., *J. Chem. Phys*, 46 (1967) 4515.
134 D. E BILLING, R. DUDLEY, B. J. HATHAWAY, P. NICHOLLS AND I. M. PROCTER, *J Chem. Soc. (A)*, (1969) 312
135 D E. BILLING, B J. HATHAWAY AND P. NICHOLLS, *J. Chem Soc. (A)*, (1969) 316

136 D. E. BILLING AND B J. HATHAWAY, *J. Chem. Soc. (A)*, (1968) 1516.
137 M. G CLARK AND R. G. BURNS, *J. Chem. Soc. (A)*, (1967) 1034.
138 J. FERGUSON, *J Chem. Phys*, 34 (1961) 1609.
139 F. A. COTTON AND J. J. WISE, *Inorg. Chem.*, 5 (1966) 1200.
140 F. A. COTTON AND J. J. WISE, *Inorg Chem*, 6 (1967) 917.
141 J. W. CARMICHAEL, JR., L. K STEINRAUF AND R. L BELFORD, *J. Chem. Phys*, 43 (1965) 3959.
142 J. GARAJ, *Chem Commun*, (1968) 904
143 D. OERLKRUG, *Z. Phys Chem.* (Frankfurt), 56 (1967) 325.
144 J. R. PILLBROW AND J. M SPAETH, *Phys Stat Solidi*, 20 (1967) 237.
145 J FERGUSON, *J Chem Phys*, 40 (1964) 3406
146 C FURLANI, E CERVONE, F. CALZONA AND B BALDANZA, *Theoret. Chem Acta.*, 7 (1967) 375
147 B J HATHAWAY, D. E BILLING, R. J DUDLEY, R J FEREDAY AND A A G. TOMLINSON, *J. Chem Soc (A)*, (1970) 806
148 C. A L BECKER, D. W. MEEK AND T. M DUNN, *J. Phys. Chem*, 72 (1968) 3588.
149 J. BAKER, R J DUDLEY, R J FEREDAY, B J. HATHAWAY AND M TYBJERG, unpublished data
150 T. R REDDY AND R SRINIVASAN, *J. Chem Phys.*, 43 (1965) 1404.
151 R BALLY, *Compt. Rend.*, 257 (1963) 425
152 I. M PROCTER, B. J. HATHAWAY, D. E. BILLING, R DUDLEY AND P NICHOLLS, *J. Chem. Soc (A)*, (1969) 1192
153 C. K JØRGENSEN, *Prog Inorg. Chem*, 4 (1962) 73.
154 J. OWEN AND J. H M THORNLEY, *Rep Prog Phys*, 29 (1966) 676
155 M GERLOCH AND J R MILLER, *Prog Inorg Chem*, 10 (1968) 1.
156 K. W H STEVENS, *Proc Roy. Soc.*, A219 (1953) 542
157 D. KIVELSON AND R. NEIMAN, *J. Chem. Phys*, 35 (1961) 149
158 B G MALMSTROM AND T. VANNGÅRD, *J. Mol Biol*, 2 (1960) 118
159 J M BARBOUR, D A MORTON-BLAKE AND A L PORTE, *J Chem Soc. (A)*, (1968) 878.
160 W B. LEWIS, M ALEI AND L O. MORGAN, *J Chem Phys*, 45 (1966) 4003
161 H A KUSKA, M. T ROGERS, R E DRULLINGER, *J Phys. Chem*, 71 (1967) 109.
162 T C CHIANG, *J. Chem Phys*, 48 (1968) 1814.
163 H R GERSMANN AND J D. SWALEN, *J Chem Phys*, 36 (1962) 3221.
164 W. WINDSCH AND M. WELTER, *Z. Naturforsch*, 22a (1967) 1
165 F A. COTTON AND J. J WISE, *Inorg. Chem*, 6 (1967) 915.
166 C FURLANI, A SGAMELLOTTI, F. MAGRINI AND D. CORDISCHE, *J. Mol. Spect*, 24 (1967) 270.
167 M. SHARNOFF, *J. Chem. Phys*, 42 (1965) 3383
168 H S JARRETT, *J. Chem. Phys*, 28 (1958) 1260
169 S YAMADA AND R TSUCHIDA, *Bull Chem Soc. Japan*, 27 (1954) 156
170 M A HITCHMAN, C DOLSON AND R. L. BELFORD, *J. Chem. Phys*, 50 (1969) 1195
171 A PAJUNEN, *Suomen Kem*, 40 (1967) 32.
172 F. MAZZI, *Rend Soc. Mineral Italiana*, 9 (1953) 148
173 R RAJAN, *J. Chem. Phys*, 37 (1962) 1901
174 A. BAGLIO, Ph D. Thesis, Rutgers University, 1965
175 E BULUGGIU, A. DALL'OLIO, G. DASCOLA AND V. VARACCA, *Phys. Rev*, 179 (1969) 289.
176 M. A. HITCHMAN, private communication
177 R. RAJAN AND T R REDDY, *J Chem Phys*, 39 (1963) 1140.
178 P B AYSCOUGH, *Electron Spin Resonance in Chemistry*, Methuen, 1967, p. 160
179 W. LOW, *Solid State Physics*, Suppl 2 (1962)
180 G E PAKE, *Paramagnetic Resonance*, Benjamin, 1962
181 P. W. ANDERSON AND P. R WEISS, *Rev. Mod Phys*, 25 (1953) 269; P R LOCHER AND C J GORTEN, *Physica*, 28 (1962) 797
182 D. M S BAGGULEY AND J H. E GRIFFITHS, *Proc Roy Soc*, A201 (1950) 366
183 B BLEANEY AND K. D BOWERS, *Proc. Roy. Soc.*, A214 (1952) 451.